# ENGAGEMENT OF GRP78 AUTOANTIBODIES WITH CELL SURFACE GRP78 ON ENDOTHELIAL CELLS DRIVE TISSUE FACTOR ACTIVATION

# ENGAGEMENT OF ANTI-GRP78 AUTOANTIBODIES WITH CELL SURFACE GRP78 ON ENDOTHELIAL CELLS DRIVE TISSUE FACTOR ACTIVATION

By:

JACK CHEN, BHSc

A Thesis Submitted to the School of Graduate Studies

In Partial Fulfillment of the Requirements for the Degree

Master of Science

MASTER OF SCIENCE (MSc) (2022)

Medical Sciences
(Blood and Vasculature)

McMaster University
Hamilton, Ontario, Canada

TITLE: ENGAGEMENT OF ANTI-GRP78 AUTOANTIBODIES WITH CELL SURFACE GRP78 ON ENDOTHELIAL CELLS DRIVE TISSUE FACTOR ACTIVATION

AUTHOR: Jack Chen, B. BHSc. (McMaster University)

SUPERVISOR: Dr. Richard C. Austin, Ph.D, CAHS

NUMBER OF PAGES 121

## Lay Abstract

Blood clots formed following vascular injury are associated with the procoagulant activity of a protein called tissue factor. Based on the observation that autoantibodies against another protein called GRP78, which is found at the cell surface of activated endothelial cells, can promote the development of plaques in arteries. I found that the anti-GRP78 autoantibodies can promote tissue factor procoagulant activity in activated endothelial cells by enhancing cytoplasmic $Ca^{2+}$ levels. Additionally, I also found small molecules that may block the ability of the anti-GRP78 autoantibody to interact with cell surface GRP78 to activate cell surface GRP78, which may represent a potentially novel treatment strategy in the formation of blood clots.

**Abstract**

Atherothrombosis is the underlying contributor of cardiovascular disease whereby the thrombotic events following atherosclerotic plaque rupture are linked to tissue factor (TF) and its procoagulant activity (PCA). We have reported previously that the 78-kilodalton glucose-regulated protein (GRP78) observed on the cell surface of tumour cells acts as a novel signalling receptor to regulate TF PCA. Cell surface GRP78 also acts as a neoantigen known to promote an immune response that leads to the generation of anti-GRP78 autoantibodies. Given that the proinflammatory cytokine tumour necrosis factor α (TNFα) is known to contribute to atherosclerotic lesion development and promote TF expression, I investigated whether the anti-GRP78 autoantibodies against cell surface GRP78 can regulate TF PCA in TNFα-treated cultured endothelial cells. In this M.Sc. thesis, I demonstrated that TNFα treatment promotes TF PCA, an effect mediated by NF-κB activation. Additionally, treatment with TNFα was observed to elevate cell surface GRP78 expression levels. Further, anti-GRP78 autoantibodies enhanced TF PCA in endothelial cells pre-treated with TNFα. These effects of the anti-GRP78 autoantibodies were further enhanced in cells pre-treated with ER stress-inducing agents, also known to enhance cell surface GRP78 levels. I also showed that anti-GRP78 autoantibodies can also elevate intracellular $Ca^{2+}$ levels, which is known to contribute to TF activation. Sequestering the anti-GRP78 autoantibody or blocking the anti-GRP78 autoantibody from cell surface GRP78 attenuated anti-GRP78 autoantibody-induced TF PCA. In this study, we identified small chemical compounds predicted to bind to cell surface GRP78 (termed GRP78 binders) that inhibited anti-GRP78 autoantibody-induced TF PCA. Together, these findings provide evidence that the anti-GRP78 autoantibodies can

contribute to enhanced TF PCA and that disrupting the engagement of the anti-GRP78 autoantibody to cell surface GRP78 with these GRP78 binders may represent a potential therapeutic strategy for the treatment and management of atherothrombosis.

## ACKNOWLEDGEMENTS

I would give my sincerest gratitude to my supervisor, Dr. Richard Austin, for his kindness and support throughout my time as a graduate student and for giving me the opportunity and freedom to explore this project. His mentorship has allowed for personal development and become a better researcher. I am honoured and privileged to be part of his research group at St. Joseph's Healthcare Hamilton. I would also like to thank my committee members, Dr. Bernardo Trigatti and Dr. Peter Gross, who have enhanced this project through their constructive feedback and guidance.

Further, I would like to thank both prior and current members of the Austin Laboratory for their technical help and support during my time in the lab. I am truly thankful to Dr. Edward G. Lynn for overseeing my training as an undergraduate CO-OP student and graduate student in the Austin laboratory and for the advice and technical expertise throughout the years I have been in the lab. I would also like to give appreciation to former members of the lab, Dr. Ali Al-Hashimi, Dr. Paul Lebeau, and Dr. Khrystyna Platko, who introduced me to the world of the wet lab and have supported me and taught me valuable life lessons and the balance between lab work and life outside of the lab.

I am also grateful for the support and friendship of my best friend, Benjamin Nguyen, who has always been there when I needed a friend the most. I am also indebted to my parents, who, without their support, encouragement, and love, I would not have had the strength to complete my studies.

**Table of Contents**

Abstract ..... iv
Table of Figures ..... x
List of Abbreviations ..... xi
1. Introduction ..... 1
1.1. Atherothrombosis and Tissue Factor (TF) ..... 1
1.1.1. Atherothrombosis ..... 1
1.1.2. The Role of TF in the Coagulation Cascade ..... 2
1.1.3. TF Expression ..... 6
1.1.4. TF Protein Structure and Post-Translational Modifications ..... 7
1.1.5. TF Encryption and Proposed Mechanisms of TF De-encryption ..... 11
1.1.5.1. TF Disulfide Bond Isomerization ..... 14
1.1.5.2. TF Dimerization ..... 15
1.1.5.3. TF Compartmentalization in Lipid Rafts/Caveolae ..... 15
1.1.5.4. Endocytosis of TF·FVIIa ..... 16
1.1.5.5. Altered Phospholipid Asymmetry ..... 17
1.2. Endoplasmic Reticulum (ER) ..... 19
1.2.1. ER Functions ..... 19
1.2.2. ER Stress and the Unfolded Protein Response ..... 19
1.2.3. ER Chaperones ..... 24
1.2.4. GRP78 ..... 24
1.2.5. Cell Surface GRP78 ..... 28
2. Rationale, Hypothesis, and Objectives of Study ..... 31
2.1. Rationale ..... 31
2.2. Hypothesis ..... 31
2.3. Objectives ..... 31
2.3.1. Overall Objectives ..... 31
2.3.2. Specific Objectives ..... 32
3. Experimental Procedures ..... 35
3.1. Cell Line and Culture Conditions ..... 35
3.2. Cell Treatments ..... 35
3.3. Identification of GRP78 binders (Atomwise Inc., San Francisco, CA) ..... 35
3.4. Anti-GRP78 Autoantibody Isolations ..... 36

3.5. Measurement of TF PCA ..... 36
3.6. Fura-2 AM $Ca^{2+}$ Assay ..... 37
3.7. Immunofluorescent Staining ..... 38
3.7.1. Immunofluorescent Staining of Intracellular Proteins ..... 38
3.7.2. Immunofluorescent Staining of Cell Surface Proteins ..... 38
3.8. Production and Purification of Recombinant Human GRP78 ..... 39
3.9. ATPase Activity Measurements ..... 40
3.10. Immunoblotting ..... 40
3.11. Enzyme-linked Immunosorbent Assay (ELISA) ..... 41
3.12. Statistical Analysis ..... 41
4. Results ..... 43
4.1. TNFα Contributes to TF PCA Through NF-κB in Endothelial Cells ..... 43
4.2. Recombinant Human GRP78 Does Not Alter TNFα-induced TF PCA ..... 49
4.3. Anti-GRP78 Autoantibody Induces TF PCA in teloHAECs ..... 52
4.4. Thapsigargin and Tunicamycin Enhance Anti-GRP78 Autoantibody Induced TF PCA ..... 56
4.5. Anti-GRP78 Autoantibodies Enhances Cytosolic $Ca^{2+}$ Levels ..... 60
4.6. CNVKSDKSC Peptide Attenuates Anti-GRP78 Autoantibody-Induced TF PCA ..... 63
4.7. Anti-GRP78 Autoantibody Induces TF PCA Mediated by Functional TF ..... 66
4.8. Heparin or Enoxaparin Attenuates Anti-GRP78 Autoantibody-mediated TF PCA in teloHAECs ..... 69
4.9. Identification of GRP78 Binders That Inhibited TNFα- and Anti-GRP78 Autoantibody-induced TF PCA in teloHAECs ..... 72
4.10. GRP78 binders B07* and B08* Reduces the ATPase Activity of rhGRP78 ..... 76
4.11. B07* Inhibits the Binding of the Anti-GRP78 Autoantibody to rhGRP78- and to KLH-CNVSDKSC-coated Plates ..... 79
5. Discussion ..... 83
5.1. TNFα Contributes to Enhanced TF PCA Through NF-κB Activation ..... 84
5.2. TNFα Enhances Cell Surface GRP78 Levels ..... 84
5.3. Regulation of TF PCA by Cell Surface GRP78 and the Anti-GRP78 Autoantibody ..... 85
5.4. Anti-GRP78 autoantibody enhances TF PCA ..... 87
5.5. Small Molecule Inhibitors of Cell Surface GRP78 ..... 88
6. Future Directions ..... 92
7. Summary ..... 94

References ..... 95

## Table of Figures

Figure 1. TF and the coagulation cascade. ..... 4
Figure 2. Structure of TF ..... 9
Figure 3. Proposed mechanisms of TF de-encryption ..... 12
Figure 4. The role of GRP78 in the ER ..... 22
Figure 5. Schematic of GRP78 ..... 26
Figure 6. A schematic representing the predicted cellular events following the engagement of the anti-GRP78 autoantibody and cell surface GRP78 ..... 33
Figure 7. TNFα promotes TF PCA mediated by NF-κB activation in cultured endothelial cells. ..... 45
Figure 8. TNFα promotes NF-κB nuclear localization in cultured endothelial cells. ..... 47
Figure 9. rhGRP78 does not activate TF PCA in TNFα-treated teloHAECs ..... 50
Figure 10. The anti-GRP78 autoantibody enhances TF PCA in teloHAECs. ..... 54
Figure 11. Thapsigargin and tunicamycin enhances the anti-GRP78 autoantibody-mediated TF PCA in TNFα-treated teloHAECs. ..... 58
Figure 12. Anti-GRP78 autoantibodies increases cytosolic $Ca^{2+}$ levels. ..... 61
Figure 13. CNVKSDKSC conformational peptide inhibits the anti-GRP78 autoantibody-induced TF PCA. ..... 64
Figure 14. Anti-TF antibodies inhibit the anti-GRP78 autoantibody-induced TF PCA in TNFα-treated teloHAECs ..... 67
Figure 15. Pre-treatment with either heparin or enoxaparin blocked anti-GRP78 autoantibody-induced TF PCA in teloHAECs. ..... 70
Figure 16. Screening of small molecules predicted to bind to cell surface GRP78 on anti-GRP78 autoantibody-induced TF PCA. ..... 74
Figure 17. B07* and B08* inhibits rhGRP78 ATPase activity. ..... 77
Figure 18. Small molecules inhibit the binding of anti-GRP78 autoantibodies to rhGRP78 or KLH-CNVSDKSC conjugate peptide. ..... 81

## List of Abbreviations

| | |
|---|---|
| ADP | Adenosine diphosphate |
| *apoE*$^{-/-}$ | Apolipoprotein E-deficient |
| Asn | Asparagine |
| ATF6 | Activating transcription factor |
| ATP | Adenosine triphosphate |
| AutoAb | Autoantibody |
| bEND3.1 | Brain-derived endothelial cells |
| BSA | Bovine serum albumin |
| $Ca^{2+}$ | Calcium ion |
| CHOP | C/EBP homologous protein |
| Cys | Cysteine |
| DSF | Differential scanning fluorimetry |
| DTT | Dithiothreitol |
| ECM | Extracellular matrix |
| eIF2α | Eukaryotic transcription factor 2α |
| ELISA | Enzyme-linked Immunosorbent Assay |
| ER | Endoplasmic Reticulum |
| ERAD | ER-associated degradation |
| FBS | Fetal bovine serum |
| FI/FIa | Fibrinogen/ Fibrin |
| FII/FIIa | Factor II; Thrombin |
| FIII/FIIIa | Factor III; prothrombin/ thrombin |
| FIX/FIXa | Factor IX/ IXa (activated) |
| FV/FVa | Factor V/ Factor V (activated) |
| FVIII/FVIIIa | Factor VIII/ Factor VIII (activated) |
| FX/FXa | Factor X/ Factor X (activated) |
| FXI/FXIa | Factor XI/ XIa (activated) |
| FXII/FXIIa | Factor XII/ Factor XII (activated) |
| GFP | Green fluorescent protein |
| GRP78 | Glucose-regulated protein 78 kDa |
| GRP78$^{-/-}$ | GRP78 knockout |
| GRP78$^{+/-}$ | GRP78 heterozygote |
| GRP94 | Glucose-regulated protein 94 kDa |
| HBSS | Hank's buffered salt solution |
| HEK293 | Human embryonic kidney 293 |
| HRP | Horseradish peroxidase |
| HSP70 | Heat shock protein 70 kDa |
| HSP90 | Heat shock protein 90 kDa |
| ICAM-1 | Intercellular adhesion molecule 1 |
| IKK | IκB kinase |
| IL- | Interleukin |
| IRE1 | Inositol-requiring enzyme 1 |
| IκB | Inhibitor of nuclear factor κB |
| KDEL | Lysine, aspartic acid, glutamic acid, and leucine |
| KLH | Keyhole limpet hemocyanin |

| | |
|---|---|
| LDL | Low-density lipoproteins |
| Leu | Leucine |
| LPS | Lipopolysaccharide |
| LRP | LDL receptor-related protein |
| MCP-1 | Macrophage chemoattractant protein-1 |
| MTJ-1/HTJ-1 | Murine DnaJ-like protein 1/ human DnaJ-like protein 1 |
| NF-κB | Nuclear factor κB |
| NOD/SCID | Non-obese diabetic/severe combined immunodeficiency |
| oxLDL | Oxidized low-density lipoproteins |
| Par-4 | Prostate apoptosis response 4 |
| PBS | Phosphate-buffered saline |
| PCA | Procoagulant activity |
| PDI | Protein disulphide isomerase |
| PE | Phosphatidylethanolamine |
| PERK | Protein kinase RNA-like endoplasmic reticulum kinase |
| PFA | Paraformaldehyde |
| PI | Phosphatidylinositol |
| PS | Phosphatidylserine |
| rh | Recombinant human |
| S1P | Site-1 protease |
| S2P | Site-2 protease |
| SPR | Surface Plasmon Resonance |
| TBS/TBS-T | Tris-buffered saline/Tris-buffered saline-Tween-20 |
| teloHAEC | Immortalized human aortic endothelial cells |
| TF | Tissue factor |
| $TF^{-/-}$ | TF-deficient |
| TFPI | Tissue pathway inhibitor |
| TG | Thapsigargin |
| TM | Tunicamycin |
| TNFα | Tumour necrosis factor α |
| UGGT | UDP-glucose: glycoprotein glucosyltransferase |
| UPR | Unfolded protein response |
| VCAM-1 | Vascular cell adhesion protein 1 |
| VSMC | Vascular smooth muscle cells |
| WCL | Whole-cell lysate |
| WGA | Wheat germ agglutinin |
| WT | Wild type |
| XBP1/sXBP1 | X-box binding protein/ X-box binding protein (spliced) |

# 1. Introduction

## *1.1. Atherothrombosis and Tissue Factor (TF)*

### *1.1.1. Atherothrombosis*

Atherothrombosis is an inflammatory condition characterized by superimposed thrombus formation following atherosclerotic plaque disruption, manifesting clinically as an ischaemic heart attack or stroke (1). Further, atherothrombosis is the major complication of cardiovascular disease, the leading cause of premature global mortality and a burden on the quality of life (2). Conventional cardiovascular disease risk factors, including hyperlipidemia, diabetes mellitus, obesity, lack of physical activity, age, tobacco use, and family history of cardiovascular disease, are also associated with enhanced blood thrombogenicity (3–6). Clinically, inflammatory biomarkers such as high sensitivity C-reactive protein have been used in the assessment for the risk of cardiovascular disease (7–10), highlighting the role of inflammation in cardiovascular disease and atherothrombosis (11). Although each risk factor alone is known to contribute to atherothrombotic disease independently, these risk factors are predicted to work in concert to promote the activation of inflammatory processes that lead to plaque formation and thrombotic complications that can follow (11, 12).

The process of atherothrombosis has been reported to occur in early adolescence and progress throughout adulthood (1). The initial stage of atherothrombosis is characterized by a local pro-inflammatory response induced by endothelial cell dysfunction and lipid accumulation in the arterial wall that leads to the recruitment of immune cells (13). In the activated endothelium, nuclear factor κB (NF-κB) localizes to the nucleus, enhancing the expression of proinflammatory cytokines such as tumour necrosis factor α (TNFα), IL-1β, and IL-6 which are known to promote atherosclerotic lesion development and progression

(14). Additionally, activated teloHAECs also express macrophage chemoattractant protein-1 (MCP-1) and vascular cell adhesion protein 1 (VCAM-1), intercellular adhesion molecule 1 (ICAM-1), and E-selectin (13). This process leads to the recruitment and infiltration of circulating leukocytes into the vessel wall. Further, the accumulation of macrophages that uptake cholesterol-rich lipids inside the vessel wall result in a foam-like appearance observed in the fatty streak (15). As the plaque progresses, vascular smooth muscle cells (VSMCs) migrate and proliferate within the intima resulting in the thickening of the arterial wall (15). Intimal VSMCs produce collagen- and proteoglycan-rich extracellular matrix (ECM) which together form a fibrous cap that overlies the lipid-rich core of the atherosclerotic plaque (15, 16). In advanced atherosclerotic lesions, secretion of matrix metalloproteinases by apoptotic macrophages results in ECM degradation (11). Additionally, TNFα and other proinflammatory cytokines have been reported to contribute to intimal VSMC and inhibit ECM production (17). Together, chronic ECM degradation and the loss of ECM production enhances the risk of plaque disruption and subsequent thrombotic complications (18).

### *1.1.2. The Role of TF in the Coagulation Cascade*

The enhanced thrombogenicity following vascular injury has been attributed to TF and its procoagulant activity (PCA) (19). TF is the primary activator of the extrinsic pathway of the coagulation cascade and is essential in the hemostatic response following vascular trauma (19). The coagulation cascade is a series of activations of serine proteases that result in FIa (fibrin) clot formation, which serves as a scaffold for platelet adhesion and aggregation required following vascular injury (Figure 1) (20). The two major pathways that characterize the coagulation cascade are the intrinsic clotting pathway and the

extrinsic clotting pathway, both of which result in the activation of factor (F)X and the subsequent generation of FIIa (thrombin) (21). Further, thrombin mediates the conversion of FI (fibrinogen) into fibrin monomers known to polymerize into the fibrin clot (20). Thrombin is also known to mediate the cleavage of protease-activated receptors on the platelet cell surface, resulting in platelet activation and aggregation (22). The intrinsic clotting pathway is initiated by contact activation of FXII with negatively charged surfaces and proteins (23). FXIIa converts FXI to FXIa, which in turn activates FIX (23). FIX in complex cofactors FVIIIa and $Ca^{2+}$ activates FX to generate thrombin (20). The extrinsic coagulation cascade is initiated following vascular trauma, whereby circulating FVII/FVIIa binds to FIII (TF), in which the TF·FVIIa complex catalyzes the activation of FX, leading to thrombin generation and fibrin formation (19).

**Figure 1. TF and the coagulation cascade.**

TF functions as the activator of the extrinsic pathway of coagulation following vascular injury. Cell surface TF binds to circulating FVII/FVIIa, in which the complex converts FX to FXa. FXa converts of prothrombin to thrombin, leading to fibrin clot formation. Adapted from Pérez-Pujol et al. (2012) (24).

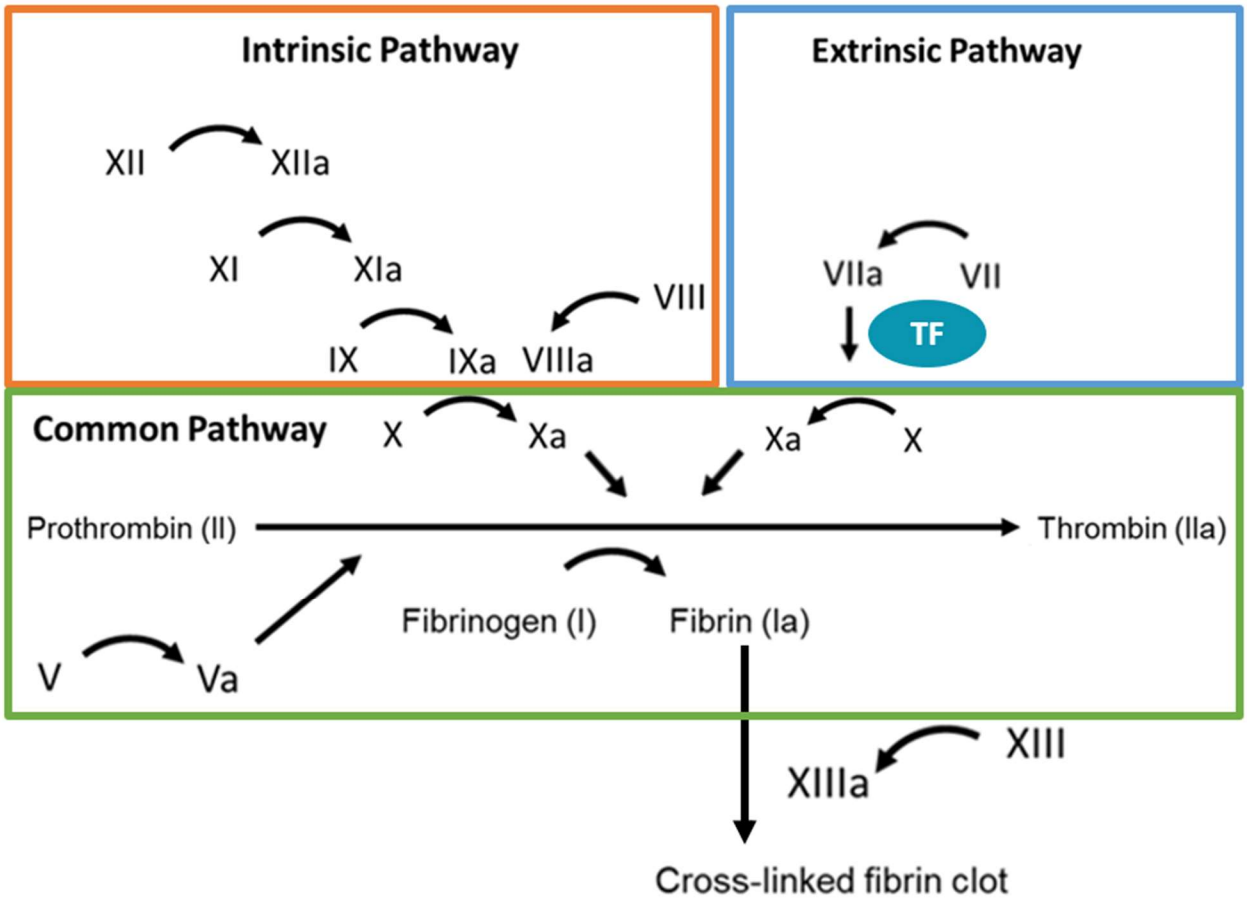
Intrinsic Pathway
XII
XIIa
XI
XIa
VIII
IX
IXa
VIIIa
Extrinsic Pathway
VIIa
VII
TF
Common Pathway
X
Xa
Xa
X
Prothrombin (II)
Thrombin (IIa)
Fibrinogen (I)
Fibrin (Ia)
V
Va
XIII
XIIIa
Cross-linked fibrin clot

### *1.1.3. TF Expression*

TF was first identified as a component within tissue extracts which induced thrombin formation when incubated in plasma (25). Additionally, TF plays a critical role during embryonic vascular development as TF-deficient ($TF^{-/-}$) mice are embryonically lethal between embryonic days 8.5 and 10.5 due to the lack of vascular integrity resulting in greater bleeding events (26). According to the Human Protein Atlas database, constitutive TF expression has been identified in several human tissues, particularly in highly vascularized tissues such as the placenta, adipose tissue, pancreas, and brain (25). High levels of TF mRNA have been identified in brain, heart, kidney, and lung tissue lysates (27). TF expression has also been identified in most tumours and is thought to contribute to tumour progression and metastasis (28, 29). In the vasculature, constitutive TF expression is found in adventitial fibroblasts and pericytes (30, 31). TF expression has also been observed in the various cell types that compose the atherosclerotic plaque (32, 33). Notably, most TF in atherosclerotic plaques is localized to lesion-resident macrophages and macrophage foam cells (32). Under normal physiological conditions, endothelial cells are reported to seldomly express TF (19). However, several studies have reported that TF expression can be induced in cultured endothelial cells in the presence of IL-1β, TNFα, and lipopolysaccharide (LPS) (34–37). Additionally, Thiruvikraman et al. reported TF expression throughout the atherosclerotic plaque, particularly in overlying endothelial cells and VSMCs within the plaque, using digoxigenin-labelled FVIIa and FX (38).

### *1.1.4. TF Protein Structure and Post-Translational Modifications*

TF is a 47-kDa integral transmembrane glycoprotein encoded by the human TF gene located on chromosome 1p21-22, composed of approximately 12.4 kilobases (39). The TF gene contains six exon sequences where exon 1 encodes a signal sequence, exon 2 to exon 5 encodes the extracellular N-terminal domain, and exon 6 encodes the transmembrane domain and the cytoplasmic C-terminal domain (Figure 2) (39, 40). Although TF was previously described as FIII, it does not share homology with other members of the coagulation cascade (39). Instead, TF is classified as a type II cytokine receptor with a structurally conserved binding domain formed by the anti-parallel beta-sandwich and the lack of a characteristic WSxWS motif found in type I receptors (39, 41). The N-terminal domain contains two extracellular immunoglobulin-like domains that form a 125° angle which functions as the binding site of FVII/FVIIa and FX (42). Previous reports have shown that the transmembrane domain does not alter the ability of TF to form a complex with FVIIa but instead plays a crucial role as a membrane anchor to facilitate and enhance the binding of the TF·FVIIa complex with FX (43). Following purification, recombinant human (rh) TF has an approximate molecular mass of 29 kDa, whereas TF purified from human cells has a molecular mass of 45-47 kDa (44). The discrepancy between the molecular mass of rhTF is due to N-linked glycosylation found on asparagine (Asn) residues 11, 124, and 137 located in the extracellular domain of TF (44). rhTF also contains disulfide bonds between cysteine (Cys) residues 49 and 57 and between 186 and 209 (44). An alternatively spliced isoform of TF was also identified in circulation that lacks exon 5 and possesses a unique exon 6 compared to full-length TF and was found in circulation due to loss of the transmembrane domain (45). The

cytoplasmic C-terminus domain of TF is not required in the coagulation cascade activation (46) but is involved in intracellular signalling pathways that contribute to cell adhesion in macrophages (47, 48).

**Figure 2. Structure of TF**

Schematic of the 4 domains of TF: the ER signal sequence (not shown), an extracellular domain, a transmembrane domain, and a cytoplasmic domain. The extracellular domain functions as the binding site of FVII/VIIa and FX. The transmembrane domain anchors TF to the cell membrane. The intracellular domain is not involved in the TF-mediated activation of FX but plays a role in TF-mediated intracellular signalling pathways. Human TF is glycosylated at residues $Asn_{11}$, $Asn_{124}$, and $Asn_{134}$, depicted as yellow circles. Human TF also forms disulfide bonds between Cys residues $Cys_{49}$ and $Cys_{57}$ and between $Cys_{186}$ and $Cys_{209}$.

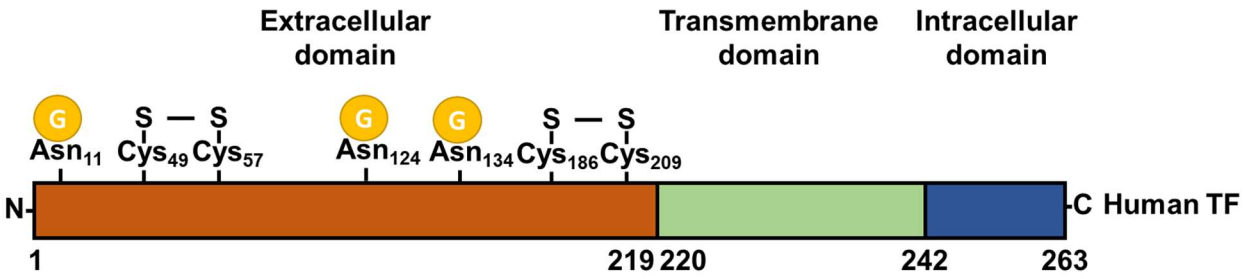
Extracellular domain
Transmembrane domain
Intracellular domain
G
S — S
Asn11 Cys49 Cys57
G
G
Asn124 Asn134
S — S
Cys186 Cys209
N-
-C Human TF
1
219 220
242
263

### *1.1.5. TF Encryption and Proposed Mechanisms of TF De-encryption*

Expression of cell surface TF does not necessarily correlate with PCA (49). Oxidized low-density lipoproteins (oxLDL) have been reported to induce TF expression in VSMCs without promoting TF PCA (50, 51). As such, current thinking suggests that at least two pools of TF exist: encrypted (non-functional) TF and de-encrypted (functional) TF (52). Furthermore, FVIIa was shown to bind to encrypted TF slowly; however, it had no detectable effect on FX activation (53). In contrast, FVII/FVIIa was shown to bind rapidly to de-encrypted TF, resulting in FXa generation (53). Several TF encryption/de-encryption mechanisms have been proposed, including i) TF disulfide bond isomerization; ii) TF dimerization; iii) TF compartmentalization in lipid rafts/caveolae; iv) TF-FVIIa endocytosis; and the v) altered phospholipid asymmetry model (Figure 3) (54). Although the specific mechanisms that regulate TF have been suggested to vary between different cell types (54).

**Figure 3. Proposed mechanisms of TF de-encryption**

There are several proposed mechanisms of TF de-encryption which may vary between cell types. A) In the TF disulfide bond isomerization model, oxidation of thiol groups of $Cys_{186}$ and $Cys_{209}$ forming a disulfide bond promotes TF de-encryption. Further, cell surface PDI may contribute to the disulfide bond formation. B) Under the TF dimerization model, TF remains encrypted when TF forms homodimers and can become de-encrypted under conditions that lead to the formation of TF monomers. C) At the cell surface, encrypted TF is also believed to reside in lipid rafts or caveolae that sequester TF away from FX and can become de-encrypted following the disruption of the caveolae. D) Endocytosis of TF·FVIIa complex mediated by TFPI with or without LRP sequesters the TF·FVIIa complex into vesicles which can be degraded or transported back to the cell surface. E) Under the anionic phospholipid asymmetry model, TF de-encryption occurs following the expression of anionic phospholipids on the outer leaflet. The illustration was generated with BioRender.

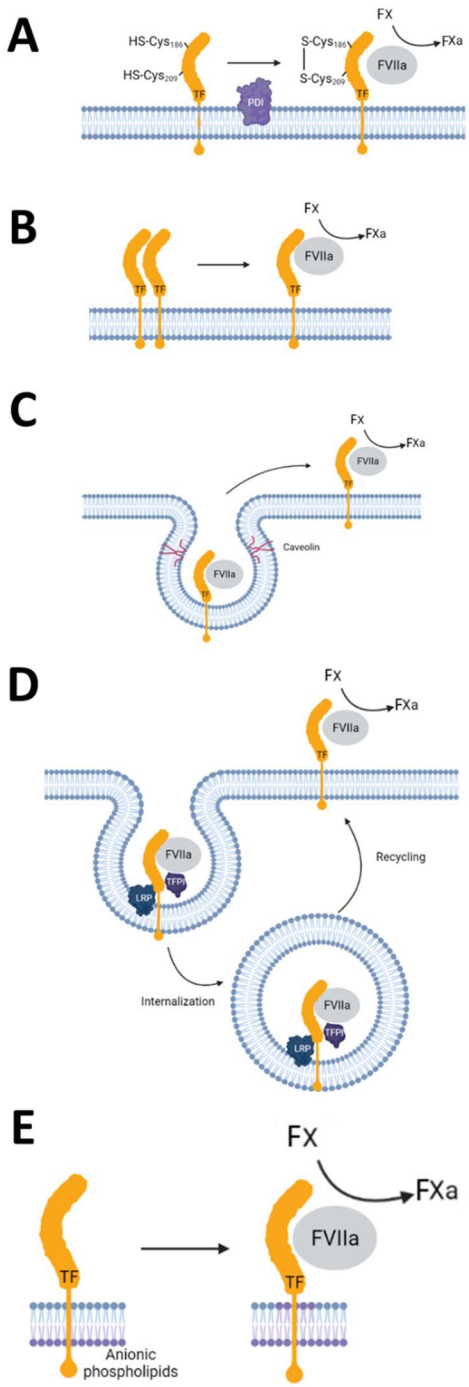
A
HS-Cys186
HS-Cys209
TF
PDI
S-Cys186
S-Cys209
FX
FXa
FVIIa
B
C
Caveolin
D
Recycling
Internalization
LRP
TFPI
E
Anionic
phospholipids

#### *1.1.5.1. TF Disulfide Bond Isomerization*

One proposed cell surface TF de-encryption mechanism involves the oxidation of extracellular residues $Cys_{186}$ and $Cys_{209}$. Although TF contains two Cys pairs ($Cys_{49}$ and $Cys_{57}$; $Cys_{186}$ and $Cys_{209}$) capable of forming disulfide bonds, the bond between $Cys_{49}$ and $Cys_{57}$ has been reported to be not required for de-encryption of TF (55). Under the view of this mechanism, $Cys_{186}$ and $Cys_{209}$ of encrypted TF contain reduced thiol groups (54). Following the oxidation between the extracellular residues $Cys_{186}$ and $Cys_{209}$, the resultant disulfide bond induces a conformational change in TF required for the binding of TF to FVII/FVIIa (55). Additionally, Ahamed et al. (2006) showed that human umbilical vein endothelial cells (HUVECs) overexpressing either $TF^{C186A}$ or $TF^{C209A}$ mutations had dramatically reduced FXa generation in comparison to cells overexpressing wild-type (WT) TF; however this mutant TF retained intracellular signalling function (56). In support of this hypothesis, it was reported that $HgCl_2$-mediated oxidation of the thiol groups of $Cys_{186}$ and $Cys_{209}$ enhanced TF PCA (57). Additionally, protein disulfide isomerase (PDI), an intracellular oxidoreductase found at the cell surface, has been observed to co-immunoprecipitate with TF using anti-TF antibodies, indicating a potential regulatory role of cell surface PDI on TF PCA (57). Further, a separate study demonstrated that purified PDI enhanced the ability of soluble TF to generate FXa. This effect was attenuated with bacitracin, known to inhibit both the oxidoreductase and chaperone function of PDI (58). Further, Versteeg and colleagues showed that inhibition of the oxidoreductase function of PDI using phenyl arsine oxide, glutathione, or dithiothreitol (DTT) failed to attenuate PDI-enhanced TF PCA, indicating that the chaperone function of PDI is required for TF de-encryption (58).

#### *1.1.5.2. TF Dimerization*

Under the TF dimerization model of TF encryption, encrypted TF is believed to arise from homodimer complexes and disassociation into TF monomers is required to induce TF PCA (49). Early chemical cross-linking studies using membrane-impermeable 3,3'-dithiobis(sulfosuccinimidyl propionate) (DTSSP) and sulfosuccinimidyl-2-(p-azidosalicylamido)ethyl-1,3-dithiopropionate (SASD) on intact cells revealed multimeric TF complexes in J82 human bladder carcinoma cells and human kidney cells overexpressing TF (59). Additionally, these multimeric TF complexes were shown to be disrupted with the reducing agent DTT (59). In a separate study, Bach and Moldow (1997) showed that the calcium ionophore ionomycin induced TF PCA in HL-60 human myeloid leukemia cells, an effect that was attenuated with the calmodulin inhibitor calmidazolium (60). The authors also indicated that pre-treatment with ionomycin attenuated DTSSP-induced cross-linking, suggesting that inhibition of TF dimerization by $Ca^{2+}$ ionophores is required for TF de-encryption. Based on these observations, it is thought that the TF dimers can sequester the binding site of FX to inhibit FXa generation (49). However, Doñate et al. (2000) showed that recombinant TF inserted with a leucine zipper dimerization domain was able to form TF homodimers (61). These TF dimer variants were shown to bind FVIIa but did not effectively alter the activation of FXa in comparison to TF monomers.

#### *1.1.5.3. TF Compartmentalization in Lipid Rafts/Caveolae*

Previous reports suggest lipid rafts may also contribute to the regulation of TF encryption/de-encryption (62). Lipids rafts are cholesterol- and sphingolipid-rich regions of the cell membrane which serve as a platform for the compartmentalization of

membrane proteins such as TF (63). Early studies revealed the expression of TF in lipid rafts in human embryonic kidney 293 (HEK293) cells (64). Additionally, methyl-β-cyclodextrin-induced disruption of the lipid rafts was shown to enhance TF PCA (64). Further, it has been suggested that TF has retained lipid rafts in the form of caveolae on the cell membrane (63). TF distribution in caveolae lipid rafts has been reported to varies between cell types, including SMCs (65), fibroblasts (66), and tumour cells (62). Moreover, Sevinsky et al. (1996) demonstrated that the formation of the TF·FVIIa·Xa complex could also induce redistribution of TF into caveolae which were suggested as a form of feedback inhibition (67). In this proposed mechanism, encrypted TF are sequestered in caveolae which lack the necessary conditions for TF PCA and become de-encrypted when TF is released into the non-lipid regions of the membrane (52). In agreement with this notion, disruption of caveolae through freeze-thawing or detergents on SMCs was shown to promote TF PCA activation (68, 69).

#### *1.1.5.4. Endocytosis of TF·FVIIa*

Another proposed mechanism of TF PCA regulation involves the endocytosis of the TF·FVIIa complex (70). Receptor-mediated endocytosis is a process of internalization of membrane proteins through membrane invagination and the formation of clathrin-coated vesicles (71). Iakhiaev et colleagues (1999) demonstrated that the binding of FVIIa to TF induced the internalization and degradation of the TF·FVIIa complex in WI-38 human embryonal lung fibroblasts (70). Although the levels of bound FVIIa depleted over time, it was shown that the cell surface TF expression levels remained unchanged, indicating that TF is recycled back to the cell surface (70). Further, TF pathway inhibitor (TFPI) may contribute to this process as the TFPI·FXa complex, further enhancing the FVIIa-induced

internalization and degradation of the TF·FVIIa complex (70). Consistent with these observations, Hamik et al. (1999) demonstrated that the binding of FVIIa and TFPI downregulated TF expression through the activation of LDL receptor-related protein (LRP)-dependent internalization and degradation of the TF·FVIIa complex. Hence, Iakhiaev et colleagues (1999) suggested two mechanisms of TF·FVIIa complex internalization: i) LRP-independent internalization or ii) LRP-independent internalization depending on the presence of TFPI/FXa (70). In a separate study, cytosolic acidification of BHK-21 hamster kidney cells leads to degradation FVIIa, indicating clathrin-coated vesicles may not be required for the internalization of the TF·FVIIa complex (72).

*1.1.5.5. Altered Phospholipid Asymmetry*

The eukaryotic cell membrane is a phospholipid bilayer with several critical differences in phospholipid compositions between the outer and inner leaflet, often characterized as an asymmetric phospholipid bilayer (73). Although most phospholipids have been observed on both leaflets, the outer leaflet primarily consists of neutral-charged and positively-charged phospholipids such as sphingomyelin and phosphatidylcholine (74, 75). In contrast, the inner leaflet contains anionic lipids such as phosphatidylethanolamine (PE), phosphatidylinositol (PI), and phosphatidylserine (PS) (74, 75). Moreover, the distribution of phospholipids is actively maintained between the two leaflets mediated by membrane-embedded translocases known as scramblases, flippase, and floppase (75). Scramblases are membrane proteins that passively facilitate the movement of phospholipids to both the outer or inner membrane leaflet (75). Flippase proteins transport lipids from the outer leaflet to the inner leaflet in an adenosine triphosphate (ATP)-dependent manner (75). Similarly, floppase is also ATP-dependent but transport

phospholipids from the inner leaflet to the outer leaflet (75). It has been reported that enhancing the concentrations of the anionic phospholipid PS promotes the binding of FVII/FVIIa to TF reconstituted in phospholipid vesicles (76). In addition, previous reports have shown that $Ca^{2+}$ ionophores are known to promote TF PCA (77). The cytosolic influx of $Ca^{2+}$ is also known to inhibit flippase function and activate scramblase, resulting in a net movement of PS towards to outer leaflet (77). In agreement with this notion, a chemical inhibitor of flippase, N-ethylmaleimide, was also shown to enhance FXa generation in fibroblast monolayers (78). Additionally, studies have demonstrated that PS can be replaced with other anionic phospholipids, including PE, which was shown to increase the sensitivity of TF to PS and enhance FXa generation (79). In support of this notion, Wolberg et al. (1999) demonstrated that sequestration of PS using annexin V only partially inhibited $Ca^{2+}$ ionophore-stimulated TF PCA, indicating that PS alone is not the sole contributor to TF de-encryption (77).

## *1.2. Endoplasmic Reticulum (ER)*

### *1.2.1. ER Functions*

The ER is a multifaceted organelle that plays critical roles, including protein folding of membrane and secreted proteins, and regulates intracellular $Ca^{2+}$ movement (80). The production of membrane-bound and secreted proteins is initiated on ER membrane-bound ribosomes and the Sec61 translocon complex, where nascent polypeptides start to fold in the ER lumen co-translationally (81, 82). The ER lumen provides a unique oxidative environment which encourages protein folding and the formation of disulfide bonds mediated by PDI (81). Maintaining ER $Ca^{2+}$ levels has also been reported to be important for the protein folding function of ER chaperones calnexin, calreticulin, the 78-kDa glucose-regulated protein (GRP78), and GRP94 (83). Also, post-translational modifications occur before their exit from the ER, including signal sequence cleavage, N-linked glycosylation, disulfide bond formation, and polypeptide oligomerization (80). Properly folded and modified polypeptides leave the ER through coat protein complex II-coated vesicles and are transported to the Golgi apparatus for further modifications (84). In contrast, unfolded or misfolded polypeptides can aggregate and disrupt ER function (84). To prevent protein aggregation and maintain ER homeostasis, ER-resident chaperones assist in protein folding until their correct conformation is achieved (84). Additionally, irreversibly misfolded polypeptides undergo ER-associated degradation (ERAD) and are translocated to the cytosol for degradation by the ubiquitin-proteasome system (84).

### *1.2.2. ER Stress and the Unfolded Protein Response*

ER stress arises from conditions that disrupt ER homeostasis, leading to an accumulation of misfolded proteins, which can overwhelm the capacity for correct protein folding (85). Pharmacological compounds that impair glycosylation, disrupt protein folding, or induce ER $Ca^{2+}$ depletion can also result in ER stress (85). Additionally, conditions such as nutrient deprivation, defects in post-translational modifications, and disruption in the ERAD pathway can elicit an ER stress response (86, 87). To mitigate uncontrolled ER stress, the signalling network known as the unfolded protein response (UPR) is activated following GRP78 dissociation from three established ER stress sensors, including activating transcription factor 6 (ATF6), inositol-requiring enzyme 1 (IRE1), and protein kinase RNA-like endoplasmic reticulum kinase (PERK) resulting in the inhibition of *de novo* protein synthesis, upregulation of protein degradation, and enhanced ER chaperone expression occurs (Figure 4) (85). Following activation, ATF6 localizes to the Golgi body, where it undergoes cleavage by site-1 protease (S1P) and site-2 protease (S2P) (85). Cleaved ATF6 functions as a transcription factor in the nucleus, where it regulates the expression of ERAD components, X-box binding protein 1 (XBP1), and ER chaperones such as GRP78 (85). Splicing of XBP1 mRNA is mediated by activated IRE1α (85). sXBP1 protein is a nuclear transcription factor that regulates the expression of ERAD components and ER chaperone proteins (85). Additionally, sXBP1 promotes ER expansion by upregulating phospholipid synthesis (88). Functionally active PERK phosphorylates eukaryotic translation initiation factor 2α (eIF2α), inhibiting *de novo* protein synthesis (88). In addition, prolonged expression of phosphorylated eIF2α also induces the expression of ATF4, a transcription factor that regulates genes involved in autophagy and resistance to oxidative stress (88). ATF6 also regulates the expression of

C/EBP homologous protein (CHOP), a transcription factor responsible for the expression of proapoptotic factors that drive ER stress-induced apoptosis (88). As a result of unresolved ER stress, chronic UPR activation is known to induce proapoptotic signalling pathways leading to cell death (88).

Our laboratory and others have shown several links exist between ER stress and atherosclerotic lesion development and progression (89–91). In support of this notion, enhanced levels of GRP78, phospho-PERK, and CHOP expression have been observed in early fatty streaks and advanced atherosclerotic lesions of apolipoprotein-deficient (*apoE*$^{-/-}$) mice (92). Further, adenoviral-mediated sXBP1 overexpression reportedly accelerates atherosclerotic lesion development (93). Markers of UPR activation have also been observed in atherosclerotic lesion-resident cells, including macrophage foam cells (94), VSMCs (95), and endothelial cells that overlie lesions (96). Additionally, *apoE*$^{-/-}$ mice given small chemical chaperones 4-phenylbutyrate or tauroursodeoxycholic acid known to protect against ER stress have been shown to protect against atherosclerotic lesion progression (91, 97, 98). Atherosclerotic lesion development have a high tendency to occur in vascular regions that are branched, bifurcated, or with high curvature due to increased exposure to shear stress (99, 100). Endothelial cells exposed to shear stress reportedly have elevated levels of IRE1, GRP78, and sXBP1 expression compared to cells exposed to laminar flow (93, 96). Another link between ER stress and atherosclerosis is homocysteine. Hyperhomocysteinemia is independent risk factor for cardiovascular disease and thrombosis (101). It was reported that treatment with homocysteine promotes protein misfolding and upregulation of GRP78 and CHOP expression in cultured endothelial cells (102).

**Figure 4. The role of GRP78 in the ER.**

GRP78 functions as a protein chaperone in the ER and facilitates nascent polypeptide folding. Under normal physiological conditions, GRP78 can be bound to ATF6, IRE1, and PERK, inhibiting the activation of these transmembrane sensors of ER stress. Under conditions of ER stress, the dissociation of GRP78 from these proteins leads to the activation of the UPR, resulting in the upregulation of ER chaperones and cochaperones, proteins involved ERAD, and attenuation of protein translation. Chronic UPR activation due to unresolved ER stress can also lead to the activation of proapoptotic pathways. The illustration was generated with BioRender.

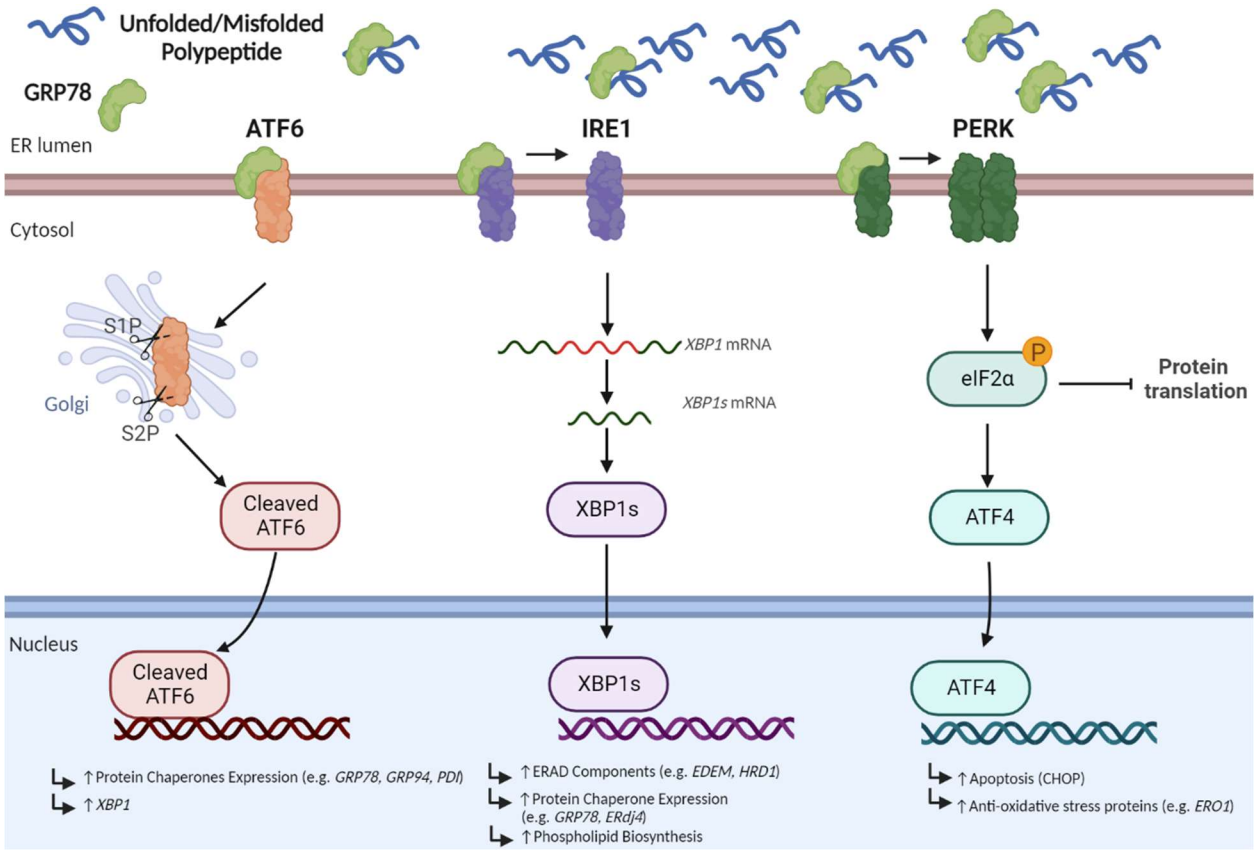
Unfolded/Misfolded Polypeptide
GRP78
ER lumen
ATF6
IRE1
PERK
Cytosol
S1P
Golgi
S2P
XBP1 mRNA
XBP1s mRNA
eIF2α
P
Protein translation
Cleaved ATF6
XBP1s
ATF4
Nucleus
Cleaved ATF6
XBP1s
ATF4
↑ Protein Chaperones Expression (e.g. GRP78, GRP94, PDI)
↑ XBP1
↑ ERAD Components (e.g. EDEM, HRD1)
↑ Protein Chaperone Expression (e.g. GRP78, ERdj4)
↑ Phospholipid Biosynthesis
↑ Apoptosis (CHOP)
↑ Anti-oxidative stress proteins (e.g. ERO1)

### *1.2.3. ER Chaperones*

Although newly translated small proteins have the capacity to spontaneously fold into their proper orientation, larger proteins typically require the assistance of ER-resident molecular chaperones to fold appropriately and efficiently to avoid protein aggregation (80). Additionally, ER chaperones prevent the premature export of misfolded proteins out of the ER as a form of quality control (80). The $Ca^{2+}$-dependent calnexin and calreticulin pathway mediates the folding of glycoproteins (103). Calnexin is an ER-membrane-bound lectin chaperone that binds newly synthesized N-linked glycosylated polypeptides similarly to its soluble homolog calreticulin, which lacks a transmembrane domain (103). Additionally, calnexin/calreticulin also allows for the binding of co-chaperones such as ERp57, which mediates the oxidation of thiol groups to form disulfide bonds (103). Other co-chaperones of calnexin/calreticulin include ERp29, which has chaperone function and cyclophilin B, which mediate protein bond isomerization (103). Subsequently, glucosidase II cleaves the glucose group from the properly folded protein inhibiting the binding of calnexin/calreticulin and transported out of the ER (104). If the protein is partially misfolded, UDP-glucose: glycoprotein glucosyltransferase (UGGT) mediates the addition of a glucose moiety to the polypeptide to allow calnexin/calreticulin to bind and continue protein folding (104).

### *1.2.4. GRP78*

Molecular chaperones assist in protein folding by binding to long hydrophobic patches exposed on nascent/misfolded polypeptides until no exposed hydrophobic patches remain (105). Subsequently, the classical chaperone folding function requires the hydrolysis of ATP to generate adenosine diphosphate (ADP) and inorganic phosphate

($P_i$) (80). In the cytosol, heat shock protein 70 (Hsp70) and Hsp90 proteins are the primary molecular chaperones that maintain the protein folding of cytosolic polypeptides. GRP78, the ER homologue of Hsp70, is one of the most well-described classical ER molecular chaperones that stabilize nascent polypeptide folding and facilitate the export of terminally misfolded polypeptides out of the ER (109). GRP78 expression was first characterized as an upregulated 78-kDa protein following the viral infection or glucose deprivation of green monkey fibroblast (CV-1) cells (106). Expression of GRP78 is observed ubiquitously throughout most tissues (25). The importance of GRP78 as an essential protein is highlighted particularly during early embryonic development as homozygous GRP78 knockout (*GRP78*$^{-/-}$) mice were found to be lethal on embryonic day 3.5 (107). Interestingly, aged heterozygous GRP78 (*GRP78*$^{+/-}$) mice with approximately half the expression of GRP78 compared to wild-type control mice, have been reported to have similar body weight and organ morphology (108).

The human GRP78 amino acid sequence is evolutionarily conserved with its yeast homolog KAR2 (109, 110). Human GRP78 also shares approximately 98-99% amino acid sequence homology with its homolog found in mice and rats (Figure 5) (111). Full-length GRP78 is a soluble protein chaperone which consists of 654 amino acids which encode for an N-terminal ER signalling sequence, an ATPase domain, a substrate-binding domain, and a C-terminal lysine, aspartic acid, glutamic acid, and leucine (KDEL) ER retention sequence KDEL retention motif (112).

**Figure 5. Schematic of GRP78.**

The schematic diagrams of human GRP78, mouse GRP78, and the yeast homolog KAR2 from *Saccharomyces cerevisiae*. The structure of GRP78 is highly conserved between species each containing an ER signalling sequence (not shown), ATPase domain (yellow), substrate-binding domain (orange), and KDEL sequence (blue).

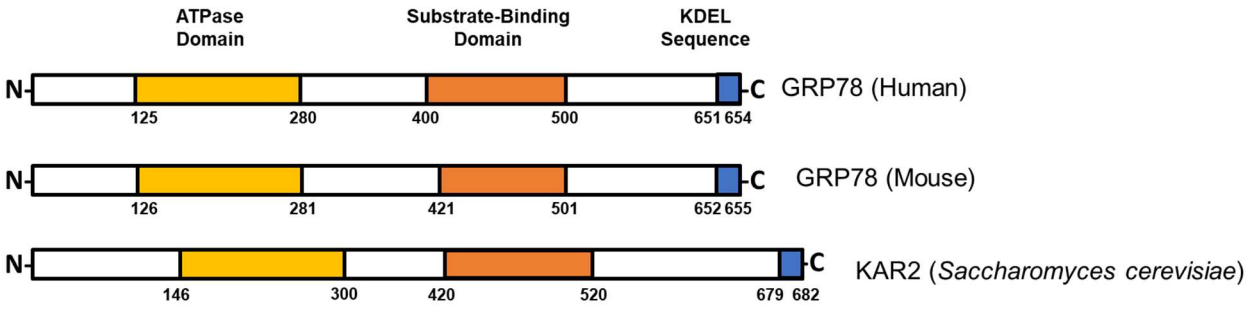
ATPase Domain
Substrate-Binding Domain
KDEL Sequence
N-
-C
GRP78 (Human)
125
280
400
500
651 654
N-
-C
GRP78 (Mouse)
126
281
421
501
652 655
N-
-C
KAR2 (Saccharomyces cerevisiae)
146
300
420
520
679 682

*1.2.5. Cell Surface GRP78*

Under certain conditions, GRP78 has been observed in several other cellular structures, including the nucleus (113) and mitochondria (114). GRP78 has also been reported on the cell surface at low levels, which can be further exacerbated under conditions of ER stress (115, 116). Moreover, cell surface GRP78 was first described as a transmembrane protein based on early transmembrane domain prediction analysis and fluorescence-activated cell sorting (FACS) analysis. However, recent biochemical studies examining the translocation of GRP78 revealed cell surface GRP78 as a non-transmembrane peripheral protein (117). The mechanisms that regulate cell surface localization of ER-resident chaperones are yet to be fully elucidated and are under current investigation (117, 118). Notably, GRP78 and other proteins that possess a lysine-aspartate-glutamate-leucine (KDEL) sequence have been observed at the cell surface (117). Under physiological conditions, KDEL-containing proteins are retained in the ER through interactions with the KDEL receptor (119). Early work on cell surface GRP78 suggested that overexpression of KDEL-containing proteins can overwhelm of the KDEL receptor due and allow GRP78 and other KDEL-containing proteins to escape the ER and localize to the cell surface (116). In agreement with this notion, ectopic overexpression of GRP78 was shown to enhance cell surface GRP78 levels in the absence of the UPR. Additionally, ER stress was recently shown to disrupt retrograde Golgi trafficking by activating proto-oncogene tyrosine-protein kinase (SRC)-mediated dispersion of the KDEL receptors (120). Interactions between GRP78 and transmembrane and secreted proteins such as $G_{\alpha}$-interacting vesicle-associated protein (121), an isoform of CD44 (122, 123), and Par-4 (124) have recently been described to

be involved in the translocation of GRP78 to the cell surface. Further, co-chaperones may also contribute the localization of GRP78 to the cell surface as knockdown of DnaJ-like protein 1 (MTJ-1/HTJ-1) has reported to reduce cell surface GRP78 levels (125).

Enhanced cell surface GRP78 expression is also associated with pathologies including cancer (126–128), rheumatoid arthritis (129), and more recently, atherosclerosis (130–132). Further, cell surface GRP78 was initially characterized as a co-receptor for activated $\alpha_2$-macroglobulin ($\alpha_2$M) that binds the N-terminal domain of cell surface GRP78 ($Leu_{98}$-$Leu_{115}$) (133). At the cell surface, GRP78 functions as a signalling receptor known to interact with several binding partners such as T-cadherin (134), Cripto (135), Kringle 5 (136), and Par-4 (124). Mintz and colleagues (2003) were first to identified cell surface GRP78 as an autoantigen that leads to the production of a pool of anti-GRP78 autoantibodies in patients with cancer (137). Of these anti-GRP78 autoantibodies, an anti-GRP78 autoantibody that recognizes the tertiary epitope within the N-terminal domain of GRP78 ($Leu_{98}$-$Leu_{115}$) is associated with disease progression and poorer prognosis in patients with prostate cancer (138). Our laboratory has previously shown that the binding of these anti-GRP78 autoantibodies to cell surface GRP78 promoted DU145-xenograft tumour growth mediate by TF in NOD/SCID mice (139). Additionally, engagement of the anti-GRP78 autoantibody to cell surface GRP78 was shown to elevate cytosolic $Ca^{2+}$ levels, enhancing TF PCA in T24/83 bladder carcinoma cells (139).

In 2003, Liu and collaborators identified the expression of cell surface GRP78 in atherosclerotic lesion-resident endothelial cells in both *apoE*$^{-/-}$ mice and human lesions (131). Similarly, Crane et al. (2018) also identified the presence of cell surface GRP78 in atherosclerotic lesion-resident endothelial cells and elevated titres of anti-GRP78

autoantibodies associated with lesion progression (130). Additionally, elevated levels of the anti-GRP78 autoantibodies were also observed in patients with established cardiovascular disease (130). Further, the engagement of anti-GRP78 autoantibodies to cell surface GRP78 was shown to activate NF-κB and enhance adhesion molecule expression in cultured endothelial cells (130). In agreement with these findings, *apoE*$^{-/-}$ mice injected with the anti-GRP78 autoantibodies had accelerated lesion progression, compared to IgG-treated control mice (130). In terms of a specific mechanism, binding of the anti-GRP78 autoantibodies to cell surface GRP78 led to activation and nuclear localization of NF-κB, increased expression of VCAM-1 and ICAM-1, thereby enhancing lesion growth (130).

# 2. Rationale, Hypothesis, and Objectives of Study

## *2.1. Rationale*

Although the role of cell surface GRP78 and the anti-GRP78 autoantibody has been studied in early lesion development, the roles of cell surface GRP78 and anti-GRP78 autoantibodies in TF PCA in the context of atherothrombosis have yet to be elucidated. It was previously reported that inhibition of cell surface GRP78 with a commercially available antibody activated TF PCA in murine brain-derived endothelial cells (bEND3.1) (140). Although the mechanism remained unclear, it was suggested cell surface GRP78 might regulate TF PCA. Our laboratory has demonstrated that engagement of the anti-GRP78 autoantibody to cell surface GRP78 also activated TF PCA in T24/83 bladder carcinoma in an intracellular $Ca^{2+}$-dependent manner (139). To further these studies, we recently collaborated with Atomwise Inc. to identify small molecules predicted to bind to GRP78 (referred to as GRP78 binders) that may disrupt the ability of the anti-GRP78 autoantibody to interact with cell surface GRP78. Given that lesion-resident endothelial cells can express both cell surface GRP78 (130) and TF (141), activation of cell surface GRP78 by the anti-GRP78 autoantibody on endothelial cells may have a potential role in the enhanced thrombogenicity following plaque rupture. However, whether the binding of the anti-GRP78 autoantibody to cell surface GRP78 affects TF PCA in endothelial cells is unknown and is the basis of my hypothesis and objectives.

## *2.2. Hypothesis*

The binding of the anti-GRP78 autoantibody to cell surface GRP78 promotes TF PCA in endothelial cells.

## *2.3. Objectives*

### *2.3.1. Overall Objectives*

The overall objective is to identify whether engagement of the anti-GRP78 autoantibody to cell surface GRP78 on endothelial cells regulates TF PCA and characterize the underlying mechanisms that impact TF PCA (Figure 6).

*2.3.2. Specific Objectives*

i. Investigating whether the interaction between cell surface GRP78 and the anti-GRP78 autoantibody promotes TF PCA in cultured human aortic endothelial cells.
ii. Determining the effect of cell surface GRP78 activation by the anti-GRP78 autoantibody on intracellular $Ca^{2+}$ levels.
iii. Identifying GRP78 binders that can bind cell surface GRP78 and block the anti-GRP78 autoantibody effect on TF PCA.

**Figure 6. A schematic representing the predicted cellular events following the engagement of the anti-GRP78 autoantibody and cell surface GRP78.**

Although GRP78 primarily resides in the ER, it can localize to the cell surface under certain conditions where it functions as a receptor. The binding of the anti-GRP78 autoantibody to residues $Leu_{98}$-$Leu_{115}$ has been previously shown to promote inositol 1,4,5-trisphosphate ($IP_3$) generation and activate $IP_3$-sensitive calcium channels on the ER membrane (139). Elevated cytoplasmic $Ca^{2+}$ can lead to disruption in cell membrane asymmetry, leading to TF PCA (77). Further, enhanced cytoplasmic $Ca^{2+}$ can also activate the canonical NF-κB pathway and promote TF PCA. Together, these intracellular events may lead to the de-encryption of TF and the subsequent generation of thrombin.

Objective ①: Investigating whether the interaction between cell surface GRP78 and the anti-GRP78 autoantibody promotes TF PCA in cultured human aortic endothelial cells.

Objective ②: Determining the effect of cell surface GRP78 activation by the anti-GRP78 autoantibody on intracellular $Ca^{2+}$ levels.

Objective ③: Identifying GRP78 binders that can bind cell surface GRP78 and block the anti-GRP78 autoantibody effect on TF PCA.

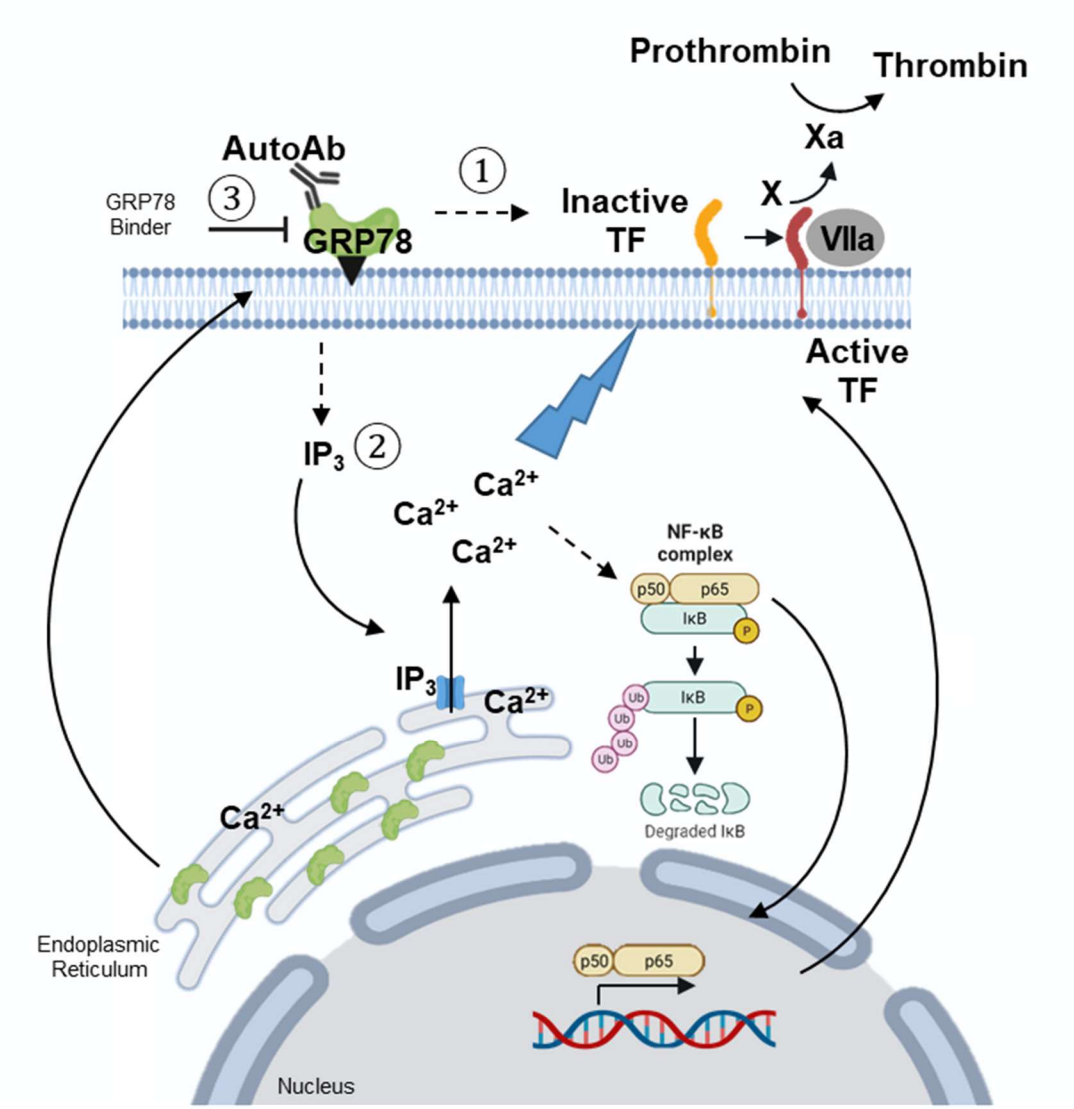
Prothrombin
Thrombin
Xa
X
VIIa
AutoAb
GRP78 Binder
3
GRP78
1
Inactive TF
Active TF
IP3
2
Ca2+
Ca2+
Ca2+
NF-κB complex
p50
p65
IκB
P
IP3
Ca2+
Ub
Degraded IκB
Ca2+
Endoplasmic Reticulum
Nucleus

# 3. Experimental Procedures

## *3.1. Cell Line and Culture Conditions*

Immortalized human aortic endothelial cells (teloHAEC) were obtained from the American Type Culture Collection (ATCC, CRL-4052) grown in endothelial cell basal medium (EGM-2; Lonza) supplemented with 2% fetal bovine serum (FBS), growth factors (EGM-2 Bullet Kit; Lonza), L-glutamine (2 mM), penicillin (100 µg/mL), and streptomycin (100 µg/mL) (Gibco, Thermo Fisher Scientific). Cells were cultured in a humidified incubator at 37°C with 5% $CO_2$.

## *3.2. Cell Treatments*

Recombinant human TNFα was purchased from R&D Systems and was used at 5 ng/mL unless otherwise stated. TPCA-1 (1 µM), an NF-κB pathway inhibitor through selective inhibition of IKK, was obtained from Caymen Chemical (142). ER stress inducers, thapsigargin (TG), a sarco/endoplasmic reticulum $Ca^{2+}$-ATPase (SERCA) pump inhibitor and tunicamycin (TM), a *N*-glycosylation inhibitor, were purchased from Caymen Chemical and were used at 1 µM and 2 µg/mL, respectively. Human IgG isolated from serum was purchased from Millipore-Sigma. Anti-green fluorescent protein (anti-GFP) antibody and anti-TF were used at a final concentration of 10 µg/mL and were obtained from Cell Signalling and Affinity Biologics, respectively. Enoxaparin (Lovenox®; Sanofi) and unfractionated heparin (Fresenius Kabi Canada) were used at a final concentration of 50 µg/mL and 50 U/mL, respectively.

## 3.3. *Identification of GRP78 binders (Atomwise Inc., San Francisco, CA*)

In collaboration with Atomwise Inc., over 3 million commercially compounds were virtually screened against human GRP78 using AtomNet™, a deep convolutional neural network for structure-based drug design(143). 86 small molecules were identified with

predicted affinity high affinity (predicted $K_D \leq 1$ μM) for the anti-GRP78 autoantibody binding site ($Leu_{98}$-$Leu_{115}$ of GRP78) and are referred to as "GRP78 binders". Additionally, 81 out of the 86 compounds were provided to us by Atomwise Inc. Each compound was denoted as A01* - G09* and used at a final concentration of 10 μM unless otherwise stated. According to Atomwise, D05* and E08* were known to be DMSO negative controls.

### *3.4. Anti-GRP78 Autoantibody Isolations*

Anti-GRP78 autoantibodies targeting the $Leu_{98}$-$Leu_{115}$ region of GRP78 were isolated from the blood of prostate cancer patients, as previously described (139). Informed consent was obtained from clinically diagnosed prostate cancer patients and approved by the Research Ethics Board of St. Joseph's Healthcare Hamilton (REB# 08-3047). Briefly, the anti-GRP78 autoantibodies were purified using the conformational peptide, CNVSDKSC (CanPeptide Inc.), that mimics the tertiary structure of the $Leu_{98}$-$Leu_{115}$ region of GRP78 (137) using SulfoLink® Immobilization Kit for Proteins (Thermo Fisher Scientific) as per manufacturer's instructions and dialyzed in phosphate-buffered saline (PBS).

### *3.5. Measurement of TF PCA*

Cell surface TF PCA defined as the amount of FXa generated was measured in intact cells continuously as previously described (144). Briefly, the chromogenic reporter substrate S-2765 (Chromogenix, Diapharma) was used to measure FXa generation indirectly. One day before the experiment, an equivalent number of cells were seeded into 96-well plates ($1\times10^4$ cells/well). Cells were subsequently pre-treated with treatments as indicated. The cells were washed in 1X Tris-buffered saline (TBS) before analysis. A

cocktail containing 1 nM of FVIIa (Enzyme Research Laboratories), 30 nM of FX (Enzyme Research Laboratories), 10 mM $CaCl_2$ (Millipore-Sigma) and 0.4 nM of S-2765 in TBS was added to each well. Either human IgG (Millipore-Sigma) or the anti-GRP78 autoantibody was diluted in 1X TBS, and a 10 µL addition was added given dose to the respective wells. The absorbance at 405 nm was measured kinetically every 2 minutes for 3 hours at 37°C. A standard curve was generated where 100 units of TF PCA were defined as the amount of activity in 1.5 µL of purified human TF equivalent to 450 µg of TF (as determined by the American Diagnostica ELISA). $V_{max}$ was calculated with SoftMax Pro and used to determine the amount of FXa generated per $1\times10^4$ cells. All assays were performed in triplicate, and data was expressed as fold change relative to the TNFα-treated group to correct the plate-to-plate variation.

### *3.6. Fura-2 AM $Ca^{2+}$ Assay*

Intracellular $Ca^{2+}$ levels were indirectly measured using the Fura-2 $Ca^{2+}$ Flux Assay Kit (Abcam) as per the manufacturer's instructions. Briefly, teloHAECs were grown to 80% confluency in black clear bottom 96-well plates. Cells were incubated with 100 µL of Fura-2 AM in 1X Pluronic F127 Plus for 1 hour at 37°C. Plates were read at 37 °C kinetically at two wavelengths (λ), $\lambda_1$ (340 nm excitation, 515 nm emission), and $\lambda_2$ (380 nm excitation, 515 nm emission), where $\lambda_1/\lambda_2$ corresponds to the ratio of Fura-2 AM dye bound to $Ca^{2+}$ over the unbound dye. Baseline measurements for each well were continuously obtained for 5 minutes and measured for an additional 20 minutes following the addition of Hank's balanced salt solution (HBSS), TG (1 µM), TM (2 µg/mL), human IgG (60 µg/mL), or the anti-GRP78 autoantibody (60 µg/mL). The area under the curve

(AUC) was determined using Graphpad Prism (version 6.01, Graphpad Software, La Jolla, CA).

### *3.7. Immunofluorescent Staining*

#### *3.7.1. Immunofluorescent Staining of Intracellular Proteins*

TeloHAECs were grown on Lab-Tek®II Chamber Slides (Thermo Fisher Scientific) until 50% confluency and cultured for 24 hours. Following treatment, cells were washed twice with 1X PBS, fixed in 4% paraformaldehyde (PFA), and permeabilized in 0.1% Triton X-100 in 1X PBS. Subsequently, cells were washed in 1X PBS and incubated in 5% bovine serum albumin (BSA; Millipore-Sigma) in 1X PBS for 1 hour. Subsequently, cells were incubated with anti-NF-κB p65 (1:200, Cell Signalling Technology; catalogue no. 8242S), or anti-β-actin (1:500, Millipore-Sigma; catalogue no. A5441) in 5% BSA in 1X PBS for 1 hour at room temperature. The cells were washed in 1X PBS and incubated with a Cy™5 AffiniPure donkey anti-rabbit IgG (1:200, Jackson ImmunoResearch Laboratory; catalogue no. 711-175-152), or appropriate Alexa Fluor® conjugated (1:200, Thermo Fisher Scientific) secondary antibody for 45 minutes at room temperature. Following incubation, cells were washed in 1X PBS three times and counterstained with DAPI (Millipore-Sigma). Cells were subsequently mounted and images were captured using EVOS FL Cell Imaging System (Thermo Fisher Scientific).

#### *3.7.2. Immunofluorescent Staining of Cell Surface Proteins*

TeloHAECs were grown on Lab-Tek®II Chamber Slides (Thermo Fisher Scientific) until 50% confluency and cultured for 24 hours. Following treatment, cells were washed with ice-cold PBS and incubated with anti-GRP78 antibody (1:200, Affinity Biologicals; lot no. AP3927), or anti-β-actin antibody (1:500, Millipore-Sigma; catalogue no. A5441) in

5% BSA in 1X PBS for 30 minutes at 4 °C. Following incubation, cells were washed twice with 1X PBS, fixed in 4% PFA, and incubated in 5% BSA (Millipore-Sigma) in 1X PBS for 1 hour. Further, cells were incubated with appropriate Alexa Fluor® conjugated secondary antibody (1:200, Thermo Fisher Scientific) or DyLight™594 donkey anti-sheep IgG conjugate (1:200, NovusBio, catalogue no. NBP1-72745DL594) secondary antibody for 45 minutes at room temperature. Cells were subsequently washed in 1X PBS and incubated with wheat germ agglutinin (WGA) (5 µg/mL, Biotium; catalogue no. 29022) for 10 minutes at room temperature. Following incubation, cells were washed in 1X PBS three times and counterstained with DAPI (Millipore-Sigma). Cells were subsequently mounted, and images were captured using EVOS FL Cell Imaging System (Thermo Fisher Scientific). Fluorescence intensity was determined using ImageJ.

### *3.8. Production and Purification of Recombinant Human GRP78*

Recombinant human GRP78 (rhGRP78) was produced and purified as previously described (139). Briefly, Rosetta DE3 cells previously transformed with a GRP78-pET-28b bacterial expression construct by Dr. Elizabeth Crane were grown in LB media in a 37°C bacterial incubator overnight. Subsequently, rhGRP78 expression was induced with isopropyl β-d-1-thiogalactopyranoside (IPTG; 500 µM) for 5 hours. Following incubation, GRP78 protein was purified using HisPur Ni-NTA Spin Columns (Thermo Fisher Scientific) as per the manufacturer's instructions. The purity of rhGRP78 was determined using SDS-PAGE and Coomassie Brillant Blue R-250 dye. Elutions containing a single band of at ~78 kDa range were subsequently dialyzed in Tris-HCl (20 mM Tris, 150 mM NaCl, 10% glycerol, pH 7.4). Functionally active rhGRP78 was determined by ATPase activity.

### *3.9. ATPase Activity Measurements*

ATPase assays were performed using ATPase/GTPase Activity Assay Kit (Millipore Sigma) as per the manufacturer's instruction. To examine ATPase activity of purified rhGRP78, rhGRP78 (0.5-1 µg) was incubated with assay buffer and ATP (Caymen Chemical, 1 mM) for 15 minutes at room temperature. Following incubation, a malachite green assay reagent was added to terminate the enzyme reaction, and absorbance was measured at 620 nm using the SpectraMax Plus384 plate reader. Phosphate concentration was determined using the phosphate standard provide by the manufacturer. Enzyme activity was calculated as per the manufacturer's instructions. To examine the ATPase activity of rhGRP78 in the presence of a small molecule, 0.5 ug of rhGRP78 with or without either a GRP78 binder (10 µM) or DMSO diluted with assay buffer and incubated for 15 minutes a room temperature before the addition of ATP (1 mM). Following incubation, a malachite green assay reagent was added to terminate the enzyme reaction, and absorbance as previously described.

### *3.10. Immunoblotting*

Total cell lysates were collected in 4X SDS lysis buffer containing a protease inhibitor cocktail (Roche) and were measured for protein concentration using DC Protein Assay (BioRad). Samples were separated on a 10% SDS-PAGE and transferred to a nitrocellulose membrane. Nitrocellulose membranes were subsequently incubated with 5% skim milk and with primary antibodies: anti-GRP78 (1:2000, Affinity Biologicals; catalogue no. AP3927) or anti-GRP94 (1:1000, Enzo Life Sciences; catalogue no. 9G10) rocking overnight at 4°C. Following incubation, membranes were washed three times in 1X TBS-Tween-20 and incubated with respective secondary antibodies conjugated to horseradish peroxidase (HRP). Membranes were washed three times in 1X TBS-Tween-

20 The signal was detected using Western Lightning® ECL Pro (PerkinElmer) chemiluminescent reagent, and blots were imaged using Chemidoc XRS+ System (Bio-Rad). Blots were probed using anti-β-actin (1:2000, Millipore-Sigma; catalogue no. A5441) antibody was used as a loading control.

### *3.11. Enzyme-linked Immunosorbent Assay (ELISA)*

Binding of anti-GRP78 autoantibodies were assessed using an ELISA originally described by Gonzalez-Gonrow et al. (138) and modified to examine binding of small molecules. Briefly, 96-well plates were coated with the CNVSKDSC peptide conjugated to KLH (3 µg/mL) (KLH-CNVSKDSC) or rhGRP78 (3 µg/mL) in coating buffer (0.1 M $NaHCO_3$, 0.5 M NaCl, pH 9.6). Plates were washed in PBS-T and blocked with 3% BSA in coating buffer and subsequently incubated with or without a GRP78 binder at indicated concentrations in 3% BSA overnight, followed by incubation with anti-GRP78 autoantibody (60 µg/mL) for 1 hour. Plates were washed and subsequently incubated with anti-human IgG conjugated to HRP and developed by adding an 3,3',5,5'-tetramethylbenzidine substrate (100 ng/mL; Millipore-Sigma) to the plate for 5 minutes, after which the reaction was stopped with 500 mM $H_2SO_4$. Absorbance was measured at 450 nm and expressed relative to secondary only control to adjust for plate-to-plate variation. All assays were performed in triplicate.

### *3.12. Statistical Analysis*

Graphpad Prism (version 6.01, Graphpad Software, La Jolla, CA) was used to analyze quantitative data. Statistical analysis between two treatment groups was analyzed using a two-tailed, unpaired Student's *t*-test, whereas comparisons between multiple groups were determined using analysis of variances (ANOVA), and a Tukey's post hoc test was

used if significant differences were identified during ANOVA. A $p < 0.05$ was considered statistically significant. All error bars represent the standard deviation of the mean.

# 4. Results

## *4.1. TNFα Contributes to TF PCA Through NF-κB in Endothelial Cells*

Under normal physiological conditions, endothelial cells express negligible levels of TF (145). However, it is reported that endothelial cells exposed to known activators of the NF-κB pathway, including TNFα, can stimulate TF expression and promote TF PCA *in vitro* (146). To investigate the effects of the anti-GRP78 autoantibodies on TF PCA in endothelial cells, we sought to generate an *in vitro* model to measure TF PCA in teloHAECs. To determine whether TF PCA could be measured in cultured endothelial cells, teloHAECs were treated with several concentrations of TNFα (0-10 ng/mL) using a previously established continuous TF PCA assay (144). As shown in Figure 7A, TNFα induces TF PCA in a dose-dependent manner compared to the PBS-treated control cells. Further, pre-treatment with the NF-κB inhibitor TPCA-1 (1 μM) protected teloHAECs against TNFα-induced TF PCA (Figure 7A). Additionally, TPCA-1 dose-dependently reduced the effect of TNFα (5 ng/mL) on TF PCA in teloHAECs (Figure 7B). Next, we characterized the impact of TNFα on TF PCA in cultured endothelial cells by individually removing components of TF assay reaction mixture including FVIIa, FX, S-2765, and $CaCl_2$ and examined TF PCA in untreated teloHAECs or cells pretreated with TNFα (5 ng/mL) or TNFα (5 ng/mL) and TG (1 μM). TG is a known activator of TF PCA in cells and was used as a positive control (144). In agreement with previous observations (144), each reagent is required to detect the active chromogenic substrate (Figure 7C). Additionally, immunofluorescent staining of endothelial cells treated with TNFα (5 ng/mL) induced NF-κB p65 nuclear localization at 12 and 24 hours (Figure 8A). However, TNFα-induced nuclear localization of NF-κB p65 was attenuated in teloHAECs pre-treated with TPCA-1 (Figure 8B). Together, these results indicated that TNFα activated NF-κB in teloHAECs

and promoted TF PCA. Accordingly, we selected to use TNFα (5 ng/mL) based on the relatively low activation of the TF PCA to examine the effects of reagents that may alter TF PCA in teloHAECs.

**Figure 7. TNFα promotes TF PCA mediated by NF-κB activation in cultured endothelial cells.**

A) TeloHAECs were incubated without or with TPCA-1 (1 μM) for 1 hour and followed with several concentrations of TNFα (0-10 ng/mL) for 24 hours and assayed for TF PCA. B) TeloHAECs were pre-treated with several concentrations of TPCA-1 (0-1 μM) for 1 hour prior to incubation with TNFα (5 μg/mL) for 24 hours. C) TeloHAECs were pretreated with either TNFα (5 ng/mL) or TNFα (5 ng/mL) and TG (1 μM) as a positive control for 24 hours. Following incubation, cells were washed and assayed for TF PCA in complete assay buffer or buffer that lacked either FVIIa, FX, chromogenic substrate S-2765, or $CaCl_2$. Each bar represents the mean ± standard deviation (n = 3 per group). *, $p < 0.05$ PBS control, one-way ANOVA; #, $p < 0.05$ versus TNFα (0 ng/mL), one-way ANOVA; ^, $p < 0.05$ versus TNFα alone (5 ng/mL), one-way ANOVA.

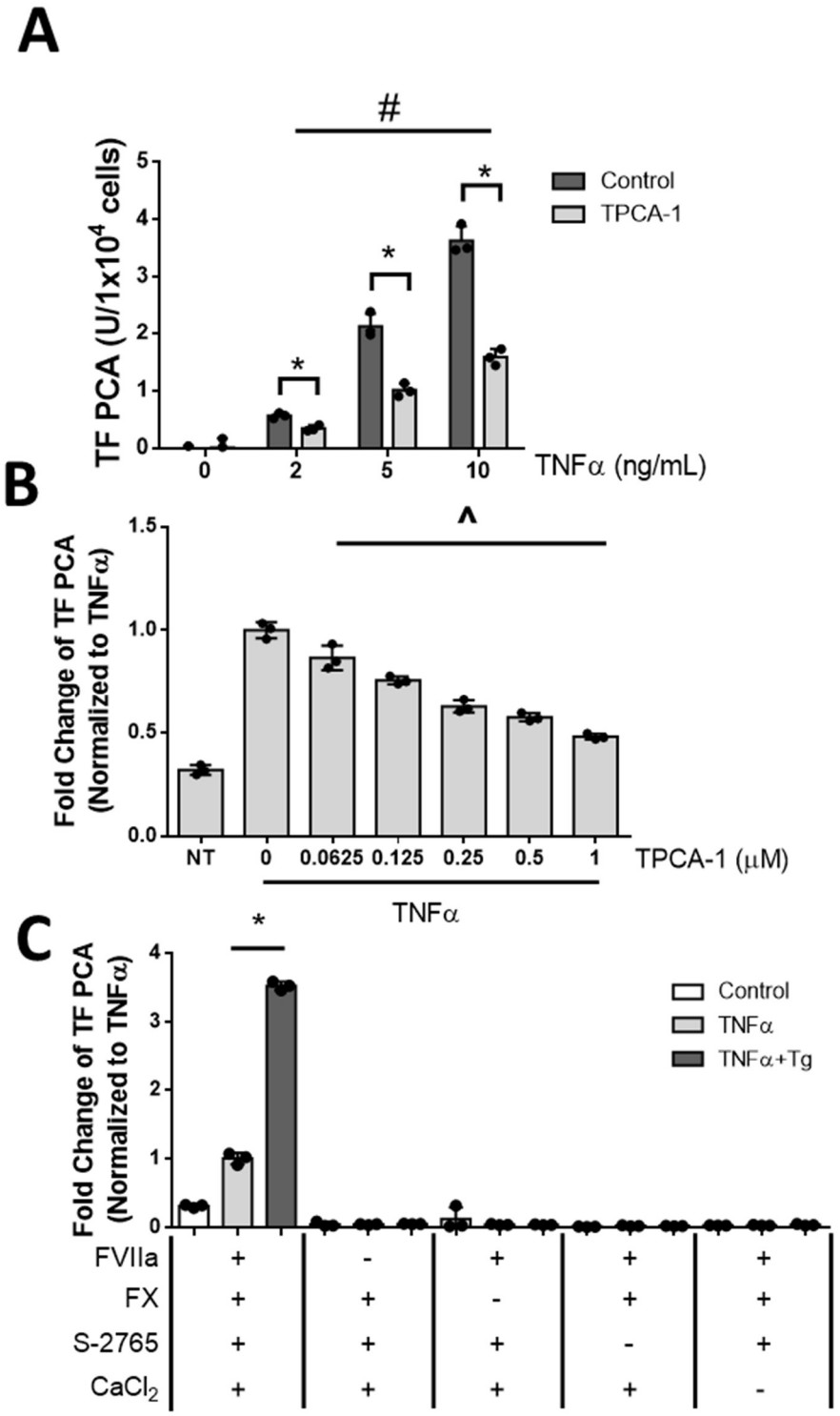
A
#
TF PCA (U/1x10^4 cells)
Control
TPCA-1
*
0
2
5
10
TNFα (ng/mL)
B
Fold Change of TF PCA (Normalized to TNFα)
NT
0
0.0625
0.125
0.25
0.5
1
TPCA-1 (μM)
TNFα
C
Fold Change of TF PCA (Normalized to TNFα)
Control
TNFα
TNFα+Tg
FVIIa
FX
S-2765
CaCl2

**Figure 8. TNFα promotes NF-κB nuclear localization in cultured endothelial cells.** Immunofluorescent staining of A) teloHAECs treated without or with TNFα (5 ng/mL) for 12 and 24 hours; B) TeloHAECs were pre-treated with either DMSO or TPCA-1 (1 μM) for 1 hour before treatment with TNFα (5 ng/mL) for 24 hours. Following incubation, cells were fixed and stained for NF-κB p65 subunit (red) and DAPI (green) and visualized using immunofluorescence imaging. Representative images of immunofluorescent staining of NF-κB p65 subunit localization and DAPI are presented. Original magnification, 20x.

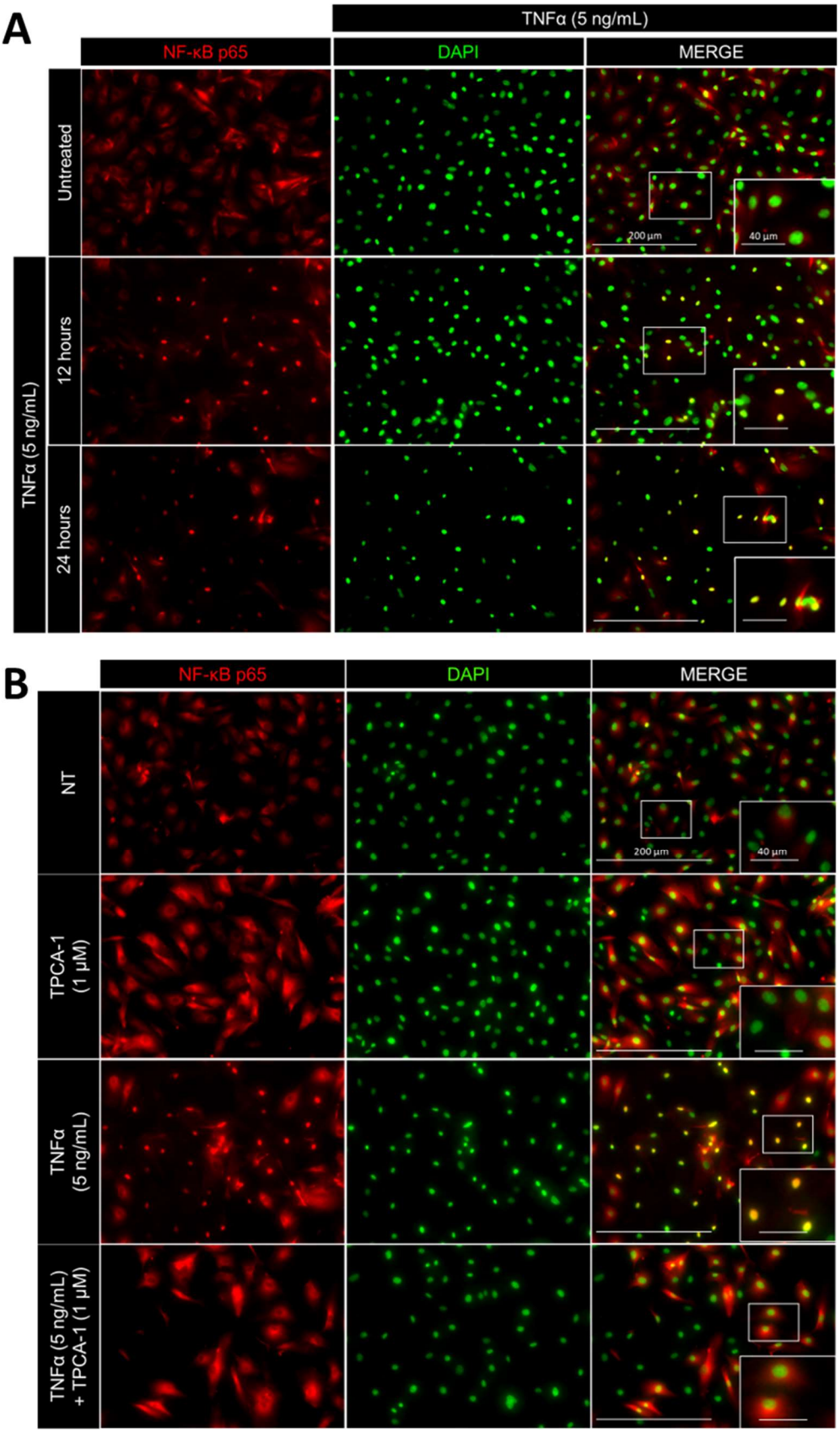
A
TNFα (5 ng/mL)
NF-κB p65
DAPI
MERGE
Untreated
TNFα (5 ng/mL)
12 hours
24 hours
200 µm
40 µm
B
NF-κB p65
DAPI
MERGE
NT
TPCA-1 (1 µM)
TNFα (5 ng/mL)
TNFα (5 ng/mL) + TPCA-1 (1 µM)
200 µm
40 µm

### *4.2. Recombinant Human GRP78 Does Not Alter TNFα-induced TF PCA*

Bhattacharjee et al. (2005) first reported that cell surface GRP78 could modulate TF PCA through a direct interaction in bEND3.1 cells (140). However, our laboratory has previously shown that 1) recombinant TF does not bind to immobilized rhGRP78 and 2) the addition of exogenous rhGRP78 does not modulate TF PCA in T24/83 bladder carcinoma cells (139). To examine whether exogenous GRP78 modulates TNFα-induced TF PCA, rhGRP78 was generated and purified from bacteria that express rhGRP78 following treatment with IPTG. The purity of the rhGRP78 isolation was determined using Coomassie blue staining of lysates obtained throughout the purification process (Figure 9A). To determine whether the bands at approximately 78 kDa correspond to GRP78, a separate gel containing each lysate was subject to immunoblotting for GRP78 expression. As shown in Figure 8B, rhGRP78 is present in the induced fraction, total fraction, elution 1, and elution 2 fractions. Additionally, the purified rhGRP78 has greater ATPase activity than BSA, indicating that the rhGRP78 is functionally active (Figure 9C). To determine whether exogenously added rhGRP78 altered TNFα-induced TF PCA, teloHAECs were pre-treated with TNFα (5 ng/mL) for 24 hours and subsequently treated with several concentration of rhGRP78 (0-50 μg/mL). As shown in Figure 9D, treatment with exogenous rhGRP78 does not appear to modulate TNFα-induced TF PCA in teloHAECs.

**Figure 9. rhGRP78 does not activate TF PCA in TNFα-treated teloHAECs**

A) Representative image of a Coomassie-stained SDS-polyacrylamide gel of fractions collected throughout the purification process of recombinant human GRP78. Bacterial cell lysates were collected using 4X SDS-PAGE lysis buffer before (lane 2) and after (lane 3) the addition of IPTG. Total soluble cell lysate (lane 4) was subsequently incubated in a His-Pur™ Ni-NTA affinity purification column and allowed to flow through (lane 5). The column was washed 3 times (lane 6-8), and eluted (lane 9-11) using an increasing gradient of imidazole. B) Immunoblot of identical samples were ran on a separate gel, transferred to a nitrocellulose membrane, and probed with an anti-GRP78 antibody. C) Functional activity of purified rhGRP78 was confirmed by measuring ATPase activity. BSA was used as a negative control. D) TNFα-treated teloHAECs were exposed to increasing concentrations of rhGRP78 (0-50 μg/mL) and assayed for TF PCA. Each bar represents the mean ± standard deviation. *, $p < 0.05$ versus BSA control, 2-tailed t-test.

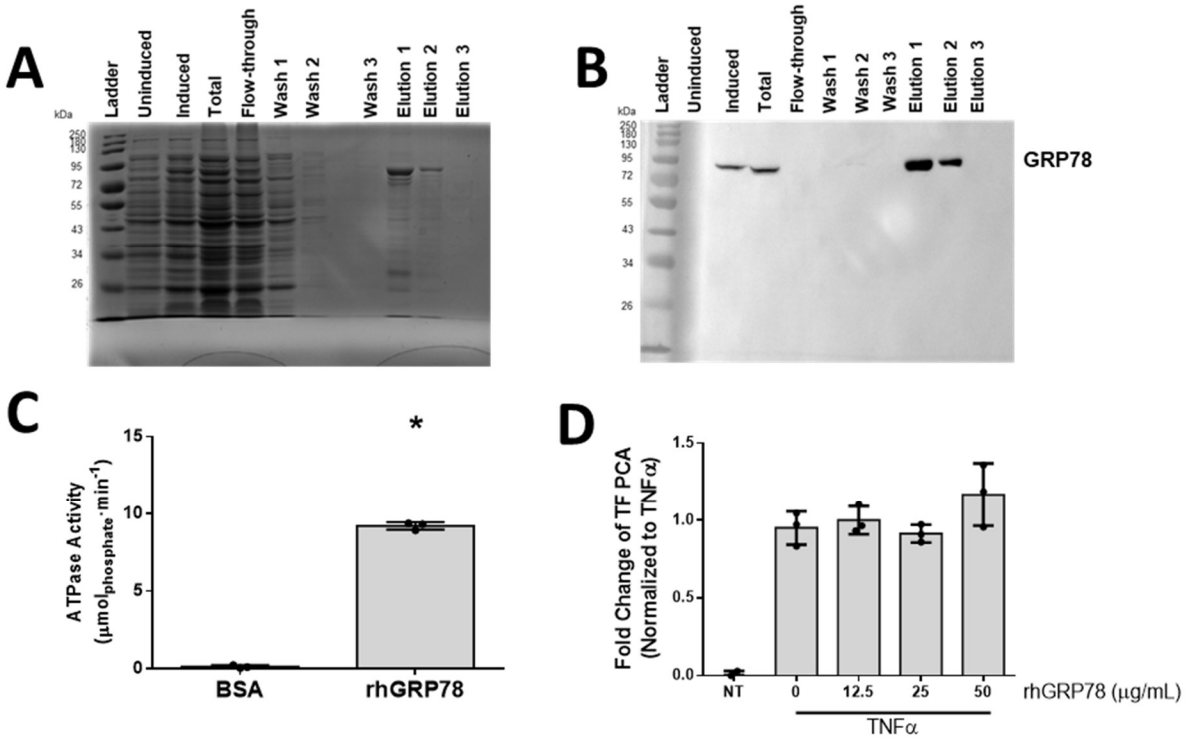
A
Ladder
Uninduced
Induced
Total
Flow-through
Wash 1
Wash 2
Wash 3
Elution 1
Elution 2
Elution 3
kDa
250
180
130
95
72
55
43
34
26
B
GRP78
C
ATPase Activity
(μmol phosphate · min-1)
15
10
5
0
*
BSA
rhGRP78
D
Fold Change of TF PCA
(Normalized to TNFα)
1.5
1.0
0.5
0.0
NT
0
12.5
25
50
rhGRP78 (μg/mL)
TNFα

### *4.3. Anti-GRP78 Autoantibody Induces TF PCA in teloHAECs*

It was reported that the anti-GRP78 autoantibodies activate TF PCA in cells that express cell surface GRP78, including T24/83 bladder carcinoma cells and DU145 prostate cancer cells (139, 147). Our lab has previously shown that pharmacological inducers of ER stress can also enhance the expression of cell surface GRP78 in cultured HAECs (130). Further, TNFα has been reported to promote UPR activation and enhanced cell surface GRP78 expression (129, 148, 149). Based on these observations, we examined the effects of TNFα on cell surface GRP78 expression in cultured endothelial cells. To examine the expression of cell surface GRP78 levels in teloHAECs, cells were either untreated or treated with TNFα (5 ng/mL) for 24 hours and subjected to immunofluorescent staining of GRP78 in non-permeabilized teloHAECs. TeloHAECs were also co-stained with fluorescently-labelled WGA, a lectin that binds cell surface glycoproteins and used to identify cell surface staining in non-permeabilized cells (150). As shown in Figure 10A, a low but detectable level of GRP78 co-localizes with WGA staining in the untreated teloHAECs, an effect that is further enhanced in endothelial cells treated with TNFα for 24 hours. Additionally, non-permeabilized teloHAECs showed little to no immunofluorescent staining of cytosolic β-actin in contrast to permeabilized cells (Figure 10B). Taken together, our data suggests that treatment with TNFα can enhance cell surface GRP78 levels in cultured teloHAECs.

Next, we examined the impact of the anti-GRP78 autoantibody on TNFα-induced TF PCA in cultured endothelial cells. Although healthy patients have been reported to have low levels of circulating anti-GRP78 autoantibodies, patients with pathological conditions such as cardiovascular disease or prostate cancer have been reported to have elevated

levels of anti-GRP78 autoantibodies (≥ 60 μg/mL) compared to healthy control patients (130, 138, 139). Based on these observations, the anti-GRP78 autoantibody concentration of 60 μg/mL was considered as a pathological concentration of autoantibody used in the current study. To investigate the effects of anti-GRP78 autoantibody on TNFα-induced TF PCA, teloHAECs were either untreated or treated with TNFα (5 ng/mL) for 24 hours and subsequently treated with either human non-specific IgG antibody (60 μg/mL) or the anti-GRP78 autoantibody (60 μg/mL) prior to the TF PCA assay. TeloHAECs treated with the anti-GRP78 autoantibody alone elevated TF PCA compared to untreated control group, an effect that was further enhanced with in cells pretreated with TNFα (Figure 10C). To further explore the effect of the anti-GRP78 autoantibody on TF PCA, teloHAECs were pre-treated with TNFα for 24 hours and subsequently treated with increasing concentrations of anti-GRP78 autoantibody (10-60 μg/mL). Our results show that the anti-GRP78 autoantibodies dose-dependently activated TF PCA in TNFα-treated teloHAECs (Figure 10D). Taken together, the anti-GRP78 autoantibody can promote TF PCA in TNFα-treated teloHAECs.

**Figure 10. The anti-GRP78 autoantibody enhances TF PCA in teloHAECs.**

A) Representative images of immunofluorescent staining of teloHAECs pretreated without or with TNFα (5 ng/mL) for 24 hours. Subsequently, non-permeabilized cells were stained for GRP78 (red), WGA (blue), or DAPI (green) and visualized using immunofluorescence imaging. Fluorescence intensity of GRP78 was quantified and expressed relative to the untreated control. B) Immunofluorescent staining of β-actin (cyan) in either permeabilized or non-permeabilized teloHAECs. Original magnification, 20x. C) TeloHAECs were treated with or without TNFα (5 ng/mL) for 24 hours and subsequently treated with human IgG (60 μg/mL) or anti-GRP78 autoantibodies (AutoAb; 60 μg/mL) prior to TF PCA measurement. D) TeloHAECs were pretreated with TNFα (5 ng/mL) for 24 hours before the addition of several concentrations of anti-GRP78 autoantibodies (0-60 μg/mL) before measurement of TF PCA. Each bar represents the mean ± standard deviation (n = 3 per group). $^{\#}$, $p < 0.05$ versus untreated control group (NT), one-way ANOVA; ^, $p < 0.05$ versus AutoAb alone, one-way ANOVA. *, $p < 0.05$ versus TNFα (0 μg/mL AutoAb), one-way ANOVA.

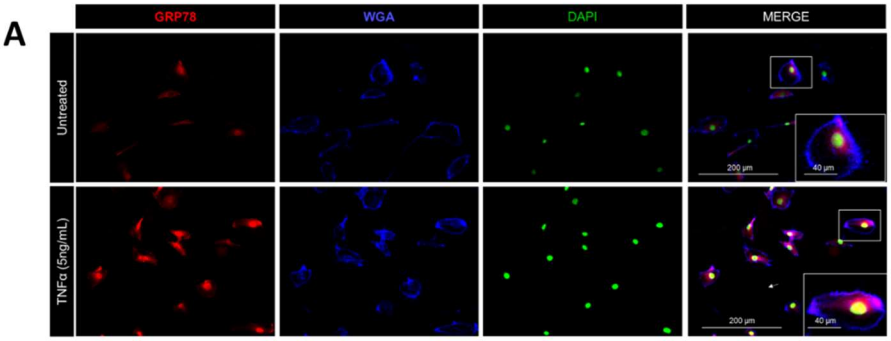
A
GRP78
WGA
DAPI
MERGE
Untreated
TNFα (5ng/mL)
200 µm
40 µm

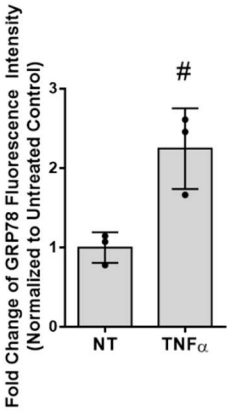
Fold Change of GRP78 Fluorescence Intensity
(Normalized to Untreated Control)
#
NT
TNFα

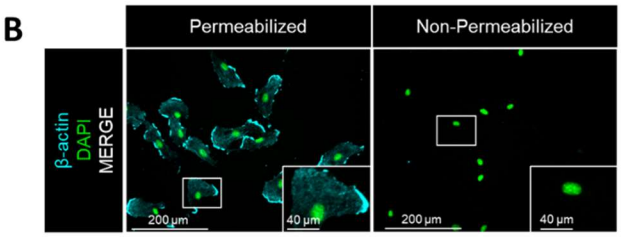
B
Permeabilized
Non-Permeabilized
β-actin
DAPI
MERGE
200 µm
40 µm

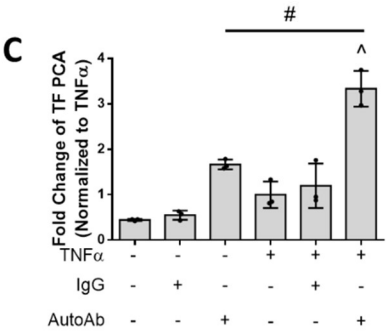
C
Fold Change of TF PCA
(Normalized to TNFα)
#
^
TNFα
IgG
AutoAb

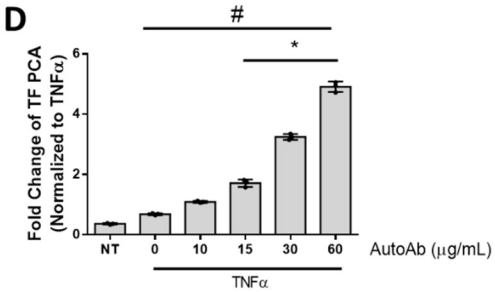
D
Fold Change of TF PCA
(Normalized to TNFα)
#
*
NT
0
10
15
30
60
AutoAb (µg/mL)
TNFα

### *4.4. Thapsigargin and Tunicamycin Enhance Anti-GRP78 Autoantibody Induced TF PCA*

Our previous studies have demonstrated that anti-GRP78 autoantibodies enhance TF PCA in cancer cells which have elevated levels of cell surface GRP78 (139). TG is a well-established SERCA pump inhibitor that results in ER $Ca^{2+}$ depletion and UPR activation (151). Similarly, TM attenuates ER N-glycosylation of *de novo* polypeptides required for maturation of certain proteins, resulting in the ER accumulation of misfolded polypeptides (151). Both TG and TM have both been shown to promote ER stress and activate the UPR, resulting in elevated total and cell surface GRP78 expression (130). Consistent with prior observations, TG (1 μM) or TM (2 μg/mL) treatments elevated total GRP78 and GRP94 protein levels relative to untreated cells (Figure 11A), a hallmark of UPR activation. Next, we investigated the effects of TG and TM on intracellular $Ca^{2+}$ levels on teloHAECs using the Fura-2 AM $Ca^{2+}$ assay. In contrast to TM which did not alter cytoplasmic $Ca^{2+}$ levels, teloHAECs treated with TG robustly enhanced cytosolic $Ca^{2+}$ levels (Figure 11B).

We next examined cell surface GRP78 levels of teloHAECs treated with TG (1 μM), TM (2 μg/mL), TNFα (5 ng/mL), TNFα (5 ng/mL) and TG (1 μM), or TNFα (5 ng/mL) and TM (2 μg/mL). As shown in Figure 11C, immunofluorescent staining of non-permeabilized teloHAECs treated with TG, TM, and TNFα show elevated cell surface GRP78 staining compared to the untreated control. Additionally, TNFα-induced cell surface GRP78 expression were further enhanced when co-treated with TG or TM (Figure 11C). Based on these observations, we investigated the effects of the anti-GRP78 autoantibody on TF PCA in teloHAECs pretreated with TNFα co-treated with or without TG or TM. TeloHAECs pre-treated with TNFα alone or with either TM or TG for 24 hours and subsequently

treated with either human IgG or the anti-GRP78 autoantibody prior to assessing TF PCA. TeloHAECs treated with the anti-GRP78 autoantibody, but not IgG, have elevated TF PCA (Figure 11D). This effect by the anti-GRP78 autoantibody was further enhanced in teloHAECs pre-treated with either TG or TM (Figure 11D). These results indicate that the anti-GRP78 autoantibody can promote TF PCA in TNFα-stimulated endothelial cells, which can be further enhanced following TG or TM treatment.

**Figure 11. Thapsigargin and tunicamycin enhances the anti-GRP78 autoantibody-mediated TF PCA in TNFα-treated teloHAECs.**

A) GRP78 and GRP94 expression was examined teloHAECs treated with either TG (1 μM), TM (2 μg/mL), or untreated using immunoblots. β-actin was used as a loading control. B) Intracellular $Ca^{2+}$ release from the ER was examined in TG (1 μM; blue triangle), TM (2 μg/mL; orange square), or HBSS (grey circle) treated teloHAECs using the high-affinity $Ca^{2+}$ dye, Fura-2 AM. Baseline fluorescence was measured at 340 nm and 380 nm was measured for 5 minutes, where TG, TM, or HBSS was added to the cells immediately after the 5-min time point. AUC was determined following the addition of each reagent. C) Immunofluorescent staining of GRP78 (red) of non-permeabilized teloHAECs. Cells were either untreated or treated with TG (1 μM), TM (2 μg/mL), or TNFα (5 ng/mL) individually, or co-treated with TNFα (5 ng/mL) with TG (1 μM) or TNFα (5 ng/mL) and TM (2 μg/mL) for 24 hours prior to treatment. Cells were subsequently countered stained with DAPI (green) and visualized using immunofluorescence imaging. Representative images of immunofluorescent staining of GRP78 (red) and DAPI (green) are presented. Original magnification, 20x. Fluorescence intensity of GRP78 was quantified and expressed relative to the untreated control. D) TeloHAECs were pretreated with TNFα alone or with either TG or TM for 24 hours before measurement of TF PCA following the addition of either human IgG (60 μg/mL) or anti-GRP78 autoantibody (AutoAb, 60 μg/mL). Each bar represents the mean ± standard deviation (n = 3 per group). ^, $p < 0.05$ versus HBSS control, one-way ANOVA; *, $p < 0.05$ versus TNFα control, one-way ANOVA; &, $p < 0.05$ versus AutoAb alone, one-way ANOVA.

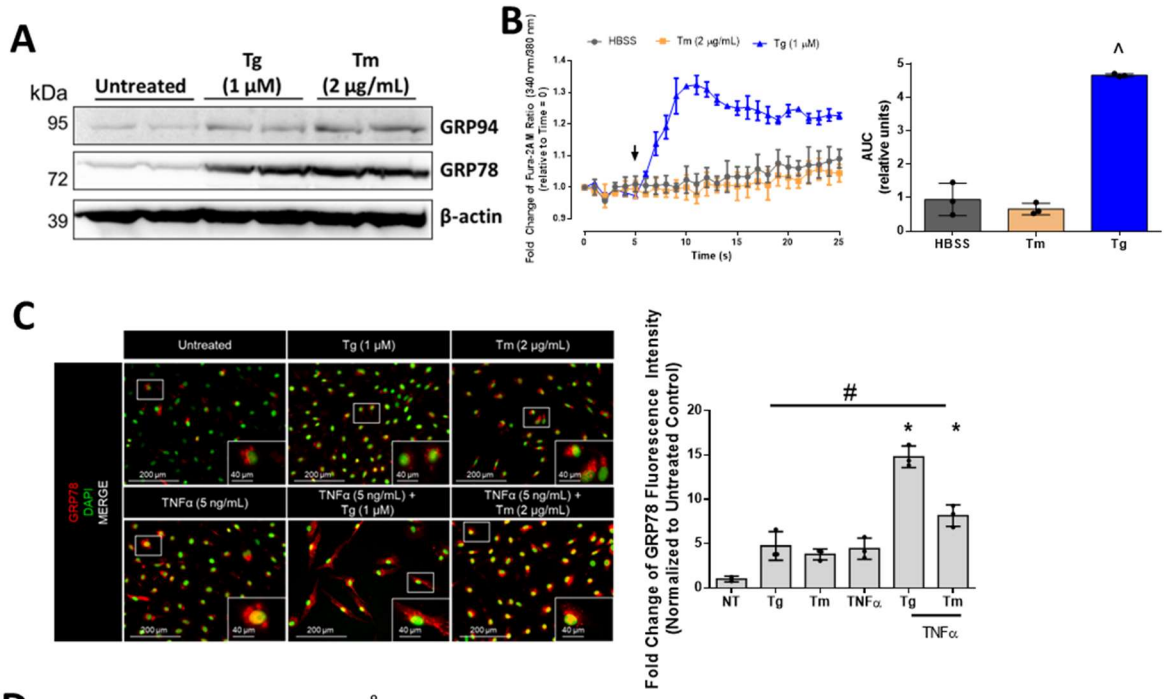
A
kDa
Untreated
Tg (1 μM)
Tm (2 μg/mL)
95
72
39
GRP94
GRP78
β-actin
B
HBSS
Tm (2 μg/mL)
Tg (1 μM)
Fold Change of Fura-2AM Ratio (340 nm/380 nm) (relative to Time = 0)
Time (s)
AUC (relative units)
HBSS
Tm
Tg
C
Untreated
Tg (1 μM)
Tm (2 μg/mL)
TNFα (5 ng/mL)
TNFα (5 ng/mL) + Tg (1 μM)
TNFα (5 ng/mL) + Tm (2 μg/mL)
GRP78
DAPI
MERGE
Fold Change of GRP78 Fluorescence Intensity (Normalized to Untreated Control)
NT
Tg
Tm
TNFα
Tg
Tm
TNFα

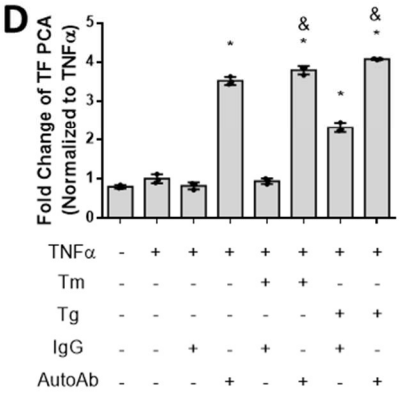
D
Fold Change of TF PCA (Normalized to TNFα)
TNFα
Tm
Tg
IgG
AutoAb

### *4.5. Anti-GRP78 Autoantibodies Enhances Cytosolic $Ca^{2+}$ levels*

Enhanced cytosolic $Ca^{2+}$ has been previously shown to the phospholipid asymmetry known to promote TF PCA (152). In agreement with this notion, we and others have previously shown that the anti-GRP78 autoantibodies purified from patients with cancer can promote ER $Ca^{2+}$ release into the cytosol in cancer cells (138, 139). Based on these observations, we examined the changes in cytosolic levels of $Ca^{2+}$ over time in teloHAECs following treatment with HBSS, TG (1 μM), TM (2 μg/mL), non-specific IgG antibodies (60 μg/mL), or the anti-GRP78 autoantibody (60 μg/mL), where TG and TM were positive and negative controls, respectively. Consistent with previous reports, TG rapidly induces elevated cytosolic $Ca^{2+}$ levels in contrast to TM or HBSS (Figure 12A). Further, teloHAECs treated with the anti-GRP78 autoantibodies also had elevated cytosolic $Ca^{2+}$ levels compared to the non-specific IgG antibodies (Figure 12A). Given the observations that TNFα can contribute to elevated cell surface GRP78 levels (Figure 10A), we also assessed ER $Ca^{2+}$ levels following the addition of anti-GRP78 autoantibodies in TNFα-pretreated teloHAECs. In Figure 12B, the effect of the anti-GRP78 autoantibodies to increase cytosolic $Ca^{2+}$ levels were further enhanced in teloHAECs pretreated with TNFα. These results indicate that the anti-GRP78 autoantibodies alone can enhance cytosolic $Ca^{2+}$ levels which can be further enhanced following pre-treatment with TNFα.

**Figure 12. Anti-GRP78 autoantibodies increases cytosolic $Ca^{2+}$ levels.**

TeloHAECs were pre-treated A) without or B) with TNFα (5 ng/mL) for 24 hours. Intracellular $Ca^{2+}$ release was examined in using Fura-2AM where baseline measurements taken for 5 minutes and immediately treated with either HBSS (grey circle), TG (1 μM) (blue triangle), TM (2 μg/mL) (orange square), IgG (60 μg/mL) (green triangle), or the anti-GRP78 autoantibody (AutoAb, 60 μg/mL) (red diamond), and fluorescent readings were taken for an additional 20 minutes. The ratio of $Ca^{2+}$ bound (excitation 340 nm/ emission 595 nm) over unbound (excitation 380/ emission 595 nm) Fura-2 AM dye was measured and expressed as fold change relative to time = 0. Each symbol represents the mean ± standard deviation (n = 3 per group). C) AUC was determined for each treatment group. Each bar represents the mean ± standard deviation (n = 3 per group). *, $p < 0.05$ versus HBSS alone, one-way ANOVA; $^{\#}$, $p < 0.05$ versus AutoAb alone, one-way ANOVA.

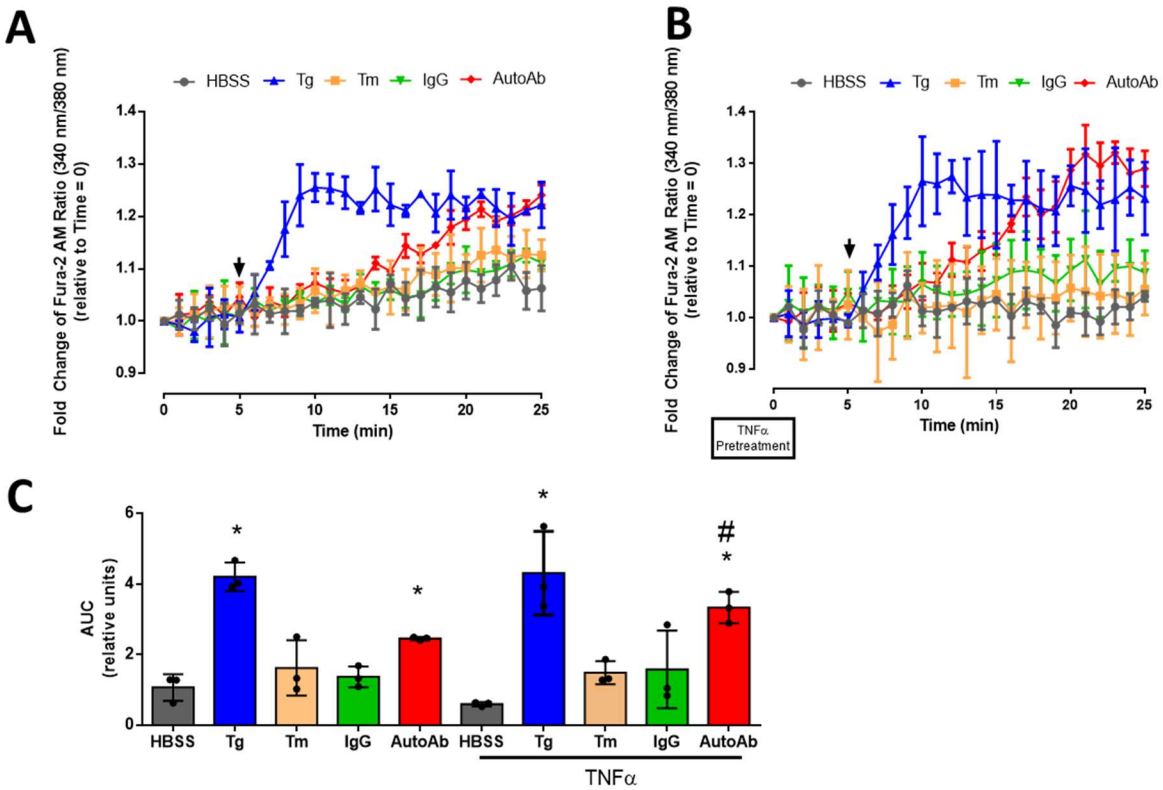
A
HBSS
Tg
Tm
IgG
AutoAb
Fold Change of Fura-2 AM Ratio (340 nm/380 nm) (relative to Time = 0)
Time (min)
B
TNFα Pretreatment
C
AUC (relative units)
HBSS
Tg
Tm
IgG
AutoAb
TNFα

### *4.6. CNVKSDKSC Peptide Attenuates Anti-GRP78 Autoantibody-Induced TF PCA*

It was previously reported that the CNVKSDKSC conformational peptide mimics the tertiary structure of the anti-GRP78 autoantibody binding region on cell surface GRP78 (138). Further, incubation of the conformational peptide with the anti-GRP78 autoantibody was shown to inhibit the ability of the anti-GRP78 autoantibody to activate cell surface GRP78 T24/83 bladder carcinoma cells and HAECs (130, 139). To extend our current findings, purified anti-GRP78 autoantibodies were incubated with or without the CNVKSDKSC conformational peptide (90 µg/mL) for 1 hour and subsequently used to treat TNFα-pretreated teloHAECs and assayed for TF PCA. The CNVKSDKSC conformational peptide alone did not modulate TF PCA in TNFα-treated teloHAECs (Figure 12). However, teloHAECs treated with the anti-GRP78 autoantibody incubated with the CNVKSDKSC conformational peptide showed marked reduction in TF PCA compared to the anti-GRP78 autoantibody-treated group (Figure 13).

**Figure 13. CNVKSDKSC conformational peptide inhibits the anti-GRP78 autoantibody-induced TF PCA.**

TeloHAECs were pre-treated with TNFα (5 ng/mL) for 24 hours prior to treatment with or without the CNVKSDKSC conformational peptide (90 μg/mL), the anti-GRP78 autoantibody (60 μg/mL) (AutoAb), or autoantibody pre-incubated with the conformational peptide for 1 hour prior to measurement of TF PCA. Each bar represents the mean ± standard deviation (n = 3 per group). *, $p < 0.05$ versus TNFα alone, one-way ANOVA; #, $p < 0.05$ versus AutoAb, one-way ANOVA.

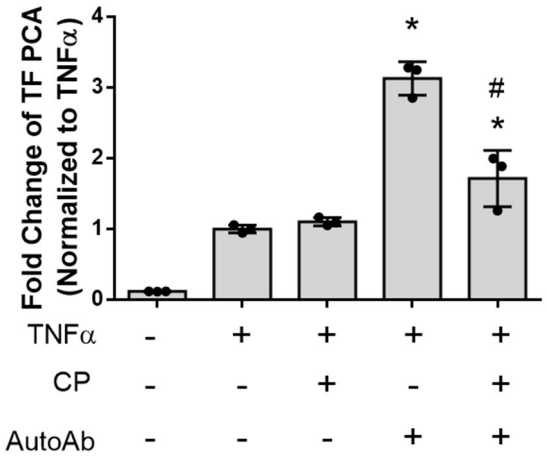
Fold Change of TF PCA
(Normalized to TNFα)
4
3
2
1
0
*
#
*
TNFα - + + + +
CP - - + - +
AutoAb - - - + +

### *4.7. Anti-GRP78 Autoantibody Induces TF PCA Mediated by Functional TF*

Several reports have demonstrated that blocking with an inhibitory anti-TF antibody effectively attenuated TF PCA in different cell types (139, 153, 154). Based on observation that the anti-GRP78 autoantibody can promote TF PCA in teloHAECs (Figure 11), we examined whether functional TF is required for the effects of the autoantibody on TF PCA. TNFα-treated teloHAECs were treated with either an inhibitory anti-TF antibody or an anti-GFP antibody control 1 hour before the addition of human IgG or the anti-GRP78 autoantibody. As shown in Figure 14, the anti-GFP antibody did not mitigate the anti-GRP78 autoantibody-induced TF PCA in TNFα-treated teloHAECs. In contrast, pre-treatment with anti-TF antibody attenuated anti-GRP78 autoantibody-mediated TF PCA. These findings indicate the effect of the anti-GRP78 autoantibody on TF PCA is mediated by functional TF on teloHAECs.

**Figure 14. Anti-TF antibodies inhibit the anti-GRP78 autoantibody-induced TF PCA in TNFα-treated teloHAECs**

TNFα-treated teloHAECs were pretreated with either an anti-GFP antibody (10 μg/mL) or an anti-TF antibody (10 μg/mL) for 1 hour prior to measurement of TF PCA following the addition of either human IgG (60 μg/mL) or anti-GRP78 autoantibody (60 μg/mL). Each bar represents the mean ± standard deviation (n = 3 per group). *, $p < 0.05$ versus TNFα alone, one-way ANOVA; #, $p < 0.05$ versus AutoAb, one-way ANOVA.

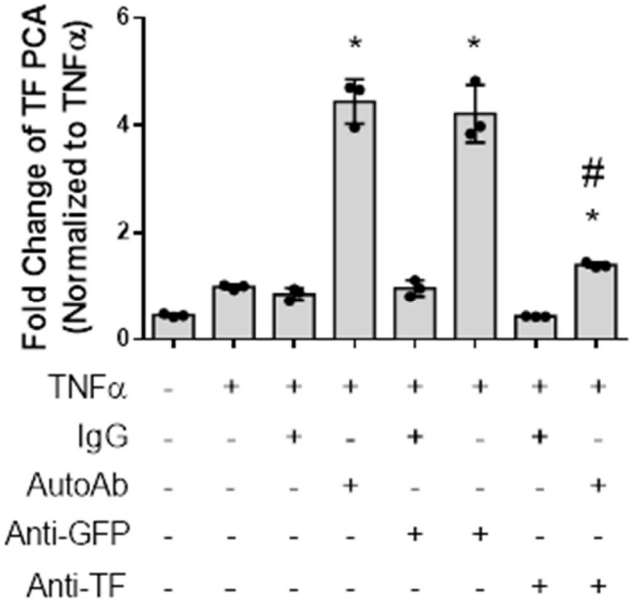
Fold Change of TF PCA
(Normalized to TNFα)
6
4
2
0
*
*
#
*
TNFα - + + + + + + +
IgG - - + - + - + -
AutoAb - - - + - - - +
Anti-GFP - - - - + + - -
Anti-TF - - - - - - + +

### *4.8. Heparin or Enoxaparin Attenuates Anti-GRP78 Autoantibody-mediated TF PCA in teloHAECs*

Previous reports demonstrate that heparin and enoxaparin could compete with the binding of the anti-GRP78 autoantibody for cell surface GRP78 on cancer cells and endothelial cells (130, 147). Pre-treatment with either heparin or enoxaparin was also shown to inhibit the binding of the anti-GRP78 autoantibody to cell surface GRP78 attenuate TF PCA in DU145 prostate cancer (147). Additionally, we have previously shown pre-treatment with enoxaparin attenuated anti-GRP78 autoantibody-induced NF-κB p65 nuclear localization in HAECs. To further investigate the effects of the anti-GRP78 autoantibody, we examined whether heparin or enoxaparin could block the effects of the anti-GRP78 autoantibody on TF PCA in teloHAECs. To assess the effects of heparin or enoxaparin on the effect of the anti-GRP78 autoantibody on TF PCA, teloHAECs were pre-treated with TNFα for 24 hours followed by heparin (50 U/mL) or enoxaparin (50 μg/mL) for 1 hour before treatment with the anti-GRP78 autoantibody. As shown in Figure 15, we observed that the pre-treatment with heparin or enoxaparin attenuated the anti-GRP78 autoantibody-induced activation of TF PCA.

**Figure 15. Pre-treatment with either heparin or enoxaparin blocked anti-GRP78 autoantibody-induced TF PCA in teloHAECs.**

TNFα-treated teloHAECs were treated with either unfractionated heparin (50 units/mL) or enoxaparin (50 μg/mL) for 1 hour prior the addition of anti-GRP78 autoantibody (AutoAb, 60 μg/mL). Each bar represents the mean ± standard deviation (n = 3 per group). *, $p < 0.05$ versus TNFα alone, one-way ANOVA; #, $p < 0.05$ versus AutoAb, one-way ANOVA.

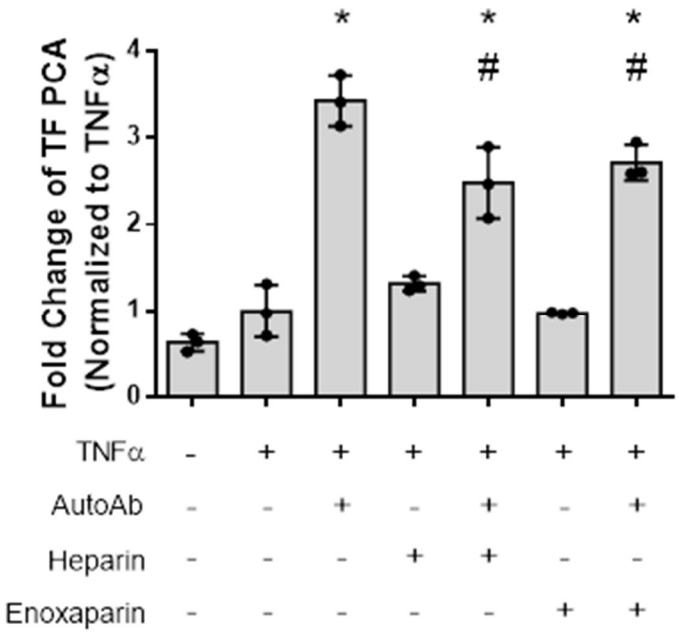
Fold Change of TF PCA
(Normalized to TNFα)
0
1
2
3
4
*
*
*
#
#
TNFα - + + + + + +
AutoAb - - + - + - +
Heparin - - - + + - -
Enoxaparin - - - - - + +

### *4.9. Identification of GRP78 Binders That Inhibited TNFα- and Anti-GRP78 Autoantibody-induced TF PCA in teloHAECs*

Based on our current findings, we show that both unfractionated heparin and enoxaparin can inhibit anti-GRP78 autoantibody induced TF PCA in TNFα-treated teloHAECs. However, the use of heparin and heparin-derived molecules are limited due to a risk of excessive bleeding (155). As such, we sought to identify small molecules that may alter the ability of the anti-GRP78 autoantibody to bind to cell surface GRP78. In collaboration with Atomwise Inc. 86 compounds were originally identified using AtomNet, the first deep convolutional neural network capable of screening millions of commercially available compounds for binding affinity prediction (143). Following discussions with Atomwise Inc. regarding the insolubility of several compounds, we sought to screen a newly generated set of compounds predicted to bind to GRP78 and assess the effects of these compounds in the presence of either human IgG or the anti-GRP78 autoantibodies. 81 of the 86 of the initial set of GRP78 binders were provided to our laboratory and denoted as A01*-G09*, where compounds D05* and E08* were revealed as the internal DMSO vehicle control of the second set of compounds. TeloHAECs were incubated with TNFα (5 ng/mL) and a GRP78 binder (10 μM, A01*-G09*) for 24 hours and subsequently treated with either human IgG (60 μg/mL) or the anti-GRP78 autoantibodies (60 μg/mL) prior to assessing TF PCA. Additionally, we observed the formation of precipitates in teloHAECs treated with 23 compounds (A03*, A07*, A09*, B01*, B12*, C06*, C10*, D01*, D04*, D11*, E02*, E04*, E05*, E07*, E10*, E11*, E12*, F03*, F06*, F09*, F11*, G05*, and G09*) independent of either IgG or anti-GRP78 autoantibody treatment. As such, these compounds were omitted from further investigation. In Figure 16A, teloHAECs treated with compounds A01*, A04*, B10*, B11*, C08*, C12*, D02*, D03*, D06*, D07*,

D09*, and D12* (Group 1) had significantly lower TF PCA compared to the DMSO vehicle control group treated with either IgG or the anti-GRP78 autoantibody. Further, we observed that teloHAECs treated with B03*, B04*, B07*, and B08* (Group 2) did not alter TF PCA compared to the vehicle control group treated with IgG but had reduced anti-GRP78 autoantibody-induced TF PCA compared to the DMSO vehicle control group (Figure 16B, 16C). Based on these observations and in accordance with Specific Objective III of this study, we selected Group 2 compounds for further evaluation as these compounds may disrupt the interaction between the anti-GRP78 autoantibody and cell surface GRP78. Although potentially interesting in terms of direct effects on ER luminal GRP78, Group 1 compounds were not further investigated in this research project.

**Figure 16. Screening of small molecules predicted to bind to cell surface GRP78 on anti-GRP78 autoantibody-induced TF PCA.**

TeloHAECs were treated with or without TNFα (5 ng/mL) and a GRP78 binder (10 μM) for 24 hours and subsequently treated with either human IgG antibodies (60 μg/mL) or anti-GRP78 autoantibody (AutoAb; 60 μg/mL) prior to assessing TF PCA. A) Compounds that inhibited TF PCA in the presence of either human IgG antibodies or anti-GRP78 autoantibodies (Group 1) and B) compounds that attenuated anti-GRP78 autoantibody-induced TF PCA (Group 2). C) Structures of Group 2 compounds. Each bar represents the mean ± standard deviation (n = 3 per group). *, $p < 0.05$ versus DMSO and IgG, one-way ANOVA; #, $p < 0.05$ versus DMSO and AutoAb, one-way ANOVA.

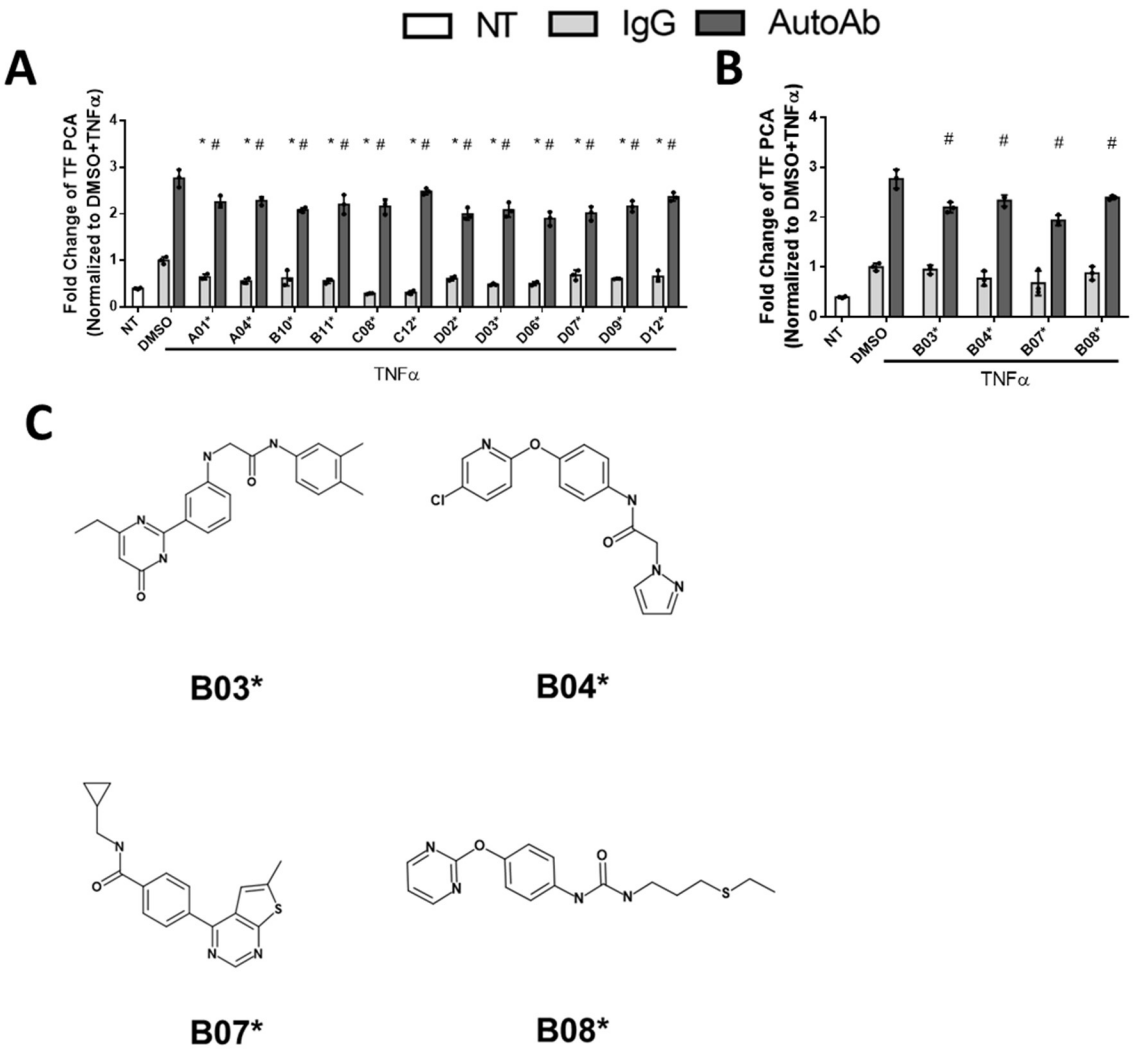
NT
IgG
AutoAb
A
B
C
Fold Change of TF PCA
(Normalized to DMSO+TNFα)
NT
DMSO
A01*
A04*
B10*
B11*
C08*
C12*
D02*
D03*
D06*
D07*
D09*
D12*
B03*
B04*
B07*
B08*
TNFα
B03*
B04*
B07*
B08*

### *4.10. GRP78 binders B07* and B08* Reduces the ATPase Activity of rhGRP78*

According to Atomwise Inc., GRP78 binders that were examined in this project are predicted to bind to the regions of GRP78 at or near the anti-GRP78 autoantibody binding region on cell surface GRP78. Previous findings demonstrated that compounds that directly bind to GRP78 but not in the ATPase domain can also alter the ATPase function of GRP78 (156). Given the relative proximity of the anti-GRP78 autoantibody binding region and the ATPase domain of human GRP78, we examined whether Group 2 GRP78 binders altered the ATPase activity of rhGRP78. To examine ATPase activity, rhGRP78 was incubated with each Atomwise compound in Group 2 (10 μM) for 15 minutes prior to assessing for ATPase activity. In contrast to B03* or B04*, rhGRP78 incubated with B07* or B08* had reduced ATPase activity compared to the rhGRP78 incubated with the DMSO vehicle control (Figure 17). Based on these observations these compounds may interact at or near the ATPase binding site of rhGRP78 and potentially with cell surface GRP78 and will be further evaluated using more sensitive methods to detect potential interactions between B07* and B08* and GRP78.

**Figure 17. B07* and B08* inhibits rhGRP78 ATPase activity.**

ATPase activity of rhGRP78 were assayed in the presence of either an indicated GRP78 binder (10 μM) or DMSO vehicle control. ATPase activity was measured following incubation of rhGRP78 (500 ng) and an Atomwise compound (10 μM) individually or DMSO, and subsequently incubated with ATP (1 mM) for 30 minutes prior to the addition of malachite green reagent. BSA was used as a negative control. Each bar represents the mean ± standard deviation (n = 3 per group). *, $p < 0.05$ versus BSA and DMSO control, one-way ANOVA; #, $p < 0.05$ versus rhGRP78 and DMSO control, one-way ANOVA.

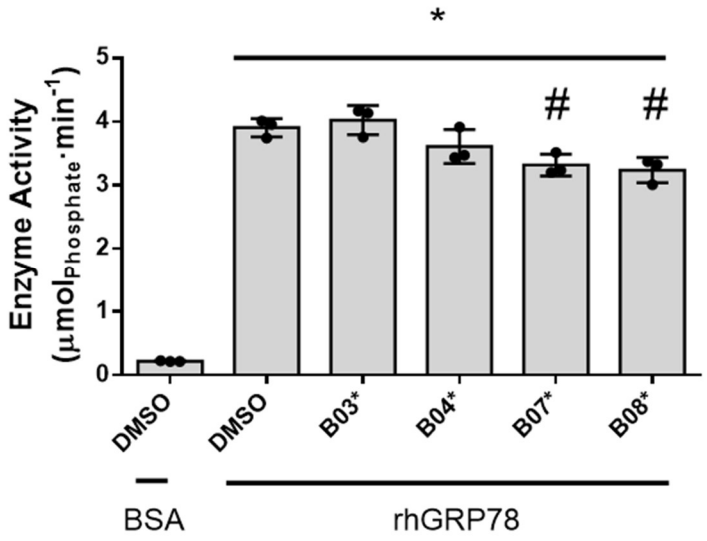
*
#
#
Enzyme Activity
(μmol$_{Phosphate}$·min$^{-1}$)
5
4
3
2
1
0
DMSO
DMSO
B03*
B04*
B07*
B08*
BSA
rhGRP78

*4.11. B07* Inhibits the Binding of the Anti-GRP78 Autoantibody to rhGRP78- and to KLH-CNVSDKSC-coated Plates*

rhGRP78- and KLH-CNVSDKSC- coated plates have previously been used in ELISAs to quantify levels of anti-GRP78 autoantibodies in both human and mouse plasma (130, 138, 147). Moreover, the CNVSDKSC conformational peptide has previously been shown to mimic the anti-GRP78 autoantibody binding region ($Leu_{98}$-$Leu_{115}$) on cell surface GRP78 (137). As such, we examined the use of the anti-GRP78 autoantibodies for an indirect ELISA using rhGRP78 or the KLH-CNVSDKSC conjugate as the antigen coated onto microtitre plates. Using a previously established ELISA method (138), increasing concentrations of anti-GRP78 autoantibodies (0-60 µg/mL) were observed to dose-dependently enhanced absorbance levels relative to secondary only control wells in both rhGRP78-coated (Figure 18A) or CNVSDSKC-coated (Figure 18B) wells. The concentration of the anti-GRP78 autoantibody, 60 µg/mL, was used in subsequent ELISA experiments based on the levels of autoantibodies found in patients with cardiovascular disease or prostate cancer (130, 138). Next, we investigated whether the interaction with the autoantibody and rhGRP78- and KLH-CNVSDKSC could be disrupted using enoxaparin or heparin. Both enoxaparin and heparin were observed to inhibit the binding of the anti-GRP78 autoantibodies to rhGRP78-coated wells (Figure 17C) but not to KLH-CNVSDKSC-coated plates (Figure 17D).

Based on these observations, we selected B07* and assessed whether this compound could disrupt the binding of the anti-GRP78 autoantibody to either rhGRP78- or KLH-CNVSDKSC-coated. rhGRP78- or KLH-CNVSDKSC-coated plates were blocked and incubated with either DMSO or B07* (0.1-100 µM) for 24 hours and subsequently incubated with the anti-GRP78 autoantibody for 1 hour. At 10 µM and 100 µM, the B07*

attenuated the binding of the anti-GRP78 autoantibody to rhGRP78 (Figure 18E) or KLH-CNVSDKSC (Figure 18F) compared to the DMSO control. Taken together, our findings indicates that B07* as a potential candidate compound and warrants further studies into the mechanism by which B07* functions to disrupt the interaction between the anti-GRP78 autoantibody and cell surface GRP78.

**Figure 18. Small molecules inhibit the binding of anti-GRP78 autoantibodies to rhGRP78 or KLH-CNVSDKSC conjugate peptide.**

Relative binding of the anti-GRP78 autoantibody was assessed using ELISA using A) rhGRP78- or B) KLH-CNVSDKSC conjugate as the antigen. Plates were incubated with indicated concentrations of the anti-GRP78 autoantibody (AutoAb) for 1 hour prior to the ELISA method. Indicated concentrations of either enoxaparin or heparin were incubated on C) rhGRP78- or D) KLH-CNVSDKSC conjugate-coated plates were incubated for 24 hours prior to incubation with the anti-GRP78 autoantibody (60 μg/mL). Indicated concentrations of B07* at indicated concentration (0.1-100 μM) or DMSO vehicle control was incubated in E) rhGRP78- or F) KLH-CNVSDKSC conjugate-coated plates for 24 hours prior to the incubation with the anti-GRP78 autoantibody (60 μg/mL). Absorbance values were expressed relative to the secondary only control wells. Each bar represents the mean ± standard deviation (n = 3 per group). $^{*}$, $p < 0.05$ versus anti-GRP78 autoantibody and DMSO control, one-way ANOVA; $^{\#}$, $p < 0.05$ versus secondary only control, one-way ANOVA.

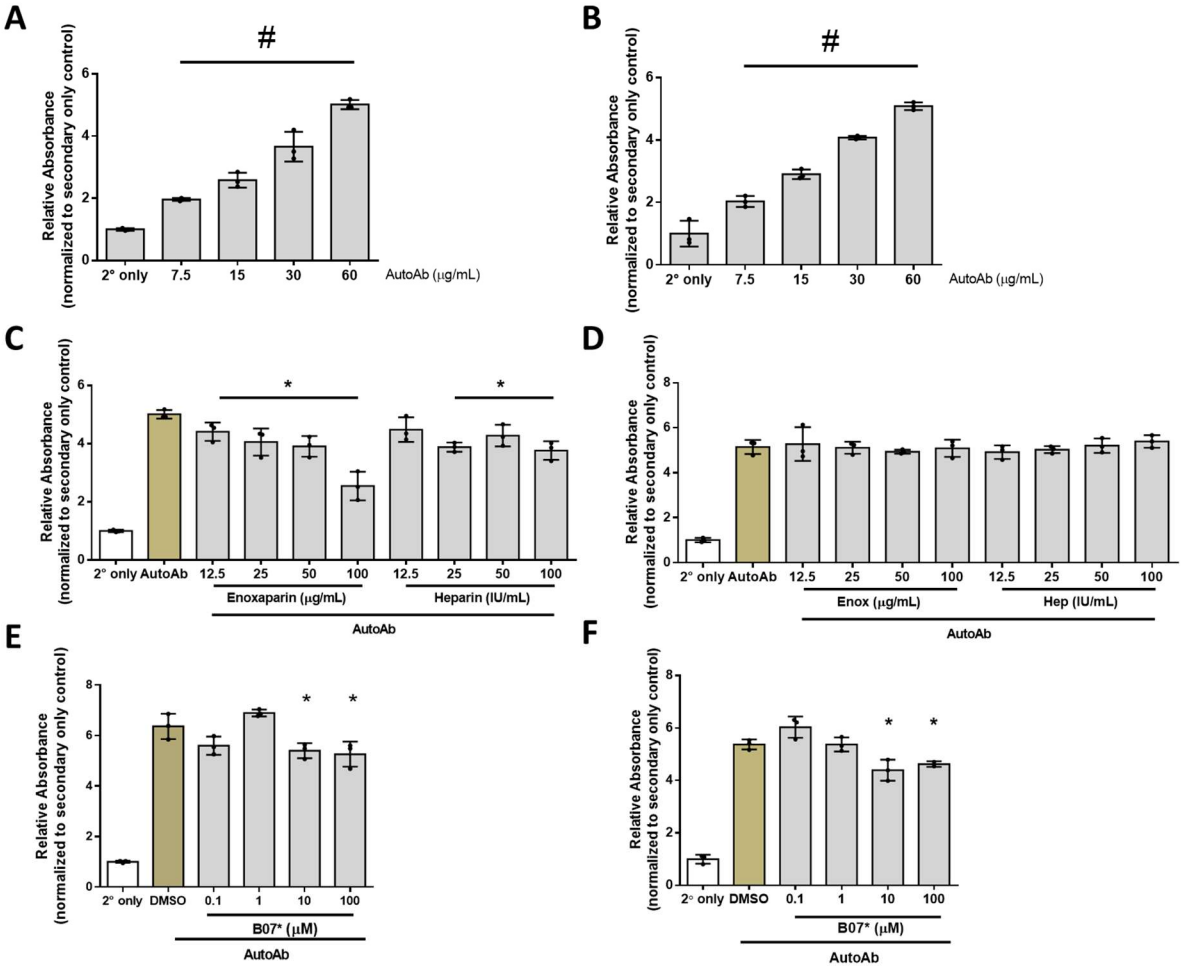
A
#
Relative Absorbance
(normalized to secondary only control)
2° only
7.5
15
30
60
AutoAb (μg/mL)
B
#
Relative Absorbance
(normalized to secondary only control)
2° only
7.5
15
30
60
AutoAb (μg/mL)
C
*
*
Relative Absorbance
(normalized to secondary only control)
2° only
AutoAb
12.5
25
50
100
12.5
25
50
100
Enoxaparin (μg/mL)
Heparin (IU/mL)
AutoAb
D
Relative Absorbance
(normalized to secondary only control)
2° only
AutoAb
12.5
25
50
100
12.5
25
50
100
Enox (μg/mL)
Hep (IU/mL)
AutoAb
E
*
*
Relative Absorbance
(normalized to secondary only control)
2° only
DMSO
0.1
1
10
100
B07* (μM)
AutoAb
F
*
*
Relative Absorbance
(normalized to secondary only control)
2° only
DMSO
0.1
1
10
100
B07* (μM)
AutoAb

## 5. Discussion

During this M.Sc. research project, I investigated the role of activation of cell surface GRP78 by the anti-GRP78 autoantibody on TF PCA in teloHAECs and identify potential compounds that may disrupt the interaction between cell surface GRP78 and the anti-GRP78 autoantibody. Given that endothelial cells express very low amounts of TF, teloHAECs were pre-treated of cells with TNFα which also serve to mimic the local proinflammatory conditions observed in the atherosclerotic plaque (157). I utilized a TNFα pre-treatment in the cell culture model system to evaluate the effect of the soluble rhGRP78, the anti-GRP78 autoantibody, and GRP78 binders on TF PCA. Using this cell culture model system, I showed that exogenous GRP78 did not activate TF PCA in cultured TNFα-treated teloHAECs. We also demonstrate that TNFα alone can promote cell surface GRP78 levels in cultured teloHAECs. Additionally, I showed that anti-GRP78 autoantibody treated endothelial cells can activate TF PCA which can further enhance TNFα-stimulated endothelial cells (144). This effect of the anti-GRP78 autoantibody was further elevated in endothelial cells pre-treated with ER stress-inducing agents also known to enhance cell surface GRP78 levels (130). Additionally, I also show that the effect of the anti-GRP78 autoantibody on TF PCA can be attenuated with pre-treatment of cells with either enoxaparin, heparin, or sequestering the anti-GRP78 autoantibody with CNVSDKSC conformational peptide. Additionally, inhibiting TF with an inhibitory antibody was also shown to attenuates anti-GRP78 autoantibody-induced TF PCA in TNFα-pretreated teloHAECs. Further, I demonstrated that the anti-GRP78 autoantibodies enhances cytosolic $Ca^{2+}$ levels over time using the Fura-2 AM calcium assay. I also identified a small molecule that alone has no effect on TF PCA but can reduce the anti-GRP78 autoantibody-mediated effect on TF PCA, potentially through disrupting the

interaction with cell surface GRP78 and the autoantibody. Together, these findings support the hypothesis that anti-GRP78 autoantibodies can activate TF PCA in teloHAECs.

### *5.1. TNFα Contributes to Enhanced TF PCA Through NF-κB Activation*

TNFα and other pro-inflammatory cytokines are known to play a pathological role in the progression of atherosclerotic lesion development (158). The binding of these pro-inflammatory cytokines to their respective receptors leads to activation of the classical NF-κB pathway where the IKK phosphorylates IκB, allowing NF-κB to freely localizes to the nucleus to upregulate the expression of inflammatory cytokines and adhesion molecules (159). Several reports have shown that TNFα-induced NF-κB activation can also upregulate TF expression and TF PCA in cultured human endothelial cells (36, 160). In support of previous findings, we show that TNFα dose-dependently activates TF PCA in cultured endothelial cells mediated by the activation of NF-κB (35, 36). Additionally, we show that TPCA-1, a selective IKK2 inhibitor, dose-dependently inhibits TNFα-induced TF PCA. Our data indicated that TNFα (5 ng/mL) was sufficient to activate NF-κB with a modest increase in TF PCA relative to the untreated control. Previous studies have established similar levels of TNFα were sufficient to evaluate the effects of compounds on NF-κB activity in endothelial cells (161). As such, we examined endothelial cells treated with TNFα (5 ng/mL) to evaluate the effect of several components of the TF assay in teloHAECs. In the current study, we showed TF assay reactions cannot proceed if the reaction mixture lacks either FVIIa, FX, S-2765, or $CaCl_2$, consistent with findings reported by Caldwell et al. (144).

### *5.2. TNFα Enhances Cell Surface GRP78 Levels*

Under normal conditions, the majority of GRP78 is localized to the ER, where it functions as sensor and protein chaperone for unfolded proteins (85). However, it has been well-established that GRP78 can localize to the cell surface where it functions as a signalling receptor under pharmacological or pathological conditions (162). Using immunofluorescent staining of non-permeabilized cells, we showed that teloHAECs treated with TNFα have increased staining of GRP78, indicating that TNFα can elevate levels of cell surface GRP78. The effect of TNFα to elevate cell surface GRP78 levels was further enhanced with pharmacological compounds TG and TM which have previously been shown to enhance cell surface GRP78 levels (130). To compliment these findings, other techniques such as cell surface biotinylation or FACS analysis will be conducted to confirm the presence of cell surface GRP78 in TNFα-treated teloHAECs. Consistent with the current findings, it was recently reported that exposure to pro-inflammatory cytokines IL-1β, IFN-γ, and TNFα can enhance the level of cell surface GRP78 without changing total GRP78 levels in EndoC-βH1 human pancreatic beta cells (149). Further, Vig et al. demonstrated that the co-chaperone, DNAJC3, is required for the trafficking GRP78 localization in EndoC-βH1 human pancreatic beta cells (149). Based on these observations, future studies will evaluate whether inhibiting DNAJC3 expression can alter cell surface GRP78 levels in TNFα-treated teloHAECs and the alter the ability of anti-GRP78 autoantibody to promote TF PCA.

### *5.3. Regulation of TF PCA by Cell Surface GRP78 and the Anti-GRP78 Autoantibody*

A study by Bhattacharjee et al. (2005) first demonstrated a potential relationship between cell surface GRP78 and TF activation in murine bEND3.1 endothelial cells (140). Immunoprecipitation and immunofluorescent staining studies revealed cell surface

GRP78 and TF can co-localize at the cell surface and negatively regulate TF PCA through direct interaction with TF (140). However, a major limitation of that study is that the studies were conducted in murine endothelial cells artificially overexpressing GRP78 mediated by adenoviral transfection (140). Moreover, Bhattacharjee and colleagues showed that gel-immobilized TF was able to bind to rhGRP78 (140). In a separate study, surface plasmon resonance (SPR) experiments conducted by our laboratory showed that immobilized rhGRP78 fails to bind recombinant TF nor regulate TF PCA in T24/83 bladder carcinoma cells (139). Consistent with these findings, our current studies show that exogenous rhGRP78 did not modulate TF PCA in TNFα-treated teloHAECs and further supports the notion that rhGRP78 does not bind to the cell surface through TF.

Interestingly, Bhattacharjee et al. (2005) has also shown that a commercially available anti-GRP78 antibody enhanced FXa generation and reduced clotting time in both unstimulated and LPS-stimulated bEND3.1 cells indicating cell surface GRP78 may be regulating TF PCA through an alternative mechanism proposed in the study (140). Our laboratory has previously reported that anti-GRP78 autoantibodies against the N-terminal domain of cell surface GRP78 promotes TF PCA in T24/83 bladder carcinoma cells and DU145 prostate cancer cells (139, 147). These anti-GRP78 autoantibodies were shown to activate TF PCA through an $IP_3$-mediated and cytosolic $Ca^{2+}$-mediated mechanisms (139). In agreement with prior studies, our current findings showed that the anti-GRP78 autoantibody activation of TF PCA is mediated by elevated cytosolic $Ca^{2+}$ levels, suggesting that a similar mechanism of TF activation by cell surface GRP78 may occur between cultured endothelial cells and cancer cells. Based on our current observations, further investigations will be conducted to determine whether pre-treatment with 8-(N,N-

diethylamino)octyl-3,4,5-trimethoxybenzoate and 2-aminoethoxydiphenyl borate, compounds previously shown to inhibit $IP_3$-mediated $Ca^{2+}$-release (163), can also attenuate the autoantibody-mediated TF PCA.

### *5.4. Anti-GRP78 autoantibody enhances TF PCA*

Using TNFα-stimulated endothelial cells, we demonstrated that the anti-GRP78 autoantibody specific for the $Leu_{98}$-$Leu_{115}$ epitope of GRP78 induced TF PCA in a dose-dependent manner. It was reported that circulating anti-GRP78 autoantibody levels were observed in healthy volunteers (~5-7 μg/mL) and significantly elevated in patients with prostate cancer (~60 μg/mL) (138). Hence, the 60 μg/mL concentration of the anti-GRP78 autoantibody was considered the pathological concentration for our evaluation of TF PCA in our endothelial cell culture model. Other autoantibodies such as anti-phospholipid autoantibodies found in patients with rheumatoid arthritis or coronavirus disease 2019 (COVID-19) have been reported to be associated with an increased risk of thrombosis (164, 165). Although our laboratory has previously demonstrated that patients with established cardiovascular disease have elevated levels of anti-GRP78 autoantibodies, further work is required to determine anti-GRP78 autoantibody titres in patients with enhance the risk of a thrombotic event (166). Although our findings suggest that the anti-GRP78 autoantibody can promote TF PCA in endothelial cells *in vitro*, these findings are limited as there may be competing or inhibitory processes that prevent TF PCA. However, this project may warrant further studies investigating the effect of the anti-GRP78 autoantibodies in animal models of atherothrombosis.

Another important finding was that teloHAECs treated with the anti-GRP78 autoantibodies pre-incubated with the conformational peptide prior to cell treatment

reduced TF PCA compared to the anti-GRP78 autoantibody alone. This finding is consistent with that of Crane et al. (2018) who showed that incubation of the anti-GRP78 autoantibody with the conformational peptide attenuated anti-GRP78 autoantibody-induced VCAM-1 and ICAM-1 mRNA expression (130). A possible explanation for these findings might be that the conformational peptide sequesters the anti-GRP78 autoantibody and limits its interaction with cell surface GRP78. Additionally, the results of this study show that pre-treatment of the anti-TF antibody inhibited the effect of the anti-GRP78 autoantibody to promote TF PCA. These results are in line with those observed in Al-Hashimi et al. (2010) demonstrating that functional TF is required for anti-GRP78 autoantibody-induced TF PCA (139). Together, these findings support the hypothesis that the anti-GRP78 autoantibodies promote TF PCA in endothelial cells and that peptides known to bind the autoantibodies can mitigate this effect.

### *5.5. Small Molecule Inhibitors of Cell Surface GRP78*

Unfractionated heparin and enoxaparin are glycosaminoglycans known to exert their anticoagulant effects through interaction with antithrombin III (167). Prior reports have shown that cultured endothelial cells incubated with enoxaparin at several time points have reduced coagulant activity without antithrombin III (168). However, the authors did not provide a mechanism by which enoxaparin exerts the anticoagulant effect in endothelial cells. In a separate study, a heparin-binding domain LIGRT ($Leu_{98}$-$Thr_{102}$) was identified near the anti-GRP78 autoantibody binding site on cell surface GRP78 (138). Here, I demonstrated that both enoxaparin and unfractionated heparin inhibited the binding of the anti-GRP78 autoantibodies to rhGRP78 using an ELISA. Additionally, unfractionated heparin and enoxaparin inhibited anti-GRP78 autoantibody-induced TF

PCA. These results corroborate previous findings that heparins can alter the binding of the anti-GRP78 autoantibody to cell surface GRP78 (130, 147). Surprisingly, enoxaparin nor heparin attenuated the binding of the anti-GRP78 autoantibody to KLH-CNVSKDSC. Given that the CNVSKDSC only resembles the tertiary conformation of the anti-GRP78 autoantibody binding site on cell surface GRP78 ($Leu_{98}$-$Leu_{115}$), it is likely that the octapeptide may not fully mimic the heparin binding domain ($Leu_{98}$-$Thr_{102}$). or that there are additional residues that stabilize the interaction between heparin molecules and GRP78 (138). Another possible explanation is that the conjugation of KLH to CNVSKDSC sterically hinders the interaction between the heparins and GRP78. Future investigations into the binding of enoxaparin and heparin to KLH-CNVSKDSC will be conducted.

Heparin and other heparin-derivatives are limited in a clinical setting, often due to an elevated risk of bleeding (155). Hence, we sought to identify other small molecules that could bind to GRP78 and potentially compete with the binding of the anti-GRP78 autoantibody to cell surface GRP78. In collaboration with Atomwise Inc., we obtained several small chemical compounds predicted to bind to regions near or within the anti-GRP78 autoantibody binding site on cell surface GRP78. To identify compounds that may disrupt the interaction between cell surface GRP78 and the autoantibody in endothelial cells, we utilized our continuous TF assay described in **section 4.1** to screen the effect of the Atomwise compounds on TF PCA in the presence or absence of the anti-GRP78 autoantibody. Interestingly, we identified compounds that reduced TF PCA independent of the anti-GRP78 autoantibody (Group 1) and compounds that only reduced anti-GRP78 autoantibody-mediated TF PCA (Group 2). Given that Group 1 compounds function independently of the anti-GRP78 autoantibody treatment, these compounds are likely not

interacting with cell surface GRP78 to reduce TF PCA and were removed from further examination in this project. Group 2 compounds were observed to attenuate the anti-GRP78 autoantibody-induced TF PCA and were selected for further investigated whether these compounds could interact with GRP78. Although Group 2 compounds were observed to inhibit approximately 30% of TF PCA relative to the DMSO control group, these compounds were selected for further evaluation as structural modifications may further improve the efficacy of these compounds.

Prior reports have demonstrated that compounds that directly bind to GRP78 but not in the ATPase domain can also inhibit the ATPase function of GRP78 (156). As such, a functional assay was used to examine ATPase activity of rhGRP78 and identified that compounds B07* and B08* inhibited rhGRP78 ATPase activity in contrast to B03* and B04*. A possible explanation for these results may be that B07* and B08* may bind to rhGRP78 at a greater affinity than B03* or B04*. To supplement these findings, more sensitive techniques including SPR or differential scanning fluorimetry (DSF) will be utilized to further evaluate the binding affinities of the compounds B07* and B08* to GRP78. Given that those techniques were not readily available, we modified a previously established ELISA method used to quantify levels of anti-GRP78 autoantibodies found in plasma (138). Recently, small molecules that interfere with the binding of monoclonal anti-amyloid-β antibodies to immobilized amyloid-β peptide were identified using the ELISA method (169). Based on these observations, we utilized a similar approach to assess the whether the compounds B07* could attenuate the binding of the anti-GRP78 autoantibody to either rhGRP78 or to the conformational peptide that mimics the binding site on cell surface GRP78 using the ELISA method. The results of this study showed

that B07* dose-dependently reduced the binding of the anti-GRP78 autoantibody to the immobilized conformational peptide or rhGRP78, which suggests that the B07* compound may potentially interfere with the ability of the anti-GRP78 autoantibody to interact with cell surface GRP78 and inhibit TF PCA. Further, work is currently being performed to characterize the interaction between cell surface GRP78 and B07* and its structural derivatives and how they may disrupt the interaction between anti-GRP78 autoantibody and cell surface GRP78. Given that we have previously shown that the anti-GRP78 autoantibodies can promote and accelerate atherosclerotic lesions in *apo*E$^{-/-}$ mice, further work will be conducted to examine the effect of B07* on the anti-GRP78 autoantibody-mediated atherosclerotic lesion development and progression, and in animal models of atherothrombosis.

## 6. Future Directions

*i. Investigating whether the interaction between cell surface GRP78 and the anti-GRP78 autoantibody promotes TF PCA in cultured human aortic endothelial cells.*

In collaboration with Affinity Biologicals, we have recently generated an anti-GRP78 antibody produced in sheep immunized with full-length human GRP78 or the KLH-CNVSDKSC conjugate. Figures 10-11 show that the antibody against full length GRP78 can detect rhGRP78 and GRP78 from cell lysates and tissue lysates in immunoblot applications. Ongoing work is currently being undertaken to examine the use of this antibody in other applications such as immunohistochemistry and immunoprecipitation. Using the ELISA method, we have also observed that sheep antibodies against the KLH-CNVSDKSC conjugate can inhibit the binding of the anti-GRP78 autoantibody using ELISA (data not shown). Additionally, we have also observed that this antibody alone does not promote TF PCA in DU145 prostate cancer cells (data not shown). Further, prior reports have shown that anti-GRP78 antibodies can disrupt the binding of the anti-GRP78 autoantibody from engaging to cell surface GRP78 in tumor cells (127). To extend our current findings, TNFα-treated teloHAECs treated with the sheep anti-GRP78 antibody with or without the human anti-GRP78 autoantibody will be assessed for TF PCA. These studies will further elaborate whether the binding of anti-GRP78 antibodies to cell surface GRP78 can modulate the effects of the anti-GRP78 autoantibodies on TF PCA.

*ii. Determining the effect of cell surface GRP78 activation by the anti-GRP78 autoantibody on intracellular $Ca^{2+}$ levels*

Our current findings indicate that the anti-GRP78 autoantibodies can mediate TF PCA through enhancing cytosolic $Ca^{2+}$ levels. To supplement these findings, intracellular $Ca^{2+}$ levels will be evaluated in teloHAECs pre-treated with either heparin or enoxaparin prior to the addition of the anti-GRP78 autoantibody to examine whether blocking the binding

of the anti-GRP78 autoantibody attenuates autoantibody-mediated increases in cytosolic $Ca^{2+}$ levels using the Fura-2 AM kinetic assay. Further, Al-Hashimi et al. previously demonstrated that the activation cell surface GRP78 by the anti-GRP78 autoantibody induced ER $IP_3$-receptor-mediated $Ca^{2+}$ release (139). Moreover, Mag-Fluo-4 AM has recently been described as a novel method to quantify ER $Ca^{2+}$ levels in live cells (151). Based on these observations, ER $Ca^{2+}$ levels will be quantified using Mag-Fluo-4 AM following the treatment with the anti-GRP78 autoantibodies on teloHAECs cells pretreated with or without TNFα. To compliment these findings, kinetics of ER $Ca^{2+}$ release can visualized through transfection of a genetically encoded calcium sensor, CatchER$^+$, and fluorescence microscopy (170).

*iii. Identifying small molecule inhibitors of the cell surface GRP78/anti-GRP78 autoantibody complex.*

This study identified several compounds predicted to bind to GRP78 that can alter anti-GRP78 autoantibody-induced TF PCA (Group 2). Given that the anti-GRP78 autoantibody has been shown to bind to immobilized rhGRP78 using Biacore surface plasmon resonance (139), binding affinity of Group 2 compounds for GRP78 will be determined using surface plasmon resonance in both the presence or absence of the anti-GRP78 autoantibody. These studies can be supplemented with DSF to confirm whether these small molecules can disrupt the binding ability of the anti-GRP78 autoantibody to cell surface GRP78. Following these experiments, modifications to the chemical structures of these GRP78 binders will be conducted to further enhance the affinity for cell surface GRP78.

Although the binding of the anti-GRP78 autoantibodies to cell surface GRP78 can promote TF PCA in our cell culture model, it remains to be determined whether these

effects of anti-GRP78 autoantibodies occurs in animal models of atherothrombosis. Plaque rupture is a rare event in murine models of atherosclerosis (171). However, plaque injury models have been described in *apoE*$^{-/-}$ mice, particularly the Rose Bengal photochemical injury model (172). Based on our current findings, we anticipate that anti-GRP78 autoantibody-treated *apoE*$^{-/-}$ mice will undergo thrombosis rapidly compared to IgG-treated mice following photochemical injury. Based on the potential findings of this study, a similar experiment could be replicated to investigate whether infusion of B07* or its derivatives may inhibit the anti-GRP78 autoantibody-associated thrombus formation. Together, the findings of the proposed studies may serve as foundation to identify a potentially therapeutic treatment strategy for atherothrombotic disease.

## 7. Summary

We provide evidence for the first time that the binding of anti-GRP78 autoantibodies to cell surface GRP78 contributes to TF PCA in activated endothelial cells, which may play a role in atherothrombotic disease. Additionally, we screened and identified several GRP78 binders that attenuate anti-GRP78 autoantibody-induced TF PCA. To complement the findings of this project, further work will be conducted to establish whether the anti-GRP78 autoantibody and cell surface GRP78 contributes to the progression of atherothrombosis *in vivo*. Additionally, structural modifications to compounds identified in this study are currently being undertaken to enhance the efficacy of the compounds to disrupt the binding of the anti-GRP78 autoantibody to cell surface GRP78 and to inhibit TF PCA. Future studies will allow us to continue our drug development program to create novel therapeutic compounds for the treatment and management of atherothrombotic disease by targeting cell surface GRP78.

## References


1. Viles-Gonzalez, J. F., Fuster, V., and Badimon, J. J. (2004) Atherothrombosis: A widespread disease with unpredictable and life-threatening consequences. *Eur. Heart J.* **25**, 1197–1207

2. Vilahur, G., Badimon, J. J., Bugiardini, R., and Badimon, L. (2014) Perspectives: The burden of cardiovascular risk factors and coronary heart disease in Europe and worldwide. *Eur. Hear. J. Suppl.* **16**, A7–A11

3. Hajar, R. (2017) Risk factors for coronary artery disease: Historical perspectives. *Hear. Views*. **18**, 109

4. Khot, U. N., Khot, M. B., Bajzer, C. T., Sapp, S. K., Ohman, E. M., Brener, S. J., Ellis, S. G., Lincoff, A. M., and Topol, E. J. (2003) Prevalence of conventional risk factors in patients with coronary heart disease. *JAMA*. **290**, 898

5. Steg, P. G., Bhatt, D. L., Wilson, P. W. F., D'Agostino, R., Ohman, E. M., Röther, J., Liau, C.-S., Hirsch, A. T., Mas, J.-L., Ikeda, Y., Pencina, M. J., and Goto, S. (2007) One-year cardiovascular event rates in outpatients with atherothrombosis. *JAMA*. **297**, 1197

6. Rauch, U., Osende, J. I., Fuster, V., Badimon, J. J., Fayad, Z., and Chesebro, J. H. (2001) Thrombus formation on atherosclerotic plaques: pathogenesis and clinical consequences. *Ann. Intern. Med.* **134**, 224

7. Woodward, M., Rumley, A., Welsh, P., Macmahin, S., and G., L. (2007) A comparison of the associations between seven hemostatic or inflammatory variables and coronary heart disease. *J. Thromb. Haemost.* **5**, 1795–1800

8. Ridker, P. M., Rifai, N., Pfeffer, M., Sacks, F., Lepage, S., and Braunwald, E. (2000) Elevation of tumor necrosis factor-α and increased risk of recurrent coronary events after myocardial infarction. *Circulation*. **101**, 2149–2153

9. Yousuf, O., Mohanty, B. D., Martin, S. S., Joshi, P. H., Blaha, M. J., Nasir, K., Blumenthal, R. S., and Budoff, M. J. (2013) High-sensitivity C-reactive protein and cardiovascular disease. *J. Am. Coll. Cardiol.* **62**, 397–408

10. Danesh, J., Kaptoge, S., Mann, A. G., Sarwar, N., Wood, A., Angleman, S. B., Wensley, F., Higgins, J. P. T., Lennon, L., Eiriksdottir, G., Rumley, A., Whincup, P. H., Lowe, G. D. O., and Gudnason, V. (2008) Long-term interleukin-6 levels and subsequent risk of coronary heart disease: two new prospective studies and a systematic review. *PLoS Med.* **5**, e78

11. Libby, P., and Ridker, P. M. (2006) Inflammation and atherothrombosis. *J. Am. Coll. Cardiol.* **48**, A33–A46

12. Libby, P. (2000) Multiple mechanisms of thrombosis complicating atherosclerotic plaques. *Clin. Cardiol.* **23**, 3–7

13. Crowther, M. A. (2005) Pathogenesis of atherosclerosis. *Hematology*. **2005**, 436–441

14. Tousoulis, D., Oikonomou, E., Economou, E. K., Crea, F., and Kaski, J. C. (2016) Inflammatory cytokines in atherosclerosis: current therapeutic approaches. *Eur. Heart J.* **37**, 1723–1732

15. Libby, P., Buring, J. E., Badimon, L., Hansson, G. K., Deanfield, J., Bittencourt, M. S., Tokgözoğlu, L., and Lewis, E. F. (2019) Atherosclerosis. *Nat. Rev. Dis. Prim.* **5**, 56

16. Seidman, M. A., Mitchell, R. N., and Stone, J. R. (2014) Pathophysiology of atherosclerosis. in *Cellular and Molecular Pathobiology of Cardiovascular Disease*, pp. 221–237, Elsevier, 10.1016/B978-0-12-405206-2.00012-0

17. Tang, M., and Fang, J. (2017) TNF-α regulates apoptosis of human vascular smooth muscle cells through gap junctions. *Mol. Med. Rep.* **15**, 1407–1411

18. Libby, P. (2021) The changing landscape of atherosclerosis. *Nature*. **592**, 524–533

19. Grover, S. P., and Mackman, N. (2020) Tissue factor in atherosclerosis and atherothrombosis. *Atherosclerosis*. **307**, 80–86

20. Weisel, J. W., and Litvinov, R. I. (2013) Mechanisms of fibrin polymerization and clinical implications. *Blood*. **121**, 1712–1719

21. Palta, S., Saroa, R., and Palta, A. (2014) Overview of the coagulation system. *Indian J. Anaesth.* **58**, 515

22. Coppin, L., Sokal, E., and Stéphenne, X. (2019) Thrombogenic risk induced by intravascular mesenchymal stem cell therapy: current status and future perspectives. *Cells*. **8**, 1160

23. Naudin, C., Burillo, E., Blankenberg, S., Butler, L., and Renné, T. (2017) Factor XII Contact Activation. *Semin. Thromb. Hemost.* **43**, 814–826

24. Perez-Pujol, S., Aras, O., and Escolar, G. (2012) Factor V Leiden and Inflammation. *Thrombosis*. **2012**, 1–10

25. Uhlen, M., Fagerberg, L., Hallstrom, B. M., Lindskog, C., Oksvold, P., Mardinoglu, A., Sivertsson, A., Kampf, C., Sjostedt, E., Asplund, A., Olsson, I., Edlund, K., Lundberg, E., Navani, S., Szigyarto, C. A.-K., Odeberg, J., Djureinovic, D., Takanen, J. O., Hober, S., Alm, T., Edqvist, P.-H., Berling, H., Tegel, H., Mulder, J., Rockberg, J., Nilsson, P., Schwenk, J. M., Hamsten, M., von Feilitzen, K., Forsberg, M., Persson, L., Johansson, F., Zwahlen, M., von Heijne, G., Nielsen, J., and Ponten, F. (2015) Tissue-based map of the human proteome. *Science (80-. ).* **347**, 1260419–1260419

26. Bugge, T. H., Xiao, Q., Kombrinck, K. W., Flick, M. J., Holmbäck, K., Danton, M. J. S., Colbert, M. C., Witte, D. P., Fujikawa, K., Davie, E. W., and Degen, J. L. (1996) Fatal embryonic bleeding events in mice lacking tissue factor, the cell-associated initiator of blood coagulation. *Proc. Natl. Acad. Sci.* **93**, 6258–6263

27. Mackman, N., Sawdey, M. S., Keeton, M. R., and Loskutoff, D. J. (1993) Murine tissue factor gene expression in vivo. Tissue and cell specificity and regulation by

lipopolysaccharide. *Am. J. Pathol.* **143**, 76–84

28. Han, X., Guo, B., Li, Y., and Zhu, B. (2014) Tissue factor in tumor microenvironment: a systematic review. *J. Hematol. Oncol.* **7**, 54

29. Kasthuri, R. S., Taubman, M. B., and Mackman, N. (2009) Role of tissue factor in cancer. *J. Clin. Oncol.* **27**, 4834–4838

30. Grabowski, E., Zuckerman, D., and Nemerson, Y. (1993) The functional expression of tissue factor by fibroblasts and endothelial cells under flow conditions. *Blood*. **81**, 3265–3270

31. Bouchard, B. A., Shatos, M. A., and Tracy, P. B. (1997) Human brain pericytes differentially regulate expression of procoagulant enzyme complexes comprising the extrinsic pathway of blood coagulation. *Arterioscler. Thromb. Vasc. Biol.* **17**, 1–9

32. Wilcox, J. N., Smith, K. M., Schwartz, S. M., and Gordon, D. (1989) Localization of tissue factor in the normal vessel wall and in the atherosclerotic plaque. *Proc. Natl. Acad. Sci.* **86**, 2839–2843

33. Hatakeyama, K., Asada, Y., Marutsuka, K., Sato, Y., Kamikubo, Y., and Sumiyoshi, A. (1997) Localization and activity of tissue factor in human aortic atherosclerotic lesions. *Atherosclerosis*. **133**, 213–219

34. Bevilacqua, M. P., Pober, J. S., Majeau, G. R., Cotran, R. S., and Gimbrone, M. A. (1984) Interleukin 1 (IL-1) induces biosynthesis and cell surface expression of procoagulant activity in human vascular endothelial cells. *J. Exp. Med.* **160**, 618–623

35. Conway, E. M., Bach, R., Rosenberg, R. D., and Konigsberg, W. H. (1989) Tumor necrosis factor enhances expression of tissue factor mRNA in endothelial cells. *Thromb. Res.* **53**, 231–41

36. Parry, G. C. N., and Mackman, N. (1995) Transcriptional regulation of tissue factor expression in human endothelial cells. *Arterioscler. Thromb. Vasc. Biol.* **15**, 612–621

37. Moll, T., Czyz, M., Holzmuller, H., Hofer-Warbinek, R., Wagner, E., Winkler, H., Bach, F. H., and Hofer, E. (1995) Regulation of the tissue factor promoter in endothelial cells: binding of NFκB-, AP-1-, AND Sp1-like transcription factors. *J. Biol. Chem.* **270**, 3849–3857

38. Thiruvikraman, S. V, Guha, A., Roboz, J., Taubman, M. B., Nemerson, Y., and Fallon, J. T. (1996) In situ localization of tissue factor in human atherosclerotic plaques by binding of digoxigenin-labeled factors VIIa and X. *Lab. Investig.* **75**, 451–61

39. Spicer, E. K., Horton, R., Bloem, L., Bach, R., Williams, K. R., Guha, A., Kraus, J., Lin, T. C., Nemerson, Y., and Konigsberg, W. H. (1987) Isolation of cDNA clones coding for human tissue factor: primary structure of the protein and cDNA. *Proc. Natl. Acad. Sci.* **84**, 5148–5152

40. Carson, S. D., Henry, W. M., and Shows, T. B. (1985) Tissue factor gene localized to human chromosome 1 (1pter→1p21). *Science (80-. ).* **229**, 991–993

41. Edgington, T. S., Mackman, N., Brand, K., and Ruf, W. (1991) The structural biology of expression and function of tissue factor. *Thromb. Haemost.* **66**, 067–079

42. Harlos, K., Martin, D. M. A., O'Brien, D. P., Jones, E. Y., Stuart, D. I., Polikarpov, I., Miller, A., Tuddenham, E. G. D., and Boys, C. W. G. (1994) Crystal structure of the extracellular region of human tissue factor. *Nature*. **370**, 662–666

43. Ruf, W., Rehemtulla, A., Morrissey, J. H., and Edgington, T. S. (1991) Phospholipid-independent and -dependent interactions required for tissue factor receptor and cofactor function. *J. Biol. Chem.* **266**, 2158–2166

44. Paborsky, L. R., and Harris, R. J. (1990) Post-translational modifications of recombinant human tissue factor. *Thromb. Res.* **60**, 367–376

45. Bogdanov, V. Y., Balasubramanian, V., Hathcock, J., Vele, O., Lieb, M., and Nemerson, Y. (2003) Alternatively spliced human tissue factor: a circulating, soluble, thrombogenic protein. *Nat. Med.* **9**, 458–462

46. Carson, S. D., and Bromberg, M. E. (2000) Tissue factor encryption/de-encryption is not altered in the absence of the cytoplasmic domain. *Thromb. Haemost.* **84**, 657–63

47. Cunningham, M. A., Romas, P., Hutchinson, P., Holdsworth, S. R., and Tipping, P. G. (1999) Tissue factor and factor VIIa receptor/ligand interactions induce proinflammatory effects in macrophages. *Blood*. **94**, 3413–20

48. Ott, I., Fischer, E. G., Miyagi, Y., Mueller, B. M., and Ruf, W. (1998) A role for tissue factor in cell adhesion and migration mediated by interaction with actin-binding protein 280. *J. Cell Biol.* **140**, 1241–1253

49. Rao, L. V. M., and Pendurthi, U. R. (2012) Regulation of tissue factor coagulant activity on cell surfaces. *J. Thromb. Haemost.* **10**, 2242–2253

50. Penn, M. S., Patel, C. V., Cui, M.-Z., DiCorleto, P. E., and Chisolm, G. M. (1999) LDL increases inactive tissue factor on vascular smooth muscle cell surfaces. *Circulation*. **99**, 1753–1759

51. Penn, M. S., Cui, M. Z., Winokur, A. L., Bethea, J., Hamilton, T. A., DiCorleto, P. E., and Chisolm, G. M. (2000) Smooth muscle cell surface tissue factor pathway activation by oxidized low-density lipoprotein requires cellular lipid peroxidation. *Blood*. **96**, 3056–63

52. Bach, R. R. (2006) Tissue factor encryption. *Arterioscler. Thromb. Vasc. Biol.* **26**, 456–461

53. Le, D. T., Rapaport, S. I., and Rao, L. V (1992) Relations between factor VIIa binding and expression of factor VIIa/tissue factor catalytic activity on cell surfaces. *J. Biol. Chem.* **267**, 15447–54

54. Chen, V. M., and Hogg, P. J. (2013) Encryption and decryption of tissue factor. *J. Thromb. Haemost.* **11**, 277–284

55. Rehemtulla, A., Ruf, W., and Edgington, T. S. (1991) The integrity of the cysteine 186-cysteine 209 bond of the second disulfide loop of tissue factor is required for binding of factor VII. *J. Biol. Chem.* **266**, 10294–9

56. Ahamed, J., Versteeg, H. H., Kerver, M., Chen, V. M., Mueller, B. M., Hogg, P. J., and Ruf, W. (2006) Disulfide isomerization switches tissue factor from coagulation to cell signaling. *Proc. Natl. Acad. Sci.* **103**, 13932–13937

57. Chen, S., Meng, X.-F., and Zhang, C. (2013) Role of NADPH oxidase-mediated reactive oxygen species in podocyte injury. *Biomed Res. Int.* **2013**, 1–7

58. Versteeg, H. H., and Ruf, W. (2007) Tissue factor coagulant function is enhanced by protein-disulfide isomerase independent of oxidoreductase activity. *J. Biol. Chem.* **282**, 25416–25424

59. Roy, S., Paborsky, L. R., and Vehar, G. A. (1991) Self-association of tissue factor as revealed by chemical crosslinking. *J. Biol. Chem.* **266**, 4665–8

60. Bach, R. R., and Moldow, C. F. (1997) Mechanism of tissue factor activation on HL-60 cells. *Blood*. 10.1182/blood.v89.9.3270

61. Doñate, F., Kelly, C. R., Ruf, W., and Edgington, T. S. (2000) Dimerization of tissue factor supports solution-phase autoactivation of factor VII without influencing proteolytic activation of factor X. *Biochemistry*. **39**, 11467–11476

62. Awasthi, V., Mandal, S. K., Papanna, V., Rao, L. V. M., and Pendurthi, U. R. (2007) Modulation of tissue factor–factor VIIa signaling by lipid rafts and caveolae. *Arterioscler. Thromb. Vasc. Biol.* **27**, 1447–1455

63. Sezgin, E., Levental, I., Mayor, S., and Eggeling, C. (2017) The mystery of membrane organization: composition, regulation and roles of lipid rafts. *Nat. Rev. Mol. Cell Biol.* **18**, 361–374

64. Dietzen, D. J., Page, K. L., and Tetzloff, T. A. (2004) Lipid rafts are necessary for tonic inhibition of cellular tissue factor procoagulant activity. *Blood*. **103**, 3038–3044

65. Mulder, A. B., Smit, J. W., Bom, V. J., Blom, N. R., Ruiters, M. H., Halie, M. R., and van der Meer, J. (1996) Association of smooth muscle cell tissue factor with caveolae. *Blood*. **88**, 1306–13

66. Mandal, S. K., Iakhiaev, A., Pendurthi, U. R., and Rao, L. V. M. (2005) Acute cholesterol depletion impairs functional expression of tissue factor in fibroblasts: modulation of tissue factor activity by membrane cholesterol. *Blood*. **105**, 153–160

67. Sevinsky, J. R., Rao, L. V, and Ruf, W. (1996) Ligand-induced protease receptor translocation into caveolae: a mechanism for regulating cell surface proteolysis of the tissue factor-dependent coagulation pathway. *J. Cell Biol.* **133**, 293–304

68. Giesen, P. L., and Nemerson, Y. (2000) Tissue factor on the loose. *Semin. Thromb.*

*Hemost.* **Volume 26**, 0379–0384

69. Schecter, A. D., Giesen, P. L., Taby, O., Rosenfield, C. L., Rossikhina, M., Fyfe, B. S., Kohtz, D. S., Fallon, J. T., Nemerson, Y., and Taubman, M. B. (1997) Tissue factor expression in human arterial smooth muscle cells. TF is present in three cellular pools after growth factor stimulation. *J. Clin. Invest.* **100**, 2276–2285

70. Iakhiaev, A., Pendurthi, U. R., Voigt, J., Ezban, M., and Rao, L. V. M. (1999) Catabolism of factor VIIa bound to tissue factor in fibroblasts in the presence and absence of tissue factor pathway inhibitor. *J. Biol. Chem.* **274**, 36995–37003

71. Kaksonen, M., and Roux, A. (2018) Mechanisms of clathrin-mediated endocytosis. *Nat. Rev. Mol. Cell Biol.* **19**, 313–326

72. Hansen, C. B., Pyke, C., Petersen, L. C., and Rao, L. V. M. (2001) Tissue factor–mediated endocytosis, recycling, and degradation of factor VIIa by a clathrin-independent mechanism not requiring the cytoplasmic domain of tissue factor. *Blood*. **97**, 1712–1720

73. van Meer, G., Voelker, D. R., and Feigenson, G. W. (2008) Membrane lipids: where they are and how they behave. *Nat. Rev. Mol. Cell Biol.* **9**, 112–124

74. Fujimoto, T., and Parmryd, I. (2017) Interleaflet coupling, pinning, and leaflet asymmetry - major players in plasma membrane nanodomain formation. *Front. Cell Dev. Biol.* 10.3389/fcell.2016.00155

75. Clarke, R. J., Hossain, K. R., and Cao, K. (2020) Physiological roles of transverse lipid asymmetry of animal membranes. *Biochim. Biophys. Acta - Biomembr.* **1862**, 183382

76. Bach, R., Gentry, R., and Nemerson, Y. (1986) Factor VII Binding to Tissue Factor in Reconstituted Phospholipid Vesicles: Induction of Cooperativity by Phosphatidylserinet. *Biochemistry*. **25**, 4007–4020

77. Wolberg, A. S., Monroe, D. M., Roberts, H. R., and Hoffman, M. R. (1999) Tissue factor de-encryption: ionophore treatment induces changes in tissue factor activity by phosphatidylserine-dependent and -independent mechanisms. *Blood Coagul. Fibrinolysis*. **10**, 201–10

78. Le, D. T., Rapaport, S. I., and Rao, L. V (1994) Studies of the mechanism for enhanced cell surface factor VIIa/tissue factor activation of factor X on fibroblast monolayers after their exposure to N-ethylmaleimide. *Thromb. Haemost.* **72**, 848–55

79. Neuenschwander, P. F., Bianco-Fisher, E., Rezaie, A. R., and Morrissey, J. H. (1995) Phosphatidylethanolamine augments factor VIIa-tissue factor activity: enhancement of sensitivity to phosphatidylserine. *Biochemistry*. **34**, 13988–13993

80. Braakman, I., and Hebert, D. N. (2013) Protein folding in the endoplasmic reticulum. *Cold Spring Harb. Perspect. Biol.* **5**, a013201–a013201

81. Walczak, C. P., Bernardi, K. M., and Tsai, B. (2012) Endoplasmic Reticulum-

Dependent Redox Reactions Control Endoplasmic Reticulum-Associated Degradation and Pathogen Entry. *Antioxid. Redox Signal.* **16**, 809–818

82. Johnson, A. E., and van Waes, M. A. (1999) The translocon: a dynamic gateway at the ER membrane. *Annu. Rev. Cell Dev. Biol.* **15**, 799–842

83. Coe, H., and Michalak, M. (2009) Calcium binding chaperones of the endoplasmic reticulum. *Gen. Physiol. Biophys.* **28 Spec No**, F96–F103

84. Anelli, T., and Sitia, R. (2008) Protein quality control in the early secretory pathway. *EMBO J.* **27**, 315–327

85. Austin, R. C. (2009) The unfolded protein response in health and disease. *Antioxid. Redox Signal.* **11**, 2279–2287

86. Görlach, A., Klappa, P., and Kietzmann, D. T. (2006) The endoplasmic reticulum: folding, calcium homeostasis, signaling, and redox control. *Antioxid. Redox Signal.* **8**, 1391–1418

87. Schröder, M., and Kaufman, R. J. (2005) ER stress and the unfolded protein response. *Mutat. Res. Mol. Mech. Mutagen.* **569**, 29–63

88. Hetz, C., Zhang, K., and Kaufman, R. J. (2020) Mechanisms, regulation and functions of the unfolded protein response. *Nat. Rev. Mol. Cell Biol.* **21**, 421–438

89. Zhou, J., Lhoták, S., Hilditch, B. A., Austin, R. C., Lhoták, Š., Hilditch, B. A., Austin, R. C., Lhoták, S., Hilditch, B. A., and Austin, R. C. (2005) Activation of the unfolded protein response occurs at all stages of atherosclerotic lesion development in apolipoprotein E–deficient mice. *Circulation*. **111**, 1814–1821

90. Hotamisligil, G. S. (2010) Endoplasmic reticulum stress and atherosclerosis. *Nat. Med.* **16**, 396–399

91. Lynn, E. G., Lhoták, Š., Lebeau, P., Byun, J. H., Chen, J., Platko, K., Shi, C., O'Brien, E. R., and Austin, R. C. (2019) 4-Phenylbutyrate protects against atherosclerotic lesion growth by increasing the expression of HSP25 in macrophages and in the circulation of Apoe −/− mice. *FASEB J.* **33**, 8406–8422

92. Zhou, J., Werstuck, G. H., Lhoták, S., de Koning, A. B. L. L., Sood, S. K., Hossain, G. S., Møller, J., Ritskes-Hoitinga, M., Falk, E., Dayal, S., Lentz, S. R., Austin, R. C., Lhoták, Š., de Koning, A. B. L. L., Sood, S. K., Hossain, G. S., Møller, J., Ritskes-Hoitinga, M., Falk, E., Dayal, S., Lentz, S. R., and Austin, R. C. (2004) Association of multiple cellular stress pathways with accelerated atherosclerosis in hyperhomocysteinemic apolipoprotein E-deficient mice. *Circulation*. **110**, 207–13

93. Zeng, L., Zampetaki, A., Margariti, A., Pepe, A. E., Alam, S., Martin, D., Xiao, Q., Wang, W., Jin, Z.-G. Z.-G., Cockerill, G., Mori, K., Li, Y. J., Hu, Y., Chien, S., and Xu, Q. (2009) Sustained activation of XBP1 splicing leads to endothelial apoptosis and atherosclerosis development in response to disturbed flow. *Proc. Natl. Acad. Sci.* **106**, 8326–8331

94. Feng, B., Yaol, P. M., Li, Y., Devlin, C. M., Zhang, D., Harding, H. P., Sweeney, M.,

Rong, J. X., Kuriakose, G., Fisher, E. A., Marks, A. R., Ron, D., and Tabas, I. (2003) The endoplasmic reticulum is the site of cholesterol-induced cytotoxicity in macrophages. *Nat. Cell Biol.* **5**, 781–792

95. Shanahan, C. M., and Furmanik, M. (2017) Endoplasmic reticulum stress in arterial smooth muscle cells: a novel regulator of vascular disease. *Curr. Cardiol. Rev.* 10.2174/1573403X12666161014094738

96. Civelek, M., Manduchi, E., Riley, R. J., Stoeckert, C. J., and Davies, P. F. (2009) Chronic endoplasmic reticulum stress activates unfolded protein response in arterial endothelium in regions of susceptibility to atherosclerosis. *Circ. Res.* **105**, 453–461

97. Huang, A., Young, T. L., Dang, V. T., Shi, Y., McAlpine, C. S., and Werstuck, G. H. (2017) 4-phenylbutyrate and valproate treatment attenuates the progression of atherosclerosis and stabilizes existing plaques. *Atherosclerosis*. **266**, 103–112

98. Hua, Y., Kandadi, M. R., Zhu, M., Ren, J., and Sreejayan, N. (2010) Tauroursodeoxycholic acid attenuates lipid accumulation in endoplasmic reticulum–stressed macrophages. *J. Cardiovasc. Pharmacol.* **55**, 49–55

99. Iiyama, K., Hajra, L., Iiyama, M., Li, H., DiChiara, M., Medoff, B. D., and Cybulsky, M. I. (1999) Patterns of vascular cell adhesion molecule-1 and intercellular adhesion molecule-1 expression in rabbit and mouse atherosclerotic lesions and at sites predisposed to lesion formation. *Circ. Res.* **85**, 199–207

100. Bailey, K. A., Haj, F. G., Simon, S. I., and Passerini, A. G. (2017) Atherosusceptible shear stress activates endoplasmic reticulum stress to promote endothelial inflammation. *Sci. Rep.* **7**, 8196

101. Welch, G. N., and Loscalzo, J. (1998) Homocysteine and atherothrombosis. *N. Engl. J. Med.* **338**, 1042–1050

102. Outinen, P. A., Sood, S. K., Pfeifer, S. I., Pamidi, S., Podor, T. J., Li, J., Weitz, J. I., and Austin, R. C. (1999) Homocysteine-induced endoplasmic reticulum stress and growth arrest leads to specific changes in gene expression in human vascular endothelial cells. *Blood*. **94**, 959–67

103. Kozlov, G., and Gehring, K. (2020) Calnexin cycle – structural features of the ER chaperone system. *FEBS J.* **287**, 4322–4340

104. D'Alessio, C., and Parodi, A. J. (2014) Role of UDP-glucose/glycoprotein glucosyltransferase in ER glycoprotein quality control. *Glycosci. Biol. Med.* 10.1007/978-4-431-54836-2_156-1

105. Paulsson, K., and Wang, P. (2003) Chaperones and folding of MHC class I molecules in the endoplasmic reticulum. *Biochim. Biophys. Acta - Mol. Cell Res.* **1641**, 1–12

106. Peluso, R. W., Lamb, R. A., and Choppin, P. W. (1978) Infection with paramyxoviruses stimulates synthesis of cellular polypeptides that are also stimulated in cells transformed by Rous sarcoma virus or deprived of glucose. *Proc.*

*Natl. Acad. Sci. U. S. A.* **75**, 6120–6124

107. Luo, S., Mao, C., Lee, B., and Lee, A. S. (2006) GRP78/BiP is required for cell proliferation and protecting the inner cell mass from apoptosis during early mouse embryonic development. *Mol. Cell. Biol.* **26**, 5688–5697

108. Lee, A. S., Brandhorst, S., Rangel, D. F., Navarrete, G., Cohen, P., Longo, V. D., Chen, J., Groshen, S., Morgan, T. E., and Dubeau, L. (2017) Effects of prolonged GRP78 haploinsufficiency on organ homeostasis, behavior, cancer and chemotoxic resistance in aged mice. *Sci. Rep.* **7**, 40919

109. Ting, J., and Lee, A. S. (1988) Human gene encoding the 78,000-dalton glucose-regulated protein and its pseudogene: structure, conservation, and regulation. *DNA*. **7**, 275–286

110. Rose, M. D., Misra, L. M., and Vogel, J. P. (1989) KAR2, a karyogamy gene, is the yeast homolog of the mammalian BiP/GRP78 gene. *Cell*. **57**, 1211–1221

111. Haas, I. G. (1994) BiP (GRP78), an essential hsp70 resident protein in the endoplasmic reticulum. *Experientia*. **50**, 1012–1020

112. Ibrahim, I. M., Abdelmalek, D. H., and Elfiky, A. A. (2019) GRP78: A cell's response to stress. *Life Sci.* **226**, 156–163

113. Huang, X., Gu, H. H., and Zhan, C.-G. (2009) Mechanism for Cocaine Blocking the Transport of Dopamine: Insights from Molecular Modeling and Dynamics Simulations. *J. Phys. Chem. B*. **113**, 15057–15066

114. Sun, F.-C., Wei, S., Li, C.-W., Chang, Y.-S., Chao, C.-C., and Lai, Y.-K. (2006) Localization of GRP78 to mitochondria under the unfolded protein response. *Biochem. J.* **396**, 31–39

115. Gonzalez–Gronow, M., Selim, M. A., Papalas, J., and Pizzo, S. V. (2009) GRP78: A multifunctional receptor on the cell surface. *Antioxid. Redox Signal.* **11**, 2299–2306

116. Zhang, Y., Liu, R., Ni, M., Gill, P., and Lee, A. S. (2010) Cell surface relocalization of the endoplasmic reticulum chaperone and unfolded protein response regulator GRP78/BiP. *J. Biol. Chem.* **285**, 15065–15075

117. Tsai, Y.-L., Zhang, Y., Tseng, C.-C., Stanciauskas, R., Pinaud, F., and Lee, A. S. (2015) Characterization and mechanism of stress-induced translocation of 78-kilodalton glucose-regulated protein (GRP78) to the cell surface. *J. Biol. Chem.* **290**, 8049–8064

118. Chen, J., Lynn, E. G., Yousof, T. R., Sharma, H., Macdonald, M. E., Byun, J. H., Shayegan, B., and Austin, R. C. (2022) Scratching the surface - an overview of the roles of cell surface GRP78 in cancer. *Biomed. 2022, Vol. 10, Page 1098*. **10**, 1098

119. Newstead, S., and Barr, F. (2020) Molecular basis for KDEL-mediated retrieval of escaped ER-resident proteins – SWEET talking the COPs. *J. Cell Sci.* 10.1242/jcs.250100

120. Tsai, Y.-L., Ha, D. P., Zhao, H., Carlos, A. J., Wei, S., Pun, T. K., Wu, K., Zandi, E., Kelly, K., and Lee, A. S. (2018) Endoplasmic reticulum stress activates SRC, relocating chaperones to the cell surface where GRP78/CD109 blocks TGF-β signaling. *Proc. Natl. Acad. Sci.* **115**, E4245–E4254

121. Limso, C., Ngo, J. M., Nguyen, P., Leal, S., Husain, A., Sahoo, D., Ghosh, P., and Bhandari, D. (2020) The Gα-interacting vesicle-associated protein interacts with and promotes cell surface localization of GRP78 during endoplasmic reticulum stress. *FEBS Lett.* **594**, 1088–1100

122. Tseng, C.-C., Stanciauskas, R., Zhang, P., Woo, D., Wu, K., Kelly, K., Gill, P. S., Yu, M., Pinaud, F., and Lee, A. S. (2019) GRP78 regulates CD44v membrane homeostasis and cell spreading in tamoxifen-resistant breast cancer. *Life Sci. Alliance*. **2**, e201900377

123. Tseng, C.-C., Zhang, P., and Lee, A. S. (2019) The COOH-terminal proline-rich region of GRP78 is a key regulator of its cell surface expression and viability of tamoxifen-resistant breast cancer cells. *Neoplasia*. **21**, 837–848

124. Burikhanov, R., Zhao, Y., Goswami, A., Qiu, S., Schwarze, S. R., and Rangnekar, V. M. (2009) The tumor suppressor Par-4 activates an extrinsic pathway for apoptosis. *Cell*. **138**, 377–388

125. Birukova, A. A., Singleton, P. A., Gawlak, G., Tian, X., Mirzapoiazova, T., Mambetsariev, B., Dubrovskyi, O., Oskolkova, O. V., Bochkov, V. N., and Birukov, K. G. (2014) GRP78 is a novel receptor initiating a vascular barrier protective response to oxidized phospholipids. *Mol. Biol. Cell*. **25**, 2006–2016

126. Yao, X., Liu, H., Zhang, X., Zhang, L., Li, X., Wang, C., and Sun, S. (2015) Cell surface GRP78 accelerated breast cancer cell proliferation and migration by activating STAT3. *PLoS One*. **10**, e0125634

127. de Ridder, G. G., Gonzalez-Gronow, M., Ray, R., and Pizzo, S. V. (2011) Autoantibodies against cell surface GRP78 promote tumor growth in a murine model of melanoma. *Melanoma Res.* **21**, 35–43

128. Delie, F., Petignat, P., and Cohen, M. (2012) GRP78 protein expression in ovarian cancer patients and perspectives for a drug-targeting approach. *J. Oncol.* **2012**, 1–5

129. Yoo, S.-A., You, S., Yoon, H.-J., Kim, D.-H., Kim, H.-S., Lee, K., Ahn, J. H., Hwang, D., Lee, A. S., Kim, K.-J., Park, Y.-J., Cho, C.-S., and Kim, W.-U. (2012) A novel pathogenic role of the ER chaperone GRP78/BiP in rheumatoid arthritis. *J. Exp. Med.* **209**, 871–886

130. Crane, E. D., Al-Hashimi, A. A., Chen, J., Lynn, E. G., Won, K. D., Lhoták, Š., Naeim, M., Platko, K., Lebeau, P., Byun, J. H., Shayegan, B., Krepinsky, J. C., Rayner, K. J., Marchiò, S., Pasqualini, R., Arap, W., and Austin, R. C. (2018) Anti-GRP78 autoantibodies induce endothelial cell activation and accelerate the development of atherosclerotic lesions. *JCI Insight*. **3**, e99363

131. Liu, C., Bhattacharjee, G., Boisvert, W., Dilley, R., and Edgington, T. (2003) In vivo interrogation of the molecular display of atherosclerotic lesion surfaces. *Am. J. Pathol.* **163**, 1859–1871

132. Tran-Nguyen, T. K., Chandra, D., Yuan, K., Patibandla, P. K., Nguyen, K. T., Sethu, P., Zhang, Y., Xue, J., Mobley, J. A., Kim, Y., Shoushtari, A., Leader, J. K., Bon, J., Sciurba, F. C., and Duncan, S. R. (2020) Glucose-regulated protein 78 autoantibodies are associated with carotid atherosclerosis in chronic obstructive pulmonary disease patients. *ImmunoHorizons*. **4**, 108–118

133. Misra, U. K., Gonzalez-Gronow, M., Gawdi, G., Hart, J. P., Johnson, C. E., and Pizzo, S. V. (2002) The role of GRP78 in α2-macroglobulin-induced signal transduction. *J. Biol. Chem.* **277**, 42082–42087

134. Philippova, M., Ivanov, D., Joshi, M. B., Kyriakakis, E., Rupp, K., Afonyushkin, T., Bochkov, V., Erne, P., and Resink, T. J. (2008) Identification of proteins associating with glycosylphosphatidylinositol- anchored T-cadherin on the surface of vascular endothelial cells: role for GRP78/BiP in T-cadherin-dependent cell survival. *Mol. Cell. Biol.* **28**, 4004–4017

135. Kelber, J. A., Panopoulos, A. D., Shani, G., Booker, E. C., Belmonte, J. C., Vale, W. W., and Gray, P. C. (2009) Blockade of Cripto binding to cell surface GRP78 inhibits oncogenic Cripto signaling via MAPK/PI3K and Smad2/3 pathways. *Oncogene*. **28**, 2324–2336

136. Cao, Y., Chen, A., An, S. S. A., Ji, R.-W., Davidson, D., Cao, Y., and Llinás, M. (1997) Kringle 5 of Plasminogen is a Novel Inhibitor of Endothelial Cell Growth. *J. Biol. Chem.* **272**, 22924–22928

137. Mintz, P. J., Kim, J., Do, K.-A., Wang, X., Zinner, R. G., Cristofanilli, M., Arap, M. A., Hong, W. K., Troncoso, P., Logothetis, C. J., Pasqualini, R., and Arap, W. (2003) Fingerprinting the circulating repertoire of antibodies from cancer patients. *Nat. Biotechnol.* **21**, 57–63

138. Gonzalez-Gronow, M., Cuchacovich, M., Llanos, C., Urzua, C., Gawdi, G., and Pizzo, S. V. (2006) Prostate cancer cell proliferation in vitro Is modulated by antibodies against glucose-regulated protein 78 isolated from patient serum. *Cancer Res.* **66**, 11424–11431

139. Al-Hashimi, A. A., Caldwell, J., Gonzalez-Gronow, M., Pizzo, S. V., Aboumrad, D., Pozza, L., Al-Bayati, H., Weitz, J. I., Stafford, A., Chan, H., Kapoor, A., Jacobsen, D. W., Dickhout, J. G., and Austin, R. C. (2010) Binding of anti-GRP78 autoantibodies to cell surface GRP78 increases tissue factor procoagulant activity via the release of calcium from endoplasmic reticulum stores. *J. Biol. Chem.* **285**, 28912–28923

140. Bhattacharjee, G., Ahamed, J., Pedersen, B., El-Sheikh, A., Mackman, N., Ruf, W., Liu, C., and Edgington, T. S. (2005) Regulation of tissue factor–mediated initiation of the coagulation cascade by cell surface GRP78. *Arterioscler. Thromb. Vasc. Biol.* **25**, 1737–1743

141. Kaikita, K., Takeya, M., Ogawa, H., Suefuji, H., Yasue, H., and Takahashi, K. (1999) Co-localization of tissue factor and tissue factor pathway inhibitor in coronary atherosclerosis. *J. Pathol.* **188**, 180–188

142. Podolin, P. L., Callahan, J. F., Bolognese, B. J., Li, Y. H., Carlson, K., Davis, T. G., Mellor, G. W., Evans, C., and Roshak, A. K. (2005) Attenuation of murine collagen-induced arthritis by a novel, potent, selective small molecule inhibitor of IκB Kinase 2, TPCA-1 (2-[(Aminocarbonyl)amino]-5-(4-fluorophenyl)-3-thiophenecarboxamide), occurs via reduction of proinflammatory cytokines and ant. *J. Pharmacol. Exp. Ther.* **312**, 373–381

143. Wallach, I., Dzamba, M., and Heifets, A. (2015) AtomNet: A deep convolutional neural network for bioactivity prediction in structure-based drug discovery. *arXiv*

144. Caldwell, J. A., Dickhout, J. G., Al-Hashimi, A. A., and Austin, R. C. (2010) Development of a continuous assay for the measurement of tissue factor procoagulant activity on intact cells. *Lab. Investig.* **90**, 953–962

145. Tatsumi, K., and Mackman, N. (2015) Tissue factor and atherothrombosis. *J. Atheroscler. Thromb.* **22**, 543–549

146. Li, Y.-D., Ye, B.-Q., Zheng, S.-X., Wang, J.-G. J.-T., Wang, J.-G. J.-T., Chen, M., Liu, J.-G., Pei, X.-H., Wang, L.-J., Lin, Z.-X., Gupta, K., Mackman, N., Slungaard, A., Key, N. S., and Geng, J.-G. (2009) NF-κB transcription factor p50 critically regulates tissue factor in deep vein thrombosis. *J. Biol. Chem.* **284**, 4473–4483

147. Al-Hashimi, A. A., Lebeau, P., Majeed, F., Polena, E., Lhotak, Š., Collins, C. A. F., Pinthus, J. H., Gonzalez-Gronow, M., Hoogenes, J., Pizzo, S. V., Crowther, M., Kapoor, A., Rak, J., Gyulay, G., D'Angelo, S., Marchiò, S., Pasqualini, R., Arap, W., Shayegan, B., and Austin, R. C. (2017) Autoantibodies against the cell surface–associated chaperone GRP78 stimulate tumor growth via tissue factor. *J. Biol. Chem.* **292**, 21180–21192

148. Yap, J., Chen, X., Delmotte, P., and Sieck, G. C. (2020) TNFα selectively activates the IRE1α/XBP1 endoplasmic reticulum stress pathway in human airway smooth muscle cells. *Am. J. Physiol. Cell. Mol. Physiol.* **318**, L483–L493

149. Vig, S., Buitinga, M., Rondas, D., Crèvecoeur, I., van Zandvoort, M., Waelkens, E., Eizirik, D. L., Gysemans, C., Baatsen, P., Mathieu, C., and Overbergh, L. (2019) Cytokine-induced translocation of GRP78 to the plasma membrane triggers a pro-apoptotic feedback loop in pancreatic beta cells. *Cell Death Dis.* **10**, 309

150. Chazotte, B. (2011) Labeling membrane glycoproteins or glycolipids with fluorescent wheat germ agglutinin. *Cold Spring Harb. Protoc.* **2011**, pdb.prot5623

151. Lebeau, P. F., Platko, K., Byun, J. H., and Austin, R. C. (2021) Calcium as a reliable marker for the quantitative assessment of endoplasmic reticulum stress in live cells. *J. Biol. Chem.* **296**, 100779

152. Bach, R. R. (1998) Mechanism of tissue factor activation on cells. *Blood Coagul. Fibrinolysis*. **9 Suppl 1**, S37-43

153. Rosas, M., Slatter, D. A., Obaji, S. G., Webber, J. P., Alvarez-Jarreta, J., Thomas, C. P., Aldrovandi, M., Tyrrell, V. J., Jenkins, P. V., O'Donnell, V. B., and Collins, P. W. (2020) The procoagulant activity of tissue factor expressed on fibroblasts is increased by tissue factor-negative extracellular vesicles. *PLoS One*. **15**, e0240189

154. Nestoridi, E., Kushak, R. I., Duguerre, D., Grabowski, E. F., and Ingelfinger, J. R. (2005) Up-regulation of tissue factor activity on human proximal tubular epithelial cells in response to Shiga toxin. *Kidney Int.* **67**, 2254–2266

155. Crowther, M. A., and Warkentin, T. E. (2008) Bleeding risk and the management of bleeding complications in patients undergoing anticoagulant therapy: focus on new anticoagulant agents. *Blood*. **111**, 4871–4879

156. Samanta, S., Yang, S., Debnath, B., Xue, D., Kuang, Y., Ramkumar, K., Lee, A. S., Ljungman, M., and Neamati, N. (2021) The hydroxyquinoline analogue YUM70 inhibits GRP78 to induce ER stress–mediated apoptosis in pancreatic cancer. *Cancer Res.* **81**, 1883–1895

157. Boesten, L., Zadelaar, A., Vanniewkoop, A., Gijbels, M., Dewinther, M., Havekes, L., and Vanblijmen, B. (2005) Tumor necrosis factor-a promotes atherosclerotic lesion progression in APOE*3-leiden transgenic mice. *Cardiovasc. Res.* **66**, 179–185

158. Ait-Oufella, H., Taleb, S., Mallat, Z., and Tedgui, A. (2011) Recent advances on the role of cytokines in atherosclerosis. *Arterioscler. Thromb. Vasc. Biol.* **31**, 969–979

159. Hayden, M. S., and Ghosh, S. (2014) Regulation of NF-κB by TNF family cytokines. *Semin. Immunol.* **26**, 253–266

160. Kirchhofer, D., Tschopp, T. B., Hadváry, P., and Baumgartner, H. R. (1994) Endothelial cells stimulated with tumor necrosis factor-alpha express varying amounts of tissue factor resulting in inhomogenous fibrin deposition in a native blood flow system. Effects of thrombin inhibitors. *J. Clin. Invest.* **93**, 2073–2083

161. Liu, C.-W., Sung, H.-C., Lin, S.-W. S.-R., Wu, C.-W., Lee, C.-W., Lee, I.-T., Yang, Y.-F., Yu, I.-S., Lin, S.-W. S.-R., Chiang, M.-H., Liang, C.-J., and Chen, Y.-L. (2017) Resveratrol attenuates ICAM-1 expression and monocyte adhesiveness to TNF-α-treated endothelial cells: evidence for an anti-inflammatory cascade mediated by the miR-221/222/AMPK/p38/NF-κB pathway. *Sci. Rep.* **7**, 44689

162. Misra, U. K., Gonzalez-Gronow, M., Gawdi, G., Wang, F., and Vincent Pizzo, S. (2004) A novel receptor function for the heat shock protein GRP78: silencing of GRP78 gene expression attenuates α2M*-induced signalling. *Cell. Signal.* **16**, 929–938

163. Krieger, N. S., and Bushinsky, D. A. (2011) Pharmacological inhibition of intracellular calcium release blocks acid-induced bone resorption. *Am. J. Physiol. Physiol.* **300**, F91–F97

164. Stelzer, M., Henes, J., and Saur, S. (2021) The Role of Antiphospholipid Antibodies in COVID-19. *Curr. Rheumatol. Rep.* **23**, 72

165. Kim, K.-J., Baek, I.-W., Park, K.-S., Kim, W.-U., and Cho, C.-S. (2017) Association between antiphospholipid antibodies and arterial thrombosis in patients with rheumatoid arthritis. *Lupus*. **26**, 88–94

166. Ballantyne, C. M., and Nambi, V. (2005) Markers of inflammation and their clinical significance. *Atheroscler. Suppl.* **6**, 21–29

167. Iqbal, Z., and Cohen, M. (2011) Enoxaparin: a pharmacologic and clinical review. *Expert Opin. Pharmacother.* **12**, 1157–1170

168. Martinez-Sales, V., Vila, V., Réganon, E., Oms, J. G., and Aznar, J. (2003) Effect of unfractionated heparin and a low molecular weight heparin (enoxaparin) on coagulant activity of cultured human endothelial cells. *Haematologica*. **88**, 694–9

169. Capule, C. C., and Yang, J. (2012) Enzyme-Linked Immunosorbent Assay-based method to quantify the association of small molecules with aggregated amyloid peptides. *Anal. Chem.* **84**, 1786–1791

170. Reddish, F. N., Miller, C. L., Gorkhali, R., and Yang, J. J. (2017) Monitoring ER/SR calcium release with the targeted Ca2+ sensor CatchER+. *J. Vis. Exp.* 10.3791/55822

171. Gisterå, A., Ketelhuth, D. F. J., Malin, S. G., and Hansson, G. K. (2022) Animal models of atherosclerosis–supportive notes and tricks of the trade. *Circ. Res.* **130**, 1869–1887

172. Eitzman, D. T., Westrick, R. J., Xu, Z., Tyson, J., and Ginsburg, D. (2000) Hyperlipidemia promotes thrombosis after injury to atherosclerotic vessels in apolipoprotein E–deficient mice. *Arterioscler. Thromb. Vasc. Biol.* **20**, 1831–1834